TECHNICKÁ UNIVERZITA V LIBERCI
Fakulta textilní

Nanovlákenné cévní náhrady

Disertační práce

Studijní program: P3106 – Textilní inženýrství
Studijní obor: 3106V015 – Textilní technika a materiálové inženýrství

Autor práce: **Mgr. Jana Horáková**
Vedoucí práce: prof. RNDr. David Lukáš, CSc.

Liberec 2015

TECHNICAL UNIVERSITY OF LIBEREC
Faculty of Textile Engineering

Nanofibrous vascular grafts

Dissertation

Study programme: P3106 – Textile Engineering
Study branch: 3106V015 – Textile Technics and Materials Engineering

Author: **Mgr. Jana Horáková**
Supervisor: prof. RNDr. David Lukáš, CSc.

Liberec 2015

Prohlášení

Byla jsem seznámena s tím, že na mou disertační práci se plně vztahuje zákon č. 121/2000 Sb., o právu autorském, zejména § 60 – školní dílo.

Beru na vědomí, že Technická univerzita v Liberci (TUL) nezasahuje do mých autorských práv užitím mé disertační práce pro vnitřní potřebu TUL.

Užiji-li disertační práci nebo poskytnu-li licenci k jejímu využití, jsem si vědoma povinnosti informovat o této skutečnosti TUL; v tomto případě má TUL právo ode mne požadovat úhradu nákladů, které vynaložila na vytvoření díla, až do jejich skutečné výše.

Disertační práci jsem vypracovala samostatně s použitím uvedené literatury a na základě konzultací s vedoucím mé disertační práce a konzultantem.

Současně čestně prohlašuji, že tištěná verze práce se shoduje s elektronickou verzí, vloženou do IS STAG.

Datum:

Podpis:

Abstract

There is a pressing need to develop vascular graft since no clinically available appropriate prosthesis with inner diameter less than 6 mm works in a long term after implantation. In the thesis, blood vessel substitutes made from biodegradable polymers were created and characterized as potential candidates for such a medical device. The idea of tissue engineering scaffolds is based on mimicking natural environment - extracellular matrix therefore ideal bypass graft was designed as double layered structure with defined morphology of each layer. The proposed structure was created by electrospinning of polycaprolactone (PCL). The morphology of the resulting fibers resembled inner and medial layer of native arteries suggesting that this similarity will help body to regenerate functional tissue after implantation. Besides PCL, novel polymer from the same group of polyester - copolymer polylactide-polycaprolactone (PLC 70/30) was electrospun into a tubular form. Vascular graft made from copolymer PLC created only single layered prosthesis.

Further tests were conducted with both presented electrospun materials in order to compare their bulk and surface properties. Copolymer PLC was slightly more hydrophilic than polycaprolactone. Thermal behavior revealed that copolymer is mostly amorphous with melting temperature about 110°C whereas polycaprolactone is semicrystalline polymer with melting temperature about 57°C. Mechanical strength and elongation at break of electrospun copolymer PLC was about ten times higher compared to electrospun polycaprolactone.

Biological tests using fibroblast and endothelial cell line prove the biocompatibility of both tested electrospun polymers. Higher proliferation rate was found when cells were cultured on electrospun copolymer PLC suggesting that higher hydrophilicity contributes to favorable cell adhesion. Hemocompatibility testing of produced samples were carried out using platelets. It was found that fibrous layers are more thrombogenic than smooth surface when compared with foils made from the same materials. Platelets became activated and aggregated after incubation with fibrous materials. The level of activation was increased in dynamic conditions.

Electrospun fibers were successfully used as a drug delivery system of nitric oxide (NO) that has many beneficial effects on cardiovascular system. Polycaprolactone fibers were blended with NO donors from the group of S-Nitrosothiols that are capable of long term NO release in physiological levels up to 42 days *in vitro.* After implantation of such grafts as a replacement of rat abdominal aorta, the NO release was found to strongly inhibit cellular infiltration into the medial and luminal regions of the vascular graft. The reduced presence of inflammatory cells within these regions may confer increased protection against neointimal hyperplasia from smooth muscle cells.

Keywords: Vascular grafts, Nanofibers, Electrospinning, *In vitro* tests, Nitric Oxide

Anotace

V současnosti není v klinické praxi cévní náhrada s vnitřním průměrem pod 6 mm, která by spolehlivě fungovala v dlouhodobém horizontu. Disertační práce se zabývá přípravou maloprůměrových cévních náhrad z biodegradabilních polymerů, které jsou testovány jako potenciálně vhodné materiály pro přípravu tkáňových nosičů pro vaskulární cévní systém. Hlavní myšlenkou tkáňového inženýrství je napodobování přirozeného prostředí - mezibuněčné hmoty. Proto byla ideální cévní náhrada navržena jako dvouvrstvá tubulární struktura s definovanou morfologií vláken. Tato definovaná struktura byla vytvořena elektrostatickým zvlákňováním polykaprolaktonu (PCL). Podobnost morfologie vláken s mezibuněčnou hmotou předpokládá, že po implantaci do organismu proběhne regenerace funkční tkáně. Kromě polymeru polykapronu byl testován polymer ze stejné třídy polyesterů - kopolymer polylatidu a polykaprolaktonu (PLC 70/30). Cévní náhrada připravená z toho polymeru byla tvořena pouze jednou vrstvou.

Pro porovnání vlastností polymerů byla provedena charakterizace obou elektrostaticky zvlákněných materiálů. Kopolymer PLC je mírně hydrofilnější než polykaprolakton. Termické vlastnosti obou polymerů se značně liší. Zatímco kopolymer PLC je převážně amorfní s teplotou tání okolo 110°C, polykaprolakton je semikrystalický polymer s teplotou tání kolem 57°C. Mechanická pevnost a prodloužení je přibližně desetkrát větší u elektrostaticky zvlákněného kopolymeru PLC než u polykaprolaktonu.

Biologické testování elektrostaticky zvlákněných materiálů potvrdilo biokompatibilitu obou testovaných polymerů s fibroblasty i s endotelovými buňkami. Vyšší proliferační stupeň byl pozorován při kultivaci buněk na mírně hydrofilnějším kopolymeru PLC, který zřejmě umožňuje lepší buněčnou adhezi. Vlákenné materiály byly rovněž testovány po interakci s krevními destičkami, které se po inkubaci aktivovaly a agregovaly. Mírnější aktivace byla pozorována po interakci s hladkými foliemi vyrobenými ze stejných materiálů, což dokládá, že na aktivaci destiček má vliv morfologie povrchu. Zvýšená aktivace trombocytů byla naopak pozorována při dynamické inkubaci vlákenných tubulárních vzorků.

Vlákenné tkáňové nosiče byly využity jako systém cíleného uvolňování léčiv, konkrétně oxidu dusnatého (NO), který má pozitivní účinky na kardiovaskulární systém. Vlákna polykaprolaktonu byla obohacena o donory NO ze skupiny S-Nitrosothiolů, které umožňují uvolňování NO ve fyziologickém rozmezí po 42 dní v *in vitro* podmínkách. Po implantaci cévních náhrad jako náhrada břišní části aorty u potkanů bylo zjištěno, že NO inhibuje buněčnou infiltraci do vnitřní a střední vrstvy cévní náhrady. Tento snížený výskyt zánětlivých buněk může bránit vzniku neointimální hyperplazie způsobenou hladkosvalovými buňkami v pozdějších stadiích implantace.

Klíčová slova: Cévní náhrady, Nanovlákna, Elektrostatické zvlákňování, *In vitro* testování, Oxid dusnatý

Acknowledgement

I would like to express sincere gratitude to my advisor prof. RNDr. David Lukáš, CSc. for excellent guidance and motivation during my studies. Furthermore I would like to acknowledge my supervisor specialist Ing. Petr Mikeš, PhD. for helping me with practical aspects of experimental part as well as bringing new ideas to further research. Many thanks belong to my colleagues from the Department of Nonwovens and Nanofibrous Materials, Technical University Liberec as well as from the Department of the Biomedical Engineering, Michigan Technological University where part of the thesis resulted from. I would like to thank Fulbright Commission for funding visiting scholarship in years 2013-2014. Many thanks belong to projects that supported the research presented in the thesis such as Student Grant Competition financed by the Ministry of Education, Youth and Sports (No. 4869: Development of nanofibrous scaffolds for tissue engineering and cell proliferation testing, 2012; No. 48018: The relationship between nanofibrous structure and cell distribution, 2013), project „Nanofiber materials for tissue engineering“ (No. CZ.1.05/3.1.00/14.0308, 2013-2015) financed by the European Social Fund and the state budget of the Czech Republic and project "Nanofibrous Biodegradable Small-Diameter Vascular Bypass Graft" financed by the Ministry of Health (No. 15-29241A, 2015). Since the field of tissue engineering requires the cooperation of specialists with different knowledge and skills, it is my pleasure to thank many people that were more or less involved in this broad concept of my thesis. Some of them are mentioned in special chapters but the list is not complete. The last but not least thanks belong to my family, especially my husband and my parents, for supporting me during the thesis processing.

Content

Notations

ATCC	American Type Culture Collection
BSA	Bovine serum albumine
CE	European Conformity (certification mark within the European Economic Area)
CVDs	Cardiovascular Diseases
DAPI	2-(4-amidinophenyl)-1H -indole-6-carboxamidine
DMEM	Dulbecco´s Modified Eagle Medium
EBM-2	Endothelial basal medium
EC	Endothelial cells
ECM	Extracellular matrix
EDRF	Endothelium-derived relaxing factor
EDTA	Ethylenediaminetetraacetic acid
EPC	Endothelial progenitor cells
ePTFE	Expanded polytetrafluorethylene
FBS	Fetal bovine serum
FDA	Food and Drug Administration
FESEM	Field emission scanning electrone microscopy
FITC	Fluorescein isothiocyanate
GMP	Good manufacturing practice
GP	Glycoprotein
H&E	Hematoxylin eosin staining
HUVEC	Human umbilical vein endothelial cells
MTT test	Cell viability test using 3-(4,5-dimethylthiazol-2-yl)-2,5-diphenyl-2*H*-tetrazolium bromide
MTU	Michigan Technological University
NAP	N-acetyl-D-penicillamine
NO	Nitric oxide
NOA	Nitric oxide analyzer
PBS	Phopshated buffer saline
PCL	Polycaprolactone
PDGF	Platelet-derived growth factor
PDLLA	Racemic mixture of L- and D-isoform of polylactic acid

PET	Polyethyleneterephtalate
PGA	Polyglycolic acid
PI	Propidium iodide
PLA	Polylactic acid
PLC	Copolymer polylactide-polycaprolactone
PLGA	Copolymer of polyglycolic and polylactic acid
PLLA	L-isoform of polylactic acid
PMMA	Polymethylmethacrylate
PUR	Polyurethanes
RGD	Tripeptide composed of L-Arginin, Glycin and L-Aspartic Acid mediating cell attachment
RSNO	S-Nitrosothiols
SEM	Scanning electrone microscopy
SMC	Smooth muscle cells
SNAP	S-Nitroso-N-acetyl-D-penicillamine
SNAP-cyclam	S-Nitroso-N-acetyl-D-penicillamine derivatized cyclam
TRS	Thrombocyte rich solution
VEGF	Vascular endothelial growth factor

1 Introduction

The development of new medical care and treatment lead to the ageing of the population and more tissues are needed to be repaired or restored. Transplantation is considered to be a gold standard of tissue replacement, however it could be limited due to the lack of appropriate donors. Government and other funding institutions are beware of this fact therefore a lot of grants and projects dealing with so called tissue engineering are funded nowadays. The development of tissue engineering scaffold, making them off-the shelf available in various sizes is a real challenge in today's world. Especially in the field of vascular tissue engineering there is a demand of an appropriate scaffold since no small diameter synthetic vascular graft successful in a long term after implantation has been successfully translated to clinic yet.

Cardiovascular diseases (CVDs) are the number one cause of death globally. More people die annually from CVDs than from any other cause according to World Health Organization. A large number of patients suffer from vascular damage, resulting in the need for bypass surgery. Blood vessels can be blocked through a process called atherosclerosis. Cholesterol and fibrous tissue make up a plaque and blood vessels become narrow and stiffen. If the vessel is completely occluded, new pathway for blood flow has to be created during a surgery. A graft can be either autologous using patient own vessel or man-made synthetic tube.

Since there are still limitations in the replacement of small diameter vascular grafts, the need and demand for developing more desirable grafts is increasing day by day. The thesis is focused on a contribution to the development of ideal bypass graft scaffolding material. Currently used materials are commercially fabricated from inert polymers such as expanded polytetrafluorethylene or polyethylene terephtalate known as Dacron. In the thesis, the usage of biodegradable materials is preferred since these materials possess many advantages over the inert ones. After implantation of biodegradable material, the body will start the healing response. Ideally, the scaffold structure and composition would be able to promote healing of the injured or damaged tissue. In this case, scaffold material serves as a temporary support that starts self-renewal of the tissue. Biodegradable polyesters were tested and compared in the thesis as ideal candidates for vascular tissue engineering scaffold fabrication.

The hypothesis of the dissertation was to create a vascular graft that will fulfill requirements of small diameter vascular graft in terms of morphological structure

that resembles native extracellular matrix (1), possess appropriate mechanical properties (2) and surface properties that will facilitate cell adhesion, especially endothelial cell adhesion to prevent further thrombosis (3). Synthetic vascular grafts could be improved by incorporation of nitric oxide releasing substances. The aim of long term nitric oxide release (4) was hypothesized to reach in the last experimental part of the thesis.

The theoretical part of the thesis described in chapter 2 deals with basic concepts of tissue engineering and specific knowledge concerning vascular tissue engineering. The experimental part of the dissertation is divided into 3 chapters called *Synthetic vascular grafts preparation and testing*, *Biological testing of vascular grafts and Vascular grafts releasing nitric oxide*. The first experimental chapter describes the electrospinning technique and devices used for production of nanofibrous scaffolds as well as tubular vascular grafts. Produced materials were characterized morphologically to reach the goal of creation structure similar to natural extracellular matrix (1), mechanically to verify hypothesis 2 and surface wettability was tested in relationship to the third hypothesis that was further tested in the second experimental part with the focus on *in vitro* testing of produced scaffolds. Seeding of fibroblasts and endothelial cells was carried out in order to test the hypothesis of biocompatibility of produced scaffolds for vascular tissue engineering. Cell lines were cultured on fibrous materials and their proliferation rate was analyzed using metabolic MTT test, fluorescence microscopy and scanning electrone microscopy in order to characterize biological performance of biodegradable scaffolds and to clarify the third hypothesis. As a part of biological performance, thrombogenicity of fibrous scaffold was also evaluated. The third experimental part of the thesis is devoted to the modification of vascular graft by nitric oxide release in a long term. Obtained results are discussed in the discussion chapter. In the end of the thesis, general conclusions are summarized and contribution of the achieved results to the field of vascular tissue engineering is evaluated.

2 Theoretical part

Theoretical part describes the basic concept of tissue engineering focused on the specific materials and fabrication techniques used in the thesis. Biological performance of tissue engineering scaffolds is introduced in order to explain the methods and approaches employed in the second experimental part of the thesis. Specific requirements of vascular grafts are listed and current status of the market with its limitations is outlined. Finally, the background of nitric oxide and its role in cardiovascular system is introduced since the modification was studied in the last chapter of experimental part.

2.1 Tissue Engineering

Tissue engineering is an interdisciplinary field that applies the principles of chemistry, physics, material science, engineering, cell biology and medicine to the development of biological substitutes that restore, maintain or improve tissue/organ functions (*Langer, 1993*). The combination of classical engineering and life sciences is essential. Biomedical engineering requires the cooperation of materials engineers, cell culture biologists, clinicians and many other experts in different fields in order to develop functional scaffold.

Tissue engineering field utilizes different types and forms of materials that serve as scaffolds for cell attachment. Plenty of materials are used to produce scaffolds with desired properties and several methods are combined in order to create an ideal scaffold. Cells that colonize the scaffold could be influenced by signals affecting their function or proliferation rate. The process of tissue engineering lays in 3 main categories: cells, scaffolds and signals as depicted in figure 1. All of these aspects are discussed later with specific focus on vascular tissue engineering related to the aims of the thesis.

Combination of these 3 pillars (cells, scaffolds and signals), multiple strategies of tissue engineering could be employed. So called *in vitro* tissue engineering, considered to be a traditional approach, constructs the scaffold by using cells, scaffold and bioreactor. *In vivo* tissue engineering uses the tissue environment such as peritoneal cavity or subcutaneous place for production of functional scaffolds. The last but not least possibility is called *in situ* tissue engineering. Biocompatible scaffolds are

produced and implanted suggesting that functional tissue will regenerate within the living organism in the site of implantation. This approach was utilized in the thesis because it reduces the cultivation time for *in vitro* cell expansion, leading to readily available grafts in various sizes (*Li, 2014).*

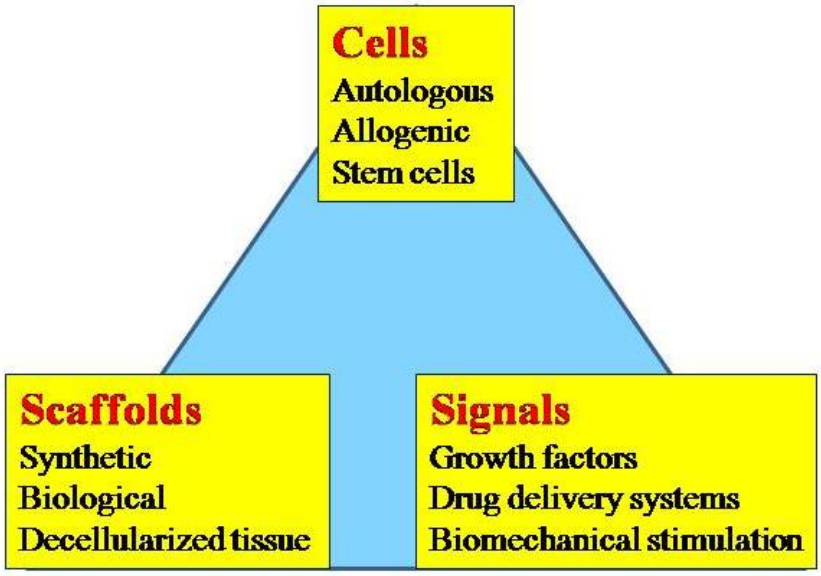

Figure 1: The description of 3 basic components of tissue engineering: cells, scaffolds and signals.

2.1.1 Scaffolds

Tissue engineering scaffolds are designed as structural and functional analogues of extracellular matrix (ECM) assuming that cells recognize their natural environment and undergo the regeneration of the damaged tissue. Extracellular matrix is a natural cell environment composed of complicated nano- and macro-architecture. Most body tissues are hierarchal fibrillar or tubular structures with various size, organization and composition that affect the tissue mechanical and biophysical properties *(Kim, 2013).* To reach this goal, many scaffold fabrication techniques has been studied, for example rapid prototyping, solvent casting and particulate leaching, electrospinning or decellularization of tissues. Specific requirements are demanded for each application but some of them are generally accepted. Scaffolds have to be fabricated from biocompatible materials that will further promote normal cell growth without any adverse tissue reactions (*Boland, 2004).* A non-viable material used in medical device

or interacted with biological system is defined as biomaterial. Metals, ceramics or polymers are widely used biomaterials in medical devices (*Bauer, 2013)*.

Materials used for scaffolds fabrication

There are still applications utilizing inert materials that are described later in the paragraph 2.2.4 (Currently used vascular grafts). On the other hand, there is a shift from usage of inert materials to biodegradable ones in the last years. It is assumed that most of the prosthetic device will be replaced by biodegradable materials that will allow the body to repair and regenerate. The overall biocompatibility of final scaffold is affected by material chemistry, molecular weight, solubility, shape and inner structure, surface wettability, degradation rate etc. (*Nair, 2007)*.

Variety of natural and synthetic polymers could be used for fabrication of tissue engineering scaffolds. Natural polymers like collagen, chitosan, gelatin, cellulose acetate, silk protein, chitin, fibrinogen possess better biocompatibility and lower immunogenicity compared to synthetic ones. On the other hand, synthetic polymers can be tailored to give a wide range of structural and functional properties such as mechanical behavior, degradation rate etc. *(Bhardwaj, 2010)*. Synthetic tissue engineering scaffolds have higher mechanical stability compared to natural based scaffolds. Moreover, it avoids the use of crosslinking agents leading to slow degradation of such a device. These polymers represent a new generation of biomaterials to mimic extracellular matrix by fibrillar structure and viscoelasticity *(Yarin, 2014)*. In biomedical applications biodegradable polyesters such as polyglycolic acid (PGA), polylactic acid (PLA) and polycaprolactone (PCL) are often used. Special attention is devoted to PCL and PLA since these polymers and their copolymer were used in the experimental part of the thesis.

Polyglycolic acid is a rigid thermoplastic polymer. Due to its high crystallinity (45-60%), it is insoluble in most organic solvents except for fluorinated organic solvents such as hexafluoro isopropanol. PGA shows excellent mechanical properties that are lost in 1-2 months after implantation. Polyglycolic acid degrades into amino acid glycine. The hydrolysis of PGA is completed within 6-12 months. Due to its high degradation rate with releasing of acidic byproducts and low solubility, PGA has been replaced by other polymers (*Nair, 2007).*

Polylactic acid is present in 3 isomeric forms: D, L and racemic mixture

PDLLA. Its L isoform (PLLA) is preferentially metabolized in the body. PLLA is a crystalline polymer (crystallinity about 37%), its crystallinity depends on molecular weight. Racemic form PDLLA is an amorphous polymer with faster degradation rate than PLLA. Polylactic acid degrades to lactic acid that enters citric acid cycle and is excreted as water and carbon dioxide. Degradation byproducts are not accumulated in the vital organs. The rate of degradation is slower than in case of PGA and is determined by crystallinity, molecular weight, morphology, porosity, site of implantation etc. (*Gunatillake, 2003).*

Polycaprolactone is a hydrophobic, semicrystalline polymer with a long degradation time (2-3 years). Its crystallinity decreases with increasing of molecular weight. It has been used in the biomedical field due to its good solubility, low melting point (59-64°C) and blend-compatibility. The degradation occurs firstly by non-enzymatic cleavage of ester groups followed by intracellular degradation of PCL fragments. The degradation product 6-hydroxylcaproic acid is further converted to acetylcoenzym-A and metabolized in citric acid cycle. Since PCL is a semicrystalline polymer, amorphous regions are preferentially degraded as depicted in the figure 2 (*Woodruff, 2010).*

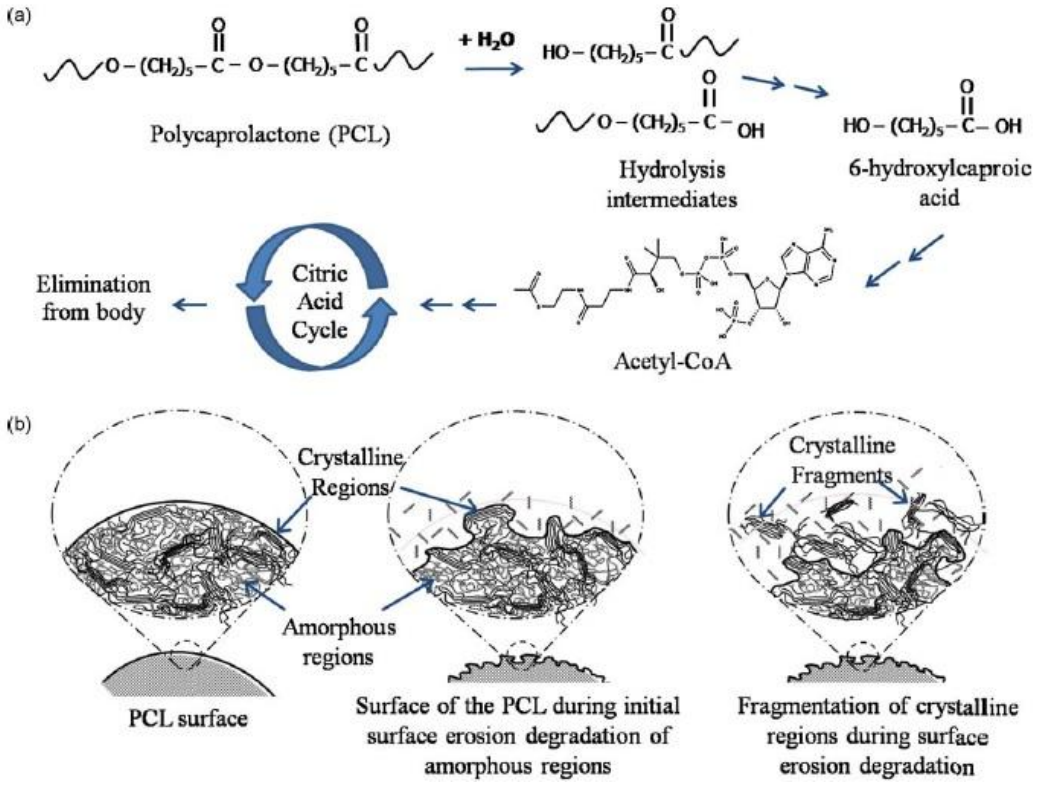

Figure 2: Hydrolytic degradation of PCL (a), schematic visualization of crystalline fragmentation during degradation (b) (Woodruff, 2010).

Some of the products made from biodegradable polyesters listed below have already been approved by Food and Drug Administration (FDA) or acquired European Conformity (CE) mark:

Monocryl suture is used in general soft tissue approximation and/or ligation. Monocryl is composed of a block copolymer of polycaprolactone with glycolide. The absorption occurs by means of hydrolysis that is completed between 91-119 days. The degradation begins as a progressive loss of tensile strength followed by a loss of mass. The sutures are produced by Ethicon (*Middleton, 2000).*

Artelon CMC Spacer is a T-shape device for ligament/tendon reinforcement, joint resurfacing or soft tissue replenishment. It is a biocompatible PCL based polyurethane urea biomaterial well tolerated in both bone and soft tissues having more than 10 years of clinical experience. The device degrades by hydrolysis that is not affected by enzymes. One half of the device that is made from PCL degrades and urethane urea part remains. The degradation is completed at about 6 years. There have not been reported any inflammatory or foreign body response accompanying implantation (*Nilsson, 2010).*

Mesofol is an implantable, resorbable surgical sheet made from a lactide-caprolactone copolymer. After implantation it is chemically broken down by hydrolytic cleavage of polymers, giving rise to 3 monomers: 6-hydroxylcaproic acid that is further metabolized to acetylcoenzym A and D-/L-lactic acid. The degradation involves molecule adhesion and fibrin attachment to both sides of the sheet. The mesh absorption time is about 4-6 weeks. The surgical sheet is used where temporary wound support is required to reinforce soft tissues *(Klopp, 2008).*

Neurolac is an FDA approved nerve guide manufactured by Polyganics having also CE mark. Neurolac offers tensionless nerve repair to further improve healing and function recovery without the need for autologous transplants. It is mechanically stable for 10-12 weeks after which degradation is observed by loss of strength and mass. The nerve guide is made from poly (D,L-lactide-ε-caprolactone) co-polyester. Both used polymers (PLA, PCL) are safe and approved for use in medical and pharmaceutical implants *(Bertleff, 2005).*

Technologies used for scaffold fabrication

Development of functional scaffold rises from the assumption of mimicking natural cellular environment – extracellular matrix. Studying of the composition and morphology of the tissue of interest is an important step when designing the scaffold structure. Afterwards, utilization of appropriate technologies that will create the proposed scaffold architecture will bring success in the development of functional scaffold. Mimicking this 3D web by nanofibers is a challenge in the modern tissue engineering *(Srouji, 2008).* Electrospinning is the most well-known method for production of nanofibrous structures. However, there are other methods that could be used to produce fibers in nanoscale such as centrifugal spinning, melt-blowing, phase separation or self-assembly *(Zhang, 2014).* Due to the versatility of electrospinning apparatus that enables mimicking of native morphology of ECM in blood vessels, this technique was chosen for experimental part of the thesis.

Nanofibers have been widely used as scaffolds for tissue engineering and regenerative medicine. Their structure is very similar to the native extracellular matrix therefore it facilitates cell adhesion and spreading *(Dahlin, 2011).* Fiber diameters in nanoscale mimic the collagen fibrils and allow cell adhesion to multiple electrospun fibers instead of many cells adhering to one microfiber *(Pham, 2006).* Electrospinning is using high electric field intensity which is affecting surface of polymeric solution. Electric forces create instabilities on the polymeric solution surface and when it reaches its critical values, the polymeric jet appears. During process, the most of the solvent has been evaporated and dry nanofibers are collected on the counter electrode. There are several physical and chemical parameters which affect this process. These parameters bring some complexity but as well some flexibility for possible modifications. One can for example control the fibrous diameter or porosity by the usage of specific solvent, molecular weight and concentration of polymer together with air humidity *(Yarin, 2014).*

2.1.2 Cells

The interaction of the cells with scaffold requires a complex assessment before implantation into the body. The thesis deals with so called *in situ* tissue engineering explained previously in subchapter 2.1 assuming that the cells will colonize the scaffold after implantation. However, the first tests with new materials have to be

tested in laboratory conditions using cell lines. In this case, cells serve as a tool for prediction of regeneration and engraftment of the scaffold following implantation. Assessment of biocompatibility of materials requires standard tests defined by the legislation. Polymers used in the thesis have been approved by FDA or acquired CE mark so their safety has been proved by companies or has been previously published by other groups *(Bertleff, 2005; Sun, 2006)*. Biocompatibility testing was designed in order to verify the cytocompatibility of electrospun fibers made from these polymers by using fibroblast cell line. For specific application in cardiovascular system, the scaffolds were also tested using endothelial cell line. Successful endothelialization of the lumen is the key factor for ensuring antithrombotic surface of implanted graft.

Scaffolds interacting with blood also require hemocompatibility testing for prediction of interactions between blood and the material. For this purpose, a part of complex hemocompatibility assessment, the scaffolds were incubated with thrombocytes predicting their thrombogenic potential that is prone to occlusion in small diameter vascular grafts.

Methods for biocompatibility assessment

Assessment of scaffold biocompatibility could be done in static or dynamic conditions. The static incubation of materials with certain cell lines was used for assessment of cellular adhesion and proliferation. Testing in dynamic conditions requires the usage of bioreactors and more closely simulate the natural environment. The construction of a bioreactor is challenging since many aspects has to be taken into account such as sterilization of the device, placing the bioreactor system into the incubator ensuring temperature of 37°C and 5% CO_2, flow of the medium through the tested scaffold etc.

Composition and morphology of tested materials plays an important role in cell behavior. Assessment of cell response to materials has to be performed using combination of techniques used in tissue culture laboratory. Measurement of cellular metabolic activity reflects the cell count so these methods result in quantitative evaluation. Metabolic assays are carried out after certain time of incubation (in the thesis after 1, 3, 7 and 14 days) so the proliferation rate of the cells could be estimated and materials cultured under the same conditions could be compared. Metabolic tests such as ***MTT test*** utilizing 3-(4,5-dimethylthiazol-2-yl)-2,5-diphenyl-

2*H*-tetrazolium bromide measures the reduction of tetrazolium salt to formazan indicating normal cell metabolism. There is a relationship between number of cells and the measured absorbance nevertheless the results are presented as measured absorbance of reduced formazan *(Freshney, 2010)*. The precise cell number could be more precisely evaluated by DNA quantification. DNA content is measured using specific device spectrofluorimeter that is not available in the laboratory of tissue engineering in TUL. Therefore, metabolic test MTT was used for quantification of cellular proliferation rate after culturing of the cells with tested materials.

Microscopic techniques are another useful tool of evaluation of interactions between cells and materials. The disadvantage of microscopic methods is their qualitative character. The observation of cellular shape and specific cellular response is described from pictures depicting cells adhered on materials. ***Fluorescence*** microscopic techniques enable the visualization of certain structures within the cells. Cellular spreading within the scaffold could be evaluated by staining of the cell nuclei by fluorescence stains binding to nucleic acids such as propidium iodide (PI) or 2-(4-amidinophenyl)-1H -indole-6-carboxamidine known as DAPI. The number of cell nuclei per specific area could be quantified and comparison of cells adhered to scaffold could be carried out. This quantification is possible when cells adhered on the surface of the material where automated image analysis could be used. When dealing with electrospun fibrous layers, the cells have a tendency to colonize both sides of tested scaffold and growth into the inner parts. The fluorescence pictures do not allow the accurate automated quantification of cells therefore alternative approaches were employed. Manual counting of the cells per field of view was used for quantification of the cells per specific area in the experimental section of the thesis.

Scanning electron microscopy (SEM) allows the observation of single cells as well as monolayer of cells on the scaffold surface with high magnification. The rate of cellular spreading corresponds with the adhesion of the cells to the surface. When the cells are rounded and small-sized, the adhesion to the material is weak. On the other hand, cells largely spread indicate satisfactory cell adhesion to the material. Evaluation of specific cellular shape requires the knowledge of normal cell morphology. After the cells adhere to materials, the proliferation rate could be estimated by the area occupied by these cells. Nevertheless, quantification is not usually possible due to the high magnifications used in SEM. Representative pictures are presented in order to depict the colonization of tested scaffolds.

Ideal scaffolds support cell adhesion within hours after seeding. When cells create strong adhesion, the process of their proliferation could start and confluent layer of the cells is created during the cultivation time. This process is detected by increasing metabolic activity of the cells measured by MTT test after certain period of incubation. Cell morphology and spreading is also observed by microscopic techniques that could be in agreement with MTT test results (more cells are observed with higher metabolic activity measured by MTT).

Hemocompatibility assessment

Thrombogenic potential of materials is a challenging question that has been investigated by other authors. The main function of platelets is the formation of mechanical plugs during the normal response to the vessel wall injury. Platelets bind to extracellular matrix components such as fibrin, collagen and laminin, to microorganisms, macrophages and surfaces of prosthetic devices. When platelets adhere to such structures, they change their regular discoid shape to irregular one with extrusion of many pseudopodia. Therefore the change of platelet morphology is a useful tool in evaluating of thrombogenicity of materials. The outermost layer of platelets is made from glycoproteins (GP) and contains various receptors. For example GP Ia/IIa facilitates adhesion to collagen, GP Ib allows adhesion to von Willebrand factor and the vascular subendothelial components and GP IIb/IIIa facilitates platelet-platelet interactions by fibrinogen ligands. Another surface receptor P-selectin is capable of binding to neutrophils and monocytes. P-selectin is located in resting platelets in the membrane of the alpha granules but after the platelets are activated, P-selectin is expressed also on plasma membrane. Platelet activation that follows their adhesion is accompanied by degranulation of platelet granules and releasing of proteins such as platelet factor 4, platelet derived growth factor, fibrinogen, von Willebrand factor, fibrinogen and other clotting factors that accelerate the activation of other platelets and contribute to platelet aggregation *(Kamath, 2001)*. Platelet adhesion and change in shape are the initial steps towards the development of thrombus therefore the assessment of thrombogenic potential of tested materials is based on evaluation of platelet shape (qualitative data) and measurement of their metabolic activity by MTT test that enables quantification.

Platelets are fragments of cytoplasm derived from the megakaryocytes of the bone marrow. Their life span is about 8-10 days. Resting platelets have discoid shape with smooth, rippled surface of the size between 1 and 2 μm *(Kamath, 2001)*. Incubation of materials with thrombocytes lead to decreasing of metabolic activity since platelets do not contain a nucleus therefore they are not able to proliferate such as cell lines used in previous experiments. The highest metabolic activity is detected immediately after the interaction with the materials followed by decreasing of metabolic activity reflecting their physiological life time. Higher absorbance measured by MTT test after 2 hours of incubation with materials and the rate of their decreasing metabolic activity indicates higher thrombogenic potential of materials.

2.2 Small diameter vascular grafts

Tissue engineering strategies has some common features that have already been described. When designing scaffolds for certain application, specific aspects have to be considered. Since tissue engineering rises from the idea of mimicking native extracellular matrix, composition and structure of vessel wall components is depicted in figure 3. Vascular tissue engineering brings many issues that have to be overcome since there is no commercially available vascular graft that will fulfill all requirements summarized in further sections. History of blood vessel substitutes is described and the most common cause of failure of currently used grafts is outlined. One of a promising modification of vascular graft is the enrichment of nitric oxide donors that have many beneficial effects on cardiovascular system. The background of nitric oxide is also a part of further chapters in theoretical as well as in experimental section.

2.2.1 Structure of native blood vessels

The native artery is an extremely complex multi layered tissue composed of a number of different extracellular matrix proteins and cell types as depicted in figure 3. In order to withstand the high flow rate, high pressure and pulsating nature of blood flow, an artery is composed of three distinct layers called the *tunica intima, tunica media* and *tunica adventitia*. Each of these layers has a different composition and plays a different physiological role *(Sell, 2009)***.** The intimal layer of the blood vessels

consists of a single layer of endothelial cells (ECs) lining the vessels internal surface *(Nerem, 2001)***.** This layer is in contact with the bloodstream therefore it provides a critical barrier to platelet activation. Intact endothelium is the only one known non-thrombogenic surface. Endothelial cells prevent thrombocytes from contact with prothrombotic elements such as collagen in the subendothelium. The endothelial cell reacts with physical and chemical stimuli within the circulation and regulates hemostasis, vasomotor tone, and immune and inflammatory responses. In addition, the endothelial cell is crucial in angiogenesis and vasculogenesis *(Sumpio, 2002)*. ECs are attached to a laminin-rich basement membrane. The ECM in *tunica intima* provides critical support for vascular endothelium and it influences ECs migration, invasion, survival and organization. ECs are attached to ECM by cell-surface integrins. Cell adhesion can be supported by interstitial fibrin and collagen I *(Davis, 2005)*.

The *tunica media* begins in the *internal elastic lamina* that separates the *tunica intima* and the *tunica media*. The middle layer is composed of smooth muscle cells (SMCs) with many functions including vasoconstriction and dilatation, synthesis of various types of collagen, elastin, and proteoglycans and vessel remodeling after injury *(Rensen, 2007).* The *tunica media* is organized into concentric lamellar units composed of elastic fibers and SMCs, separated by an interlamellar matrix containing collagens, proteoglycans and glycoproteins. Collagen fibers provide tensile stiffness whereas elastin gives the vessel the required elastic properties. Compressibility of the vessel and the deformation against pulsating blood flow are provided by proteoglycans and glycoproteins. *In vitro* studies confirm the involvement of ECM–SMC signaling in establishing and maintaining the mature tubular structure *(Brooke, 2003).* The composition of ECM in the *tunica media* regulates the activity and phenotype of SMCs *(Patel, 2006)*.

The outermost layer *tunica adventitia* extends beyond the *external elastic lamina* and is composed mainly of randomly arranged collagen fibers and fibroblasts *(Kolacna, 2007).* This outermost layer is nourished by *vasa vasorum*, thin capillaries providing an important source of nutrition *(Williams, 2006).*

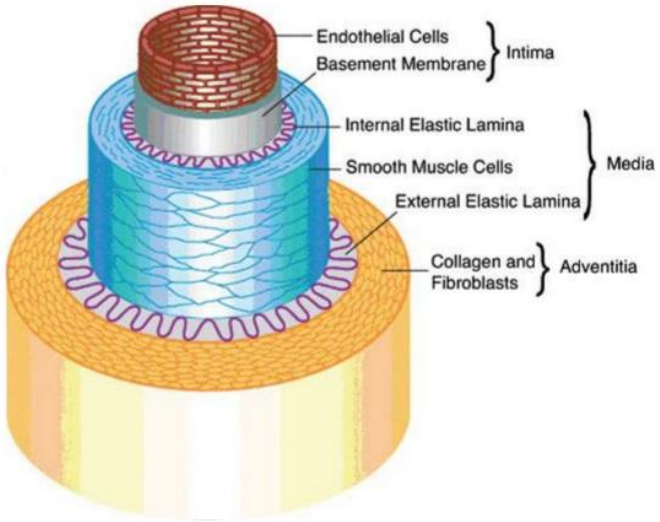

Figure 3: The structure of native blood vessel composed of 3 distinct layers: tunica intima, tunica media and tunica adventitia (Sarkar, 2006).

2.2.2 Requirements for small diameter blood vessel replacement

The issue of small diameter blood vessel replacement remains a major challenge yet to be overcome in the production of appropriate vascular grafts. Specific properties of such grafts have to be maintained not only in time of surgery but also in a long term after the implantation. The production of vascular grafts has to be cost effective, environmental friendly with consistent quality. The final product has to withstand selected sterilization technique. The graft should be available in different sizes, various inner diameters, wall thickness and length. During implantation, the graft has to be easily sutured and provided initial mechanical strength to withstand blood pressure with no bleeding. An ideal vascular graft must meet an extended list of criteria including the strength and elasticity of the vessel wall, biocompatibility, blood compatibility and biostability in the long term *(Greenwald, 2000; Arrigoni, 2006).* It also needs to adapt to the hemodynamic conditions. Vascular graft should enable the regeneration of the vessel wall therefore inert materials are replaced by biodegradable ones. The materials have to be non-immunogenic and non-toxic *(Thomas, 2003; Kakisis, 2005).*

One of the important properties that influenced cellular colonization of vascular grafts is surface wettability. It was reported that commercially used expanded polytetrafluorethylene (ePTFE) and polyethylene terephtalate (PET) vascular grafts work well for large diameter blood vessel substitutes but they fail in small diameter applications because of their hydrophobicity *(Jardine, 2005).* In general, synthetic

polymers are too hydrophobic (contact angle > 100°). Cell adhesion to the biomaterial is mediated by molecules of ECM like fibronectin, vitronectin, collagen, laminin, and fibrin. These adhesion molecules are spontaneously adsorbed from the body fluids or culture media or are deposited on the cells by themselves. If the material is too hydrophobic, these molecules are adsorbed in a denaturated or rigid form. Their geometrical conformation does not allow cells to bind to the surface because of specific sites like RGD-peptides are less accessible to integrins *(Bacakova, 2011).*

Increasing of surface wettability does not influence only cell adhesion; hydrophilic surface may also confer thromboresistance of the vascular graft. But the thrombogenicity depends more on type of material rather than on surface properties *(Kallmes, 1997)*. One of the ways of reducing hydrophobicity of materials is the covalent linkage of hydrophilic groups, for examples polyethylene glycol *(Karrer, 2005)* or polyethylene oxide *(Bergstrom, 1994).* Another method based on plasma treatment was used by *Valence et al.* Vascular grafts made from PCL underwent a cold air plasma treatment that lead to significantly increased hydrophilicity of the surface. The scaffolds were tested *in vitro* using smooth muscle cells showing more spread morphology of the cells compared to small, rounded cells cultured on the scaffolds without the plasma modification. After implantation into vascular position, the plasma treated scaffold became more infiltrated with the cells than non-treated one suggesting that increased hydrophilicity could accelerate tissue regeneration *(Valence, 2013).*

Other properties that have to be thoroughly considered are mechanical qualities. Vascular grafts should match those of natural blood vessels but currently used commercial grafts made from PET or PTFE have much stronger mechanical properties. Abdominal aorta in longitudinal direction possess tensile strength of 1,47 MPa compared to commercial graft Teflon TF-208 having tensile strength of 85,2 MPa (*How, 1992).*

After implantation, the graft will provoke an *in vivo* response known as graft healing that could be either transanastomotic or transmural. Transanastomotic healing takes place from adjacent native arteries through newly-emerged anastomosis between implanted graft and arteries as depicted in figure 4. Smooth muscle cells in the media of native artery start to proliferate and migrate into the *intima* and to the graft. Amongst relevant factors playing a crucial role in anastomotic healing belongs porosity of the graft and type of animal model. There is a remarkable difference between human and experimental models in terms of endothelialization rate

(*Beyuidenhout, 2004).* In humans, the endothelialization occurs only closely to the anastomosis (*Sauvage, 1971).* Even after years of implantation, the transanastomotic endothelialization did not exceed 1-2 cm *(Berger, 1972).* Transmural healing occurs when long vascular grafts are implanted such as femoropopliteal bypasses that could be up to 60 cm long where transanastomotic endothelialization in humans is limited. Transmural healing also depends on graft structure and proliferative and migratory capacity of the host cells. The newly formed tissue should consist of smooth muscle cells secreting its own extracellular matrix and development of *vasa vasorum* that will nourish the newly restored vessel (*Beyuidenhout, 2004).*

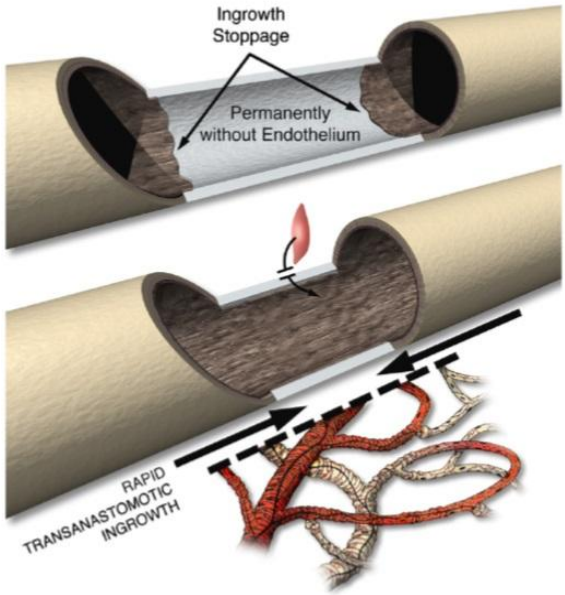

Figure 4: Schematic picture of the difference in transanastomotic endothelialization in animal models (bottom) and in humans (top) where permanently non-endothelialized graft section are present. (Zilla, 2007).

Spontaneous endothelialization of vascular graft lumen occurs by direct migration from the anastomotic edge, transmural migration and by cell transformation from endothelial progenitor cells (EPC). Despite the fact that endothelialization happens in animal models such as rats, rabbits and pigs *(Pektok 2008; Zheng, 2012; Mrowczynski, 2014)* there are difficulties in achieving spontaneous endothelialization in humans. In case of PTFE there is a little evidence of any endothelialization *(Guidon, 1993)* whereas knitted Dacron enables the formation of a patchy endothelial layer after implantation in humans *(Shi, 1999). Pektok et al.* compared healing characteristics

of vascular grafts made from electrospun PCL having average fiber diameter of 1,9 μm and commercially available ePTFE after implantation in rats. Electrospun PCL conduit showed faster endothelialization, better cellular infiltration accompanied by neovascularization after 6 months of implantation. However, the authors comment on the necessity of testing these grafts in long term studies using higher animal models *(Pektok, 2008).*

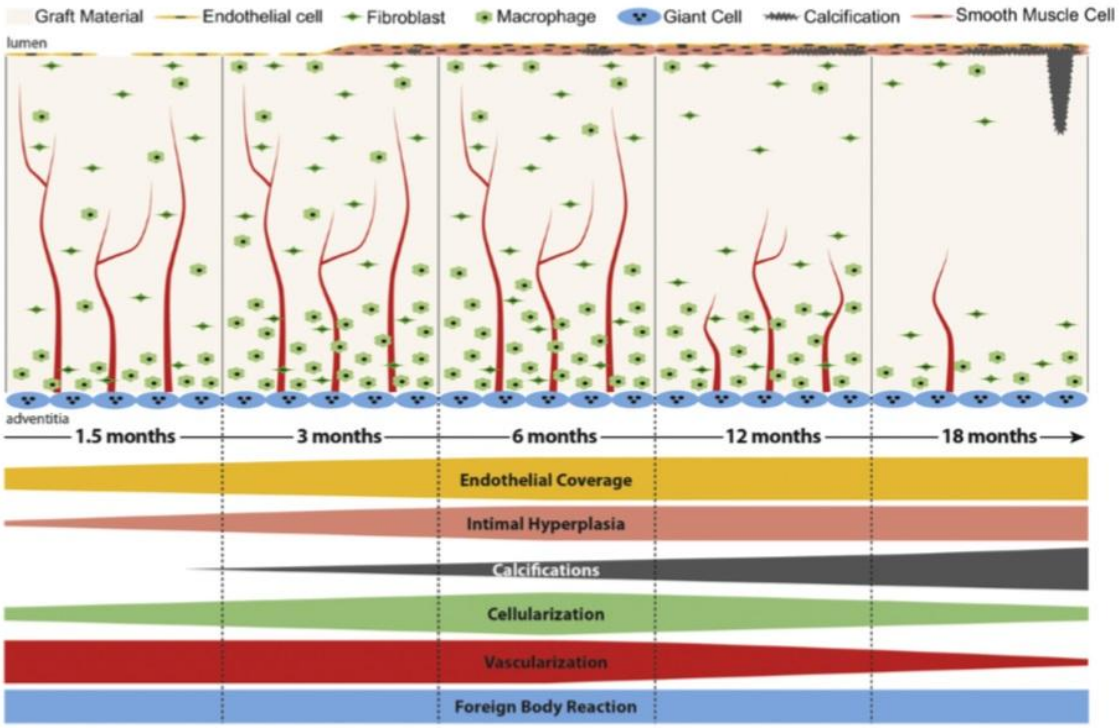

Figure 5: Prediction of vascular wall regeneration following implantation of synthetic vascular graft (Wang, 2014).

There is a gap of knowledge in tissue remodeling process following the implantation of vascular graft *in vivo.* Proposed remodeling process is described by Wang et al. in figure 5. Macrophages are the first cells infiltrating the graft. Macrophages could express either phenotype M1 (inflammatory) or phenotype M2 (anti-inflammatory, immunomodulative) that is responsible for successful tissue remodeling process. Inner surface of the graft is being endothelialized within months depending on animal model. Smooth muscle cells will penetrate the graft ensuring the physiological function of implanted graft. In the adventitial site, *vasa vasorum* will develop and nourish the newly created vessel. Some adverse effects such as calcification or foreign body response can be observed *(Wang, 2014).* The explanation of early cell-material reaction as well as long-term outcomes have to be

done in order to create a synthetic small caliber graft, resistant to thrombosis and biocompatible, that would have some advantages over traditional autologous grafts – an unlimited availability and consistent quality and patency.

2.2.3 History of blood vessel tissue engineering

The idea of small diameter blood vessel tissue engineering came from Weinberg and Bell, 1986. Their group reported the first tissue-engineered blood vessel created from collagen gels combined with bovine endothelial cells, fibroblasts and smooth muscle cells *(Weinberg, 1986)*. In 1998, L'Hereux et al. created a tissue-engineered blood vessel without supporting material. Human vascular smooth muscle cells and fibroblasts separately produced cohesive cellular sheets. By wrapping these two sheets, a tubular scaffold was created and its lumen was seeded with endothelial cells. This graft had high burst strength, positive surgical handling and a functional endothelium *(L'Hereux, 1998)*. Niklason et al. described the first successful implantation of tissue-engineered vascular graft. Smooth muscle cells were seeded on a polyglycolic acid mesh and cultivated in a bioreactor. After 8 weeks, a lumen of the vessel was seeded with endothelial cells. This graft was implanted to mini pigs showing patency up to 4 weeks *(Niklason, 1999)*. Watanabe et al. introduced a biodegradable polymer scaffold seeded with mixed cells obtained from femoral veins. After 1 week of in vitro cultivation, the scaffolds were implanted into dogs. After 6 months, the tissue-engineered vessel contained a sufficient amount of ECM without occlusion or aneurysm formation. In addition, an endothelial lining was present in the luminal surface *(Watanabe, 2001)*. The first clinical trial of a tissue-engineered blood vessel in a human was carried out by Shin'oka et al, 2001. Cells were isolated from a peripheral vein of a 4-year-old patient. A biodegradable polymer scaffold was seeded with cells and after maturation the graft replaced an occluded pulmonary artery. The patient showed no evidence of either occlusion or aneurysm change after 7 months *(Shin'oka, 2001)*.

The above mentioned studies have the disadvantage of long term vessel maturation *in vitro*. To overcome the issue of endothelial cell isolation and proliferation in *in vitro* conditions, the approach of tissue engineering *in situ* seems to be more suitable for vascular replacement. If the structure of the scaffold would mimic the native extracellular matrix, cells will infiltrate the graft and the process called remodeling will

regenerate vessel as depicted previously in figure 5. There are discussions whether this approach could be used in humans despite there are many successful studies in rats *(Notellet, 2009; Valence, 2012; Valence, 2013; Wang, 2014),* rabbits *(Tillman, 2009; Zheng, 2012)* and pigs *(Mrowczynski 2014).* Zilla et al. summarized wrong attempts in *in vivo* testing of vascular grafts in terms of inappropriate animal models used or different place of suturing in the body. The studies using inappropriate locations of the graft as well as animal with different rate of endothelialization lead to misrepresented results when the grafts were transferred to human clinical praxis *(Zilla, 2007).*

2.2.4 Currently used vascular grafts

Vascular grafts could be classified as small caliber diameter (< 6 mm), medium size (6-8 mm) and large caliber diameter (> 8 mm) *(Chlupac, 2009).* The latter are successfully used in clinical praxis for years but there is still a pressing need to develop small diameter vascular grafts that can replace failed small diameter arteries when there is an absence of endogenous grafting material. Vascular grafts could be classified into two groups based on their material composition - biological and synthetic. ***Biological grafts*** are usually the first choice in clinical use. Autologous veins (f.e. saphenous, jugular) are preferred for bypass grafting of arteries (coronary, carotid, renal etc.). However, the usage of veins in arterial circulation could cause deterioration of local hemodynamic forces. Autologous arteries such as internal mammary artery could serve as a biological graft as well but they are not readily available as autologous veins (*Beyuidenhout, 2004)*. Coronary artery bypass grafting has constantly been the mainstay of surgical revascularization of coronary artery disease. The most widely used conduits are either autologous internal thoracic arteries, saphenous veins or radial arteries. These grafts provide mechanical stability and natural antithrombogenicity *(Angelini, 1989; Cameron, 1996).* However, increase in the indications for the surgical revascularization, elderly patients' population and increased number of re-operations could be limiting for the availability of suitable autologous grafts. It is the problem of approximately 25% of all patients indicated to a coronary bypass *(Hasegawa, 2005).* A relatively significant group of patients have no vein grafts suitable for a coronary bypass owing to pre-existing vascular disease, vein stripping or vein harvesting *(Wang, 2007).* Unavailability of the autologous grafts could be an invitation for the use

of prosthetic conduits.

Synthetic grafts used in clinical praxis are represented by biostable grafts made from expanded polytetrafluorethylene and polyethylene terephtalate. Biostable materials are permanently implanted into the body since it has been recognized that no material is completely inert upon implantation (*Beyuidenhout, 2004).* In the last years, new biodegradable materials are under development amongst which polyurethane (PUR) and biodegradable polyesters has been successfully investigated. The advantages, disadvantages and healing characteristics of clinically used synthetic vascular grafts are summarized in table 1.

Table 1: Synthetic vascular grafts in clinical use (Chlupac, 2009).

Synthetic vascular grafts						
	PET (Dacron, Terylen)		**ePTFE (Teflon, Gore-Tex)**		**Polyurethane**	
	Woven	**Knitted**	**Low-porosity**	**High porosity**	**Fibrillar**	**Foamy**
Advan-tages	Better stability, lower permeability and less bleading	Greater porosity, tissue ingrowth and radial distensibility	Biostability, no dilation over time	Biostability, better cell ingrowth	Compliance, good hemo- and biocompatibility, less thrombogenicity	
Disad-vantages	Reduced compliance and tissue incorporation, low porosity, fraying at edges, infection risk	Dilation over time, infection risk	Stitch bleeding, limited incorporation, infection risk	Late neointimal desquamation, infection risk	Biodegradation in first generation, infection risk, carcinogenic?	
Healing	Inner fibrinous capsule, outer collagenous capsule, scarce endothelial islands	Fibrin luminal coverage, very sporadic endothelium, transanasto-motic endotheliali-zation in animals	Luminal fibrin and platelet carpet, connective tissue capsule with foreign body giant cells, no transmural tissue ingrowth	Macrophages and polymorphonu clear invasion, capillary sprouting, fibroblast migration, certain angiogenesis, thicker neointima, endothelializat ion in animals	Thin inner layer, outside foreign body cells, limited ingrowth	Better ingrowth with bigger pores

Polyethylene terephtalate is melt-spun and drawn into highly crystalline filaments having the diameter of 10-20 μm with high tensile strength. These filaments are bundled into multifilament yarns and then woven or knitted to form of tubular or bifurcated grafts. Woven prostheses possess poor compliance with limited elongation. Knitted PET grafts have good dimensional stability and suturing properties. Both types of PET grafts are often crimped to improve strength in radial direction and to increase elongation (*Beyuidenhout, 2004*). Another common modification of PET grafts is sealing with collagen, albumin or gelatin to eliminate blood permeability (*von Oppel, 1998).* Vascular grafts made from PET are used for large-diameter vascular graft applications with high flow such as aortic replacement.

Polytetrafluoroethylene is an inert fluorocarbon polymer with high degree of crystallinity. Expanded PTFE grafts are produced by extrusion and subsequent sintering. This non-biodegradable polymer is widely used for lower-limb bypass grafts with the inner diameter between 7 and 9 mm. These grafts are rigid in comparison with the elasticity of the host artery (*Tai, 2000; Salacinski, 2001)*.

Vascular grafts made from *polyurethanes* possess biocompatibility and elastomeric properties. The structure could be either fibrillar or foam-type. Although many grafts made from polyurethane have been developed using different fabrication techniques (f.e. weaving, knitting, electrostatic spinning, melt spinning), they have not been widely accepted for clinical use up to now *(Beyuidenhout, 2004).*

Biodegradable polyesters, such as poly-ε-caprolactone or poly-L-lactic acid have been successfully used in research for tissue engineering applications, including vascular replacement *(Vaz, 2005; Notellet, 2009; Dong, 2008; He, 2008; Wu, 2010; Hu, 2012; Huang, 2012).* The advantage of biodegradable polymers instead of inert one has already been mentioned in the paragraph 2.1.1. Therefore these type of materials were used in experimental part of the thesis - namely PCL and copolymer composed of polylactic acid and polycaprolactone (PLC). Polymer PCL has been reported by my colleagues for different tissue engineering applications such as bone tissue engineering *(Rampichova, 2013; Erben, 2015).* Based on literature, electrospun vascular grafts made from PCL were reported by several groups to be a promising candidate for vascular replacement *(Pektok, 2008; Notellet, 2009)*. PCL possesses intrinsically slow degradation rate, desirable mechanical properties, and general biocompatibility *(Woodruff, 2010).* However, insufficient regeneration of the vascular wall as well as

graft calcification was reported by Valence et al. *(2012).* Therefore novel material besides PCL was tested in order to improve function of such grafts.

Copolymer PLC composed of polylactic acid and polycaprolactone in different ratios has also been reported as a good candidate for vascular graft replacement. Mo et al. studied electrospinning conditions of copolymer PLLA and PCL in ration 75/25 proving its biocompatibility with endothelial cells and smooth muscle cells *in vitro (Mo, 2004)*. Dong et al. tested copolymer PLLA and PCL in ration 70/30 with endothelial cells for 105 days proving its long-term compatibility with the endothelial cells that is a crucial task for vascular graft function after implantation *(Dong, 2008).* He et al. rotationally seeded endothelial cells in the lumen of the graft made from copolymer PLLA and PCL in ration 70/30. After 10 days endothelial cells covered the lumen of the prepared graft during culturing *in vitro*. This construct was subsequently implanted in the rabbit showing patency for 7 weeks *(He, 2008).*

The final vascular graft could be designed as multi layered tube that will match the properties of native tissues. Different polymers, fabrication techniques as well as drug delivery systems could be employed in order to produce ideal vascular graft. Such approach has been published for example by Han et al. The scaffold was prepared by electrospinning of poly(ethylene glycol)-*b*-poly(L-lactide-co-ε-caprolactone) (PELCL), copolymer of polyglycolic acid and polylactic acid (PLGA) and PCL to ensure sufficient mechanical properties. Delivery of vascular endothelial growth factor (VEGF) and platelet-derived growth factor (PDGF) incorporated into the inner and middle layer of the graft supported new blood vessel formation and maturation with better results when compared *in vivo* as a replacement of rabbit common carotid artery for 8 weeks *(Han, 2013).* Similar study using double layered electrospun scaffold was performed by Zhang et al. The combination of gelatin, elastin, PCL and poliglecapron (PGC) was used to promote endothelialization. Human aortic endothelial cells favored the biomechanics and biochemistry of such scaffold for at least 11 days *(Zhang, 2010).* A three layered electrospun scaffold made from PCL, collagen and elastin was described by McClure et al. The combination of polymers led to construction of vascular graft with distinct properties for each layer such as fiber diameter, suture retention and compliance. Mathematical modeling was implemented in order to achieve the best mechanical combination of materials and to help the prediction of future graft optimization *(McClure, 2010).* Fiber orientation in vascular graft was studied

by Wu et al. through the combination of regulating the electric field and the rotation of collector leading to tubular scaffolds with different nanofiber orientation (circumferential, axial and its combination). They stated that such a complex nanofiber orientation can be constructed to achieve desirable macroscopic mechanical property and cell responses along specific directions *(Wu, 2010).*

2.2.5 Failure of small diameter vascular grafts

Biological vascular grafts failed mostly because of degenerative changes. These small-diameter vascular grafts proved excellent anti-thrombogenicity in *in vitro* studies, but no long term patency have been reported in coronary artery surgery. A human umbilical vein graft (Biograft, Meadox Medicals, USA; 4 mm diameter) demonstrated angiographic graft patency rates of 46 % within 3-13 months *(Silver, 1982).* A treated bovine IMA graft (Biocor BIMA Biograft, Biocor laboratory, 4 and 5 mm of diameter) was implanted in the coronary artery position of 20 patients *(Vrandecic, 1987).* Graft patency was confirmed in two patients at 6 months. A dialdehyde starch-treated bovine artery grafts (Bioflow, Bio-Vascular Inc., USA) have been used over the past few years *(Abbate, 1988; Suma, 1991).* The only one long-term follow-up clinical report was available and it reported graft patency rates of 16 % within 3-23 months *(Mitchell, 1993).* These biological grafts have a tendency to undergo degenerative changes and dilatation *(Tomizawa, 1994).*

The main ***synthetic graft*** materials are successfully used in large diameter blood replacement. However, their usage in small diameter blood vessel replacement is impossible due to the early occlusion after implantation. The major causes of graft failure have been thrombosis and intimal hyperplasia *(Esquivel, 1986).* After implantation, plasma proteins immediately adsorb to the lumen of vascular graft presenting binding sites for integrin receptors found on platelets. Apart from that fact, platelets adhere to positively charged surfaces due to their own negative charge. Thrombocytes also preferentially attach to hydrophilic surfaces. Therefore negatively charged hydrophilic materials could contribute to prevent acute thrombosis. Endothelial cell lining is known to provide a constantly tuned non-thrombogenic environment. There are numerous biochemical pathways by which endothelial cells modulate plasma protein and platelet adhesion. Basement membrane possesses moderate thrombogenicity whereas collagen in the subendothelial tissue is highly thrombogenic *(Sarkar, 2006).*

In small diameter vessel, the blood flow is lower than in vessels with larger diameter that contributes to thrombogenic potential as well together with hemodynamic changes near anastomosis *(Kapadia, 2008).*

Another complication is the development of intimal hyperplasia that is characterized by increased smooth muscle cell migration, proliferation, and synthetic activity in the inner region of a vascular graft, leading to progressive intimal wall thickening and eventual stenosis *(Lemson, 2000; Ducasse, 2003).*

The poor mechanical features and the lack of endothelial cell lining of the graft lumen are the crucial factors causing the poor patency of ePTFE vascular grafts *(Berger, 1972).* Grafts made from PET have shown poor patency rates when used in small diameter sizes or in low-flow locations *(Xue, 2003; Soldani, 2010).* Polyurethanes have been investigated as an alternative graft material more compliant than PET and PTFE. Thus, their mechanical and flow parameters are better matched to those of the native vasculature. Early attempts using polyurethane led to high rates of aneurysm formation and thrombosis compared with conventional prosthetic grafts *(Brothers, 1990).* However, some modified forms of polyurethane grafts based on nanocomposite polymers are more resistant to biodegradation *(Giudiceandrea, 1998; Seifalian, 2003).*

Synthetic materials available nowadays have not been successful in coronary artery bypass so far because of their poor long-term patency rates. Attempts to improve synthetic grafts have included embedding them with anti-thrombotic drugs, seeding with endothelial cells or developing new biomaterials. These grafts had better results than standard prostheses, but it was marginal. Heparin was rapidly lost to plasma *(Engbers, 1991).* The other grafts have been tested with dipyridamole, hirudin, tissue factor pathway inhibitor or non-thrombogenic phospholipid polymer. The surface texture of prostheses has also been altered in an attempt to increase patency and promote endothelialization *(Hoenig, 2005).*

2.2.6 Modification of vascular grafts by nitric oxide releasing substances

Modification of vascular grafts by nitric oxide (NO) releasing substances improves the biocompatibility of vascular grafts by stimulation of endothelial cell proliferation and inhibition of platelet aggregation and adhesion, inhibition of vascular smooth muscle cell proliferation and migration and leukocyte chemotaxis and activation

(Ahanchi, 2001). Therefore special attention was focused on this type of modification that is closely connected to the third experimental chapter.

The discovery of the physiological and pathophysiological roles of nitric oxide (NO) began in 1980s. In 1992, NO was called the molecule of the year by the editors of the journal *Science*. Later on in 1998, R.F. Furchgott, L.J. Ignarro and F. Murad were awarded the Nobel Prize in physiology and medicine for their contribution to elucidating the role of NO in the functions of living organisms *(Wang, 2005)*.

NO is a diatomic free radical, known as the endothelium-derived relaxing factor (EDRF). Endothelial cells produce NO that has many beneficial effects on cardiovascular system. NO is thromboresistant due to the inhibition of platelet aggregation, adhesion and activation *(Radomski, 1987)*. The affects of NO differs for certain cell types in blood vessels. Whereas NO stimulates endothelial cell proliferation *(Ziche, 1994)* and prevents endothelial cells apoptosis *(Tzeng, 1997)*, it also inhibits smooth muscle cells growth and migration *(Garg, 1989; Mooradian, 1995)*. NO possess anti-inflammatory properties due to the inhibition of leukocyte adhesion and migration *(Lefer, 1997)*. The affects of NO are summarized in figure 6.

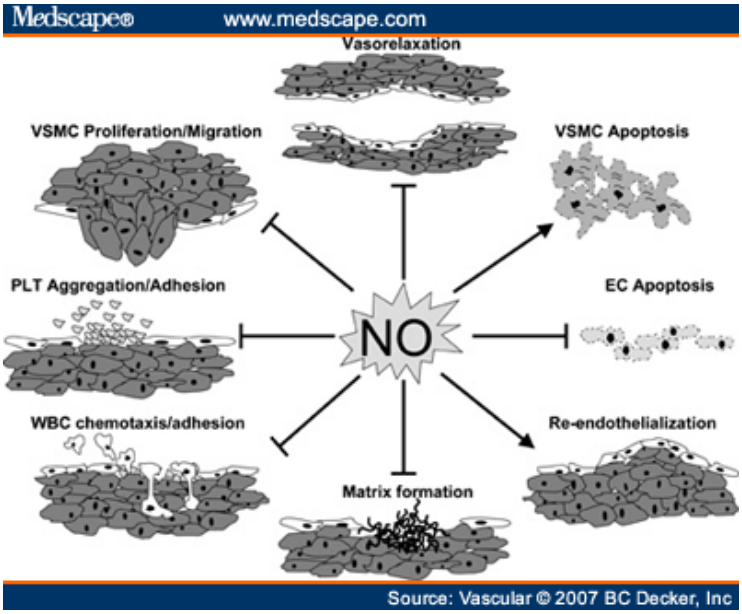

Figure 6: Beneficial properties of nitric oxide (NO) in the vasculature. EC = endothelial cell; PLT = platelet; VSMC = vascular smooth muscle cell; WBC = white blood cell. The symbol of an arrow symbolizes the acceleration of action supported by NO whereas the symbol of a segment line means the suppression/inhibition of function by NO (Popowich, 2007).

NO has limited solubility in water (2-3 mM), and it is unstable in the presence of various oxidants. This makes it difficult to introduce into biological systems in a controlled manner. Consequently, the development of chemical agents that release NO is important *(Wang, 2005)*. One promising group of NO donors is S-nitrosothiols (RSNO), which can be readily incorporated into a polymeric vascular graft. S-Nitrosothiols are present in biological systems, where they serve as a reservoir and transporter of NO *(Jourd'heuil, 2000)*. S-Nitroso-N-acetyl-D-penicillamine (SNAP) is a compound from the group of S-nitrosothiol that has been used in NO-releasing polymers having a capacity for low and controllable NO release *(Gierke, 2011)*. The S-NO bond can be cleaved through several mechanisms. These include the reduction of Cu^{2+} to Cu^{+} that reacts with RSNO to release NO, forming a sulfhydryl anion product and regenerating Cu^{2+} *(Dicks, 1996)*. Physiologically prevalent ascorbate ions are sufficient reducing agents to generate Cu^{+} from Cu^{2+}. Another mechanism of NO release is homolytic cleavage of the S-NO bond by light *(Frost, 2005)*. Therefore, the level of NO release *in vivo* is highly dependent on the presence of Cu^{2+} and ascorbic acid when using S-nitrosothiols. High levels of ascorbic acid (millimolar concentration) are found in cells such as leucocytes and tissues whereas in extracellular fluids such as plasma the levels of ascorbic acid are low (micromolar concentration). The total body content of ascorbic acid ranges between 300 mg to about 2 g and is strongly dependent on people life style *(Jacob, 2002)*. The reference value of copper in adult plasma has been reported as 16,5 ± 8,6 μmol/l *(Rukgauer, 1997)*.

Incorporation of S-nitroso-N-acetylpenicillamine into a polymer was described by Brisbois et al., who showed that SNAP-doped polymers exhibited improved hemocompatibility for a wide variety of blood-contacting materials *(Brisbois, 2013)*. NO-releasing vascular grafts that incorporate diazeniumdiolates, another group of NO donors, have been described by Fleser et al. Using a polyurethane vascular graft containing the NO donor dialkylhexadiaminediazeniumdiolate, the graft was implanted for 21 days in a sheep arteriovenous bridge graft model. It was found to have higher patency compared to controls *(Fleser, 2004)*.

NO-eluting polymers are a promising, albeit challenging, family of implantable biomaterials. The use electrospinning technology enables entrapment of NO donors in a polymer matrix, thereby providing a protected NO reservoir and making long-term release possible *(Koh, 2013; Chen, 2014)* Delivery of NO at physiological levels is crucial for device efficacy. Endothelial cells are believed to produce NO surface fluxes

of 50–400 pmol cm^{-2} min^{-1} *(Vaughn, 1998)*. An ideal vascular graft should produce an NO flux at physiological levels for several months. This promises to mitigate harmful inflammatory responses and simultaneously encourage cellular infiltration, re-endothelialization, and tissue regeneration. There has not been a NO-releasing compound or incorporated polymeric material that would meet these requirements. For instance, Hetrick et al. introduced NO-releasing implants containing diazeniumdiolates. However, 50% of the total NO was released after 5 h and more than 99% of the available donor was exhausted after 72 h *(Hetrick, 2007)*. Nichols *et al.* stated in their work the need for materials with NO release profiles exceeding 2 weeks in duration *(Nichols, 2012)*. Koh et al. used electrospun fibers with entrapped NO-releasing silica nanoparticles. Their electrospun polyurethane nanofibers exhibited a wide range of NO release totals with release durations up to 2 weeks *(Koh, 2013)*.

Fabrication of biodegradable synthetic vascular grafts seems to be a promising approach to generate appropriate scaffolds in terms of morphological similarity to the native ECM, appropriate bulk and surface properties. However, limitations in the healing response of electrospun vascular grafts made from PCL were described *(Valence, 2012)*. To overcome the issues of thrombogenicity of the grafts, lack of endothelialization of the graft lumen, intimal hyperplasia development as well as inflammatory reaction, the incorporation of nitric oxide releasing substances was introduced in the chapter 5 Vascular grafts releasing nitric oxide.

3 Synthetic vascular grafts preparation and testing

The first section of experimental part is focused on production of vascular grafts made from biodegradable polyesters. The work is based on the study of native blood vessel structure that is followed by mimicking of certain structural patterns by electrospinning technique. Additional properties like surface wettability, thermal properties and mechanical behavior are investigated in relationship to the usage of these grafts in vascular tissue engineering.

3.1 Histology of native blood vessel

First of all, the composition of native blood vessel was studied. One of the tested hypothesis rises from the idea of mimicking the natural environment of tissues in order to facilitate and support regeneration. Therefore, the tissue of interest (small diameter blood vessel) was characterized histologically and its structure was mimicked in further experiments using electrospinning technique. This section was carried out in cooperation with R. Domin from Pathology Department of Liberec Regional Hospital.

To prove the hypothesis of mimicking native ECM blood vessel components, a histological investigation of the carotid artery having similar internal diameter of 6 mm was carried out. Small diameter blood vessels were obtained from Liberec Regional Hospital. The human carotid artery as a representative specimen of small diameter blood vessel was fixed in formaldehyde followed by gradual dehydration with alcohol and soaking in toluene. Samples were embedded in paraffin and 3 μm sections were prepared for histological analysis. After removal of the embedded resin, the samples were stained with: Hematoxylin eosin (H&E) (a), Van Gieson staining specific for collagen (b), acidic orcein for elastin fibers detection (c) and specific staining for reticulin fibers (d). The stained samples were placed on slides and analyzed using Nikon ECLIPSE Ti-E/B light microscope. A thin section of the embedded tissue was prepared directly on the target for further SEM analysis.

The main components of ECM such as collagen, elastin and reticulin fibers were studied as well as the arrangement of cells in the different layers as depicted in figure 7. The wall thickness of the analyzed samples varied from 400 μm to 1000 μm along

its length. The thickness of the innermost layer, *tunica intima*, is very thin having about tens of micrometers. The middle layer thickness is the most variable one having the thickness between 200 and 600 μm. The outermost layer, *tunica adventitia*, has the thickness of about hundred micrometers but its measurement is affected by the fact that the layer continuously passes to the adjacent tissues and its borders could not be accurately determined.

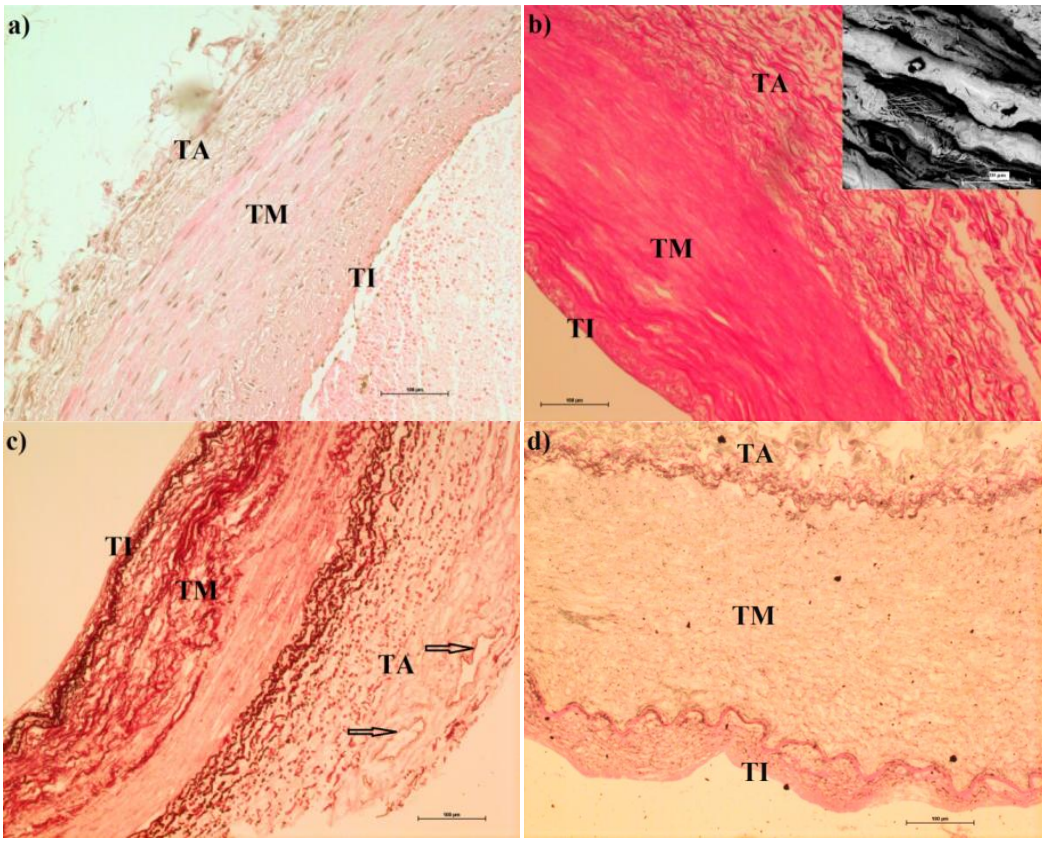

Figure 7: Hematoxylin eosin staining (a), collagen (b), elastin (c) and reticulin fibers in the tunica intima (TI), tunica media (TM) and tunica adventitia (TA). Scale bars: 100 μm. Collagen nanofibers arranged in microfibrous bundles are depicted in SEM picture intercalated in (b), scale bar: 10 μm. Black arrows in picture (c) indicate vasa vasorum in the tunica adventitia.

Hematoxylin-eosin staining depicted in figure 7a provided information about the cell arrangement in the different layers. Endothelial cells create a single layer covering the luminal surface, whereas smooth muscle cells are organized into numerous layers inside the *tunica media*. The cross section of the smooth muscle cell nuclei shows their concentric arrangement which corresponds with the organization of collagen and elastin fibers inside the middle layer. The outermost layer, *tunica adventitia*, is composed of fluffy fibers with a few fibroblasts. Collagen frequently occurs in all three

layers of native blood vessel as shown in figure 7b. The collagen nanofibers are organized in micrometer scale bundles as depicted in the top right corner of the same picture. In the figure 7c, the *vasa vasorum* can be seen in the *tunica adventitia* which nourishes the outermost layer. Elastin forms an elastic layer between the *tunica intima* and the *tunica media* called the *lamina elastica interna* (figure 7c). Elastin fibers are also present in the *tunica media* and *tunica adventitia* and give the blood vessel the desired elastic properties. Reticulin fibers depicted in figure 7d are rarely found in all three layers of native blood vessels.

The native blood vessel is composed of 2 basic components: cells and extracellular matrix that creates a functional entity. When considering an ideal biomaterial, structures closely mimicking native ECM will enable remodeling process after implantation into the body. The ideal vascular graft replacement has to (1) enable endothelialization of the lumen, (2) allow smooth muscle cells infiltration and (3) possess adequate mechanical properties. Based on these assumptions, an ideal vascular graft was designed as a double layered graft with desired properties of each layer. It has been published that nanofibers promote cellular adhesion *(Bacakova, 2011)* therefore the inner layer is intended to be a nanofibrous layer that will facilitate endothelial cell adhesion and proliferation. The thickness of the inner layer is about tens of micrometers as in native vessel. The middle layer in the native blood vessel is composed of radially oriented collagen and elastin fibers and smooth muscle cells. The layer in the thesis is designed as a microfibrous layer that will enable cellular infiltration. Nanofibers supports cell adhesion; on the other hand, their small pore sizes do not enable cellular infiltration into 3D structure. Therefore the middle layer mimicking *tunica media* within blood vessels is designed as microfibrous layer with radially oriented fibers that will have sufficient strength and allow the elongation of the graft upon implantation into the blood flow. The thickness of the layer will be about hundreds of micrometers as in native blood vessel. There could not have been changes in the wall thickness between the bypass graft and vessel wall. Therefore, the thickness will be adjusted according to specific requirements of implantation site. Finally, the outermost layer is composed of collagen fibers and fibroblast cells in the body. It is expected that this layer does not have to be mimicked because fibroblasts will infiltrate the scaffold and produce its own ECM that will help to integrate the graft to the neighboring tissues. These considerations were taken into account when designing ideal vascular graft using electrospinning of biodegradable polymers described in the following section.

The schematic design of suggested structure is depicted in figure 8 together with listed properties of inner and media layers.

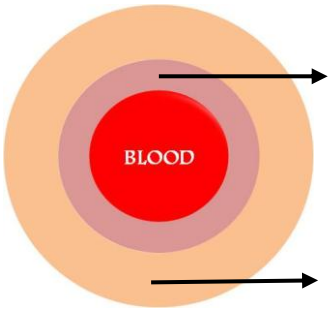

Inner layer: nanofibrous, thickness tens of micrometers, non-thrombogenic, facilitating endothelialization

Media layer: microfibrous, radially oriented fibers, thickness hundreds of micrometers, porous structure facilitating smooth muscle cell migration; elastic properties with sufficient mechanical strength

Figure 8: Structural design of double layered vascular grafts.

3.2 Vascular graft production

Biodegradable polymers were chosen for vascular graft replacement due their biocompatibility, relatively slow degradation rate and ease of processing. The main technology used for production of vascular grafts was electrospinning due to the capability of creation structure similar to native ECM. At the beginning, optimization of electrospinning parameters was done using needle electrospinning. Then, needleless electrospinning using Nanospider was carried out in order to obtain sufficient amount of samples for material characterization such as surface wettability, thermal behavior and mechanical properties. Some of the properties such as mechanical behavior and *in vitro* performance were tested in planar as well as in tubular forms of produced scaffolds. The section was done in cooperation with A. Šaman, Department of Nonwovens and Nanofibrous Materials, Faculty of Textile Engineering, Technical University of Liberec and I. Yalcin, Department of Textile Engineering, Faculty of Textile Technologies and Design, Istanbul Technical University.

3.2.1 Materials used for vascular graft fabrication

Synthetic polyesters were used for fabrication of small diameter vascular grafts, namely polycaprolactone (PCL, M_n=45,000, Sigma Aldrich) and copolymer of poly-L-lactide and polycaprolactone (PLC, 70/30, PURASORB). Polymer PCL supplied by Sigma Aldrich has the average number molecular weight of 45,000 (M_n 40,000-50,000) and polydispersity index between 1,2 and 1,8 with the mass average molecular weight

of 48,000-90,000. Copolymer PURASORB PLC 7015 is a GMP grade copolymer of L-lactide and ε-caprolactone in a 70/30 molar ratio. Content of L-lactide is determined by the supplier in the range of 67-73 mol % and caprolactone between 33 and 27 mol %. Instead of molecular weight of the polymer, inherent viscosity is determined by the supplier. The midpoint of inherent viscosity is 1,5 dl/g (ranging between 1,2 and 1,8 dl/g).

The solvent system used for electrospinning was composed of chloroform (Penta) and ethanol (Penta) 9/1 (v/v) or chloroform/ethanol/acetic acid (Penta) 8/1/1 (v/v/v). The solvent system is specified for each experiment separately. The polymeric component in the electrospinning solution ranged between 14 and 22 wt% of PCL and 2-12,5 wt% PLC. The solutions were stirring until complete dissolution and then immediately electrospun.

The behavior of PCL is well known from previous experiments done in the Department of Nonwovens and Nanofibrous Materials, Faculty of Textile Engineering, Technical University of Liberec *(Rampichova, 2013; Erben, 2015)*. Copolymer PLC has not been investigated before therefore its optimization of electrospinning solution composition and parameters was studied firstly using needle electrospinning technique.

3.2.2 Electrospinning technologies

Polymeric solutions were electrospun using different technologies in order to optimize the process itself and to produce planar as well as tubular samples of electrospun biodegradable polymers for further characterization.

Needle electrospinning using planar collector

The needle electrospinning was carried out in order to find the ideal electrospinning solution composition that was not known for novel material - copolymer PLC. The electrospinning apparatus consisted of a syringe filled with electrospinning solution, a needle, a syringe pump, a high-voltage power supply (Spellman SL 150, Direct Industry) and a flat collector covered with an aluminium foil. Needle electrospinning was performed in order to optimize polymeric concentration for further experiments. Needle diameter was 0,6 mm, used voltage 15 kV, distance between needle and collector 18 cm, feed rate 1,5 ml/h, relative humidity was kept about 50%

and temperature between 22-23°C. Copolymer PLC was dissolved in solvent system composed of chloroform/ethanol/acetic acid 8/1/1 (v/v/v) in various concentrations: 2 wt%; 3 wt%; 5 wt%; 7,5 wt%; 8 wt%; 9 wt%; 10 wt% and 12,5 wt%.

Needle electrospinning using rotating mandrel collector for fabrication of small diameter vascular grafts

Synthetic vascular grafts were prepared by electrospinning with special set up that is depicted in figure 9. Special collector in the form of rotating stainless steel mandrel was used for obtaining tubular scaffolds. Electrospinning parameters like speed of polymer dosage, voltage, distance between needle tip and collector, speed of mandrel rotation, relative humidity and temperature were recorded. The parameters are described together with resulting structures for each experiment described in further subchapters.

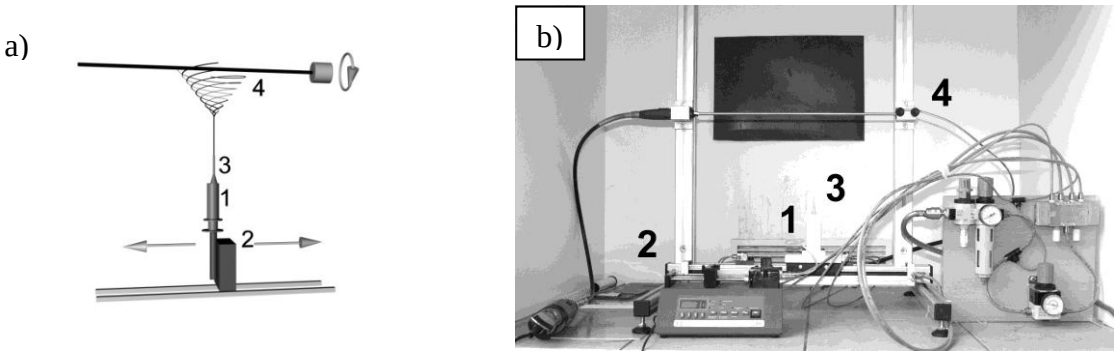

Figure 9: The schema (a) and photo (b) of electrospinning setup used for small diameter vascular grafts. Syringe pump (2) doses polymeric solution in the syringe (1) that is connected to the positively charged needle (3). Forming fibers are collected on the rotating mandrel (4).

The custom designed electrospinning apparatus consisted of a positive high-voltage power supply (Spellman SL 150, Direct Industry), a syringe pump, a plastic syringe, a hypodermic needle and a grounded stainless steel rotating mandrel (1-6 mm diameter, 20 cm length). The speed of rotation varied between 250 rpm and 15 000 rpm. Reciprocal movement of the needle spinning electrode was achieved using a linear actuator. The speed of movement was approximately 20 cm/3,5 s that corresponds with an average speed of 0,057 m/s. The length of the movement was limited to 20 cm after which was a pause of about 1,5 s in duration. Polymeric solution dosage was set to 1,5 ml/h. Time of electrospinning was adjusted to the required thickness of the graft that was measured during the fabrication process using micrometer screw gauge.

After electrospinning, the tubular scaffold was dried overnight and then removed from the mandrel by manually pushing.

Needleless electrospinning

For detailed characterization of electrospun PCL and PLC, sufficient amount of planar samples were obtained by needleless electrospinning using Nanospider^{TM} 1WS500U. Needleless electrospinning was carried out using a 0,2 mm string that was covered by polymeric solution using slots in size of 0,5 mm. The forming fibers were collected on spun bond layer that was rolled by speed of 15 mm/min. The collector was placed 17 cm above the string. The applied voltage was -10 kV and +35 kV in collector and in the string, respectively. The temperature was kept in 23°C and relative humidity between 35 and 42%.

The comparison of tested fibrous structures should reflect only polymeric composition difference between PCL and copolymer PLC, not the morphology of the layer itself. Materials with similar microfibrous structures were electrospun after a series of electrospinning solution composition optimization. PCL was dissolved in chloroform/ethanol 9/1 (v/v) in total concentration of 22 wt% to get uniform microfibrous layer having the average fiber diameter of 0,96 ± 0,76 μm. Copolymer PLC was dissolved in chloroform/ethanol/acetic acid 8/1/1 (v/v/v) at 10 wt% concentration to get similar microfibrous layer with average fiber diameter of 1,03 ± 0,71 μm. The structure of electrospun PCL and PLC is depicted in figure 10.

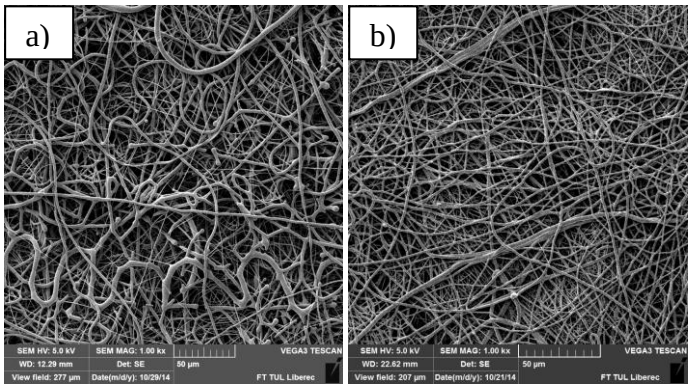

Figure 10: SEM pictures of electrospun PCL (a) and copolymer PLC (b). Scale bars 50 μm.

Characterization of electrospun layers made by needleless electrospinning

Morphology of electrospun layers was assessed by scanning electrone microscopy (SEM) and image analysis software to characterize average fiber diameter. Samples for SEM analyses were sputter coated with gold and analyzed using TESCAN Vega 3SB Easy probe (Czech Republic) or Phenom FEI scanning electrone microscope (USA). All specimens were recorded in appropriate magnification to enable image analysis of fibrous morphology. Image analysis of produced grafts was made from SEM pictures using software NIS Elements (LIM s.r.o., Czech Republic) or NIH Image J software *(Rasband, 1997-2014).* The main characteristics as fiber diameter and orientation of the fibers were measured. Fiber diameter or capsule diameter in case of beaded structure was evaluated from 100 measurements (n=100). The data were expressed as mean ± standard deviation.

Surface area of produced fibrous layers was measured by cutting the samples to the size of 1x1 cm and weighing. Ten samples were weighted and surface area was calculated in units of mg/cm^2. Thickness of the samples was measured by micrometer screw gauge. The measurements were repeated 10 times for each electrospun layer and the mean ± standard deviation was calculated. Characterization of prepared layers by needleless electrospinning is summarized in table 2 (n=10).

Table 2: Characterization of electrospun PCL and PLC

	22% PCL	**10% PLC**
Surface area [mg/cm^2]	7,65 ±1,18	3,71 ± 0,35
Thickness [μm]	289 ± 37	107 ± 8
Average fiber diameter [μm]	0,96 ± 0,76	1,03 ± 0,71

Fibers made from PCL and PLC had an average fiber diameter of about 1 μm. The morphology of electrospun fibers is comparable in these 2 polymers. Fiber diameter did not show significant difference between electrospun layers. Surface area and thickness of prepared layers was approximately twice higher in case of PCL. On the other hand, the following material analysis should reflect the effect of polymer composition or surface properties and this non-uniformity of surface area and thickness could be neglected.

3.3 Electrospinning of polycaprolactone

Since PCL is a promising material for various tissue engineering applications, the process of electrospinning and its parameters were known from previous experiments carried out in the Department of Nonwovens and Nanofibrous Materials. Therefore the optimization had started with tubular grafts production using rotating mandrel collector.

3.3.1 Optimization of polymeric concentration for vascular graft fabrication

For preparation of tubular vascular grafts made from PCL, rotating mandrel with 6 mm inner diameter was used. Electrospinning conditions were set as follows: needle diameter 0,6 mm, the distance between needle tip and collector 20 cm, speed of polymer delivery 2 ml/h, voltage 7,5 kV, polymer concentration 14 wt%, 16 wt%, 18 wt%, 20 wt%, 22 wt%, solvent system chloroform/ethanol 9/1 (v/v). In the pictures below (figure 11), morphology of electrospun PCL in different concentration is depicted.

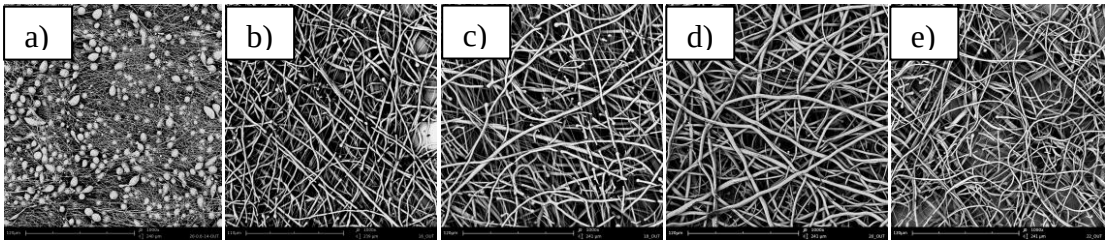

Figure 11: SEM pictures of different concentration of PCL electrospun on rotating mandrel with inner diameter of 6 mm: 14 wt % (a), 16 wt % (b), 18 wt % (c), 20 wt % (d) and 22 wt % (e). Scale bars 120 µm.

The lowest polymer concentration (14 wt %) wasn't sufficient for obtaining fibrous structure. A lot of beads are present within the structure together with thin fibers. Concentration of PCL between 16 and 22 wt % led to fibers having around more than 1 µm in diameter as shown in figure 12 where mean fiber diameter and its dependence on polymeric concentration is shown.

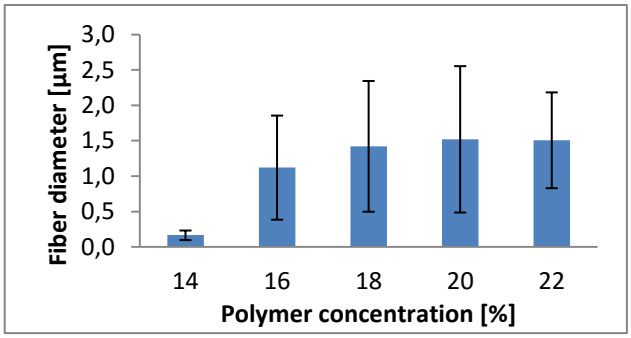

Figure 12: The function of polymer concentration and mean fiber diameter.

Further study of fiber morphology showed that there were two types of fibers present within the structure - thinner one having the diameter in nanoscale and thicker with diameter about 2 µm. The fiber diameter spectrum is depicted in figure 13 having two peaks corresponding to the statement of nano- and micro- composite structure. This structure is able to provide higher mechanical strength by microfibers as well as binding sites in nanoscale for cell attachment.

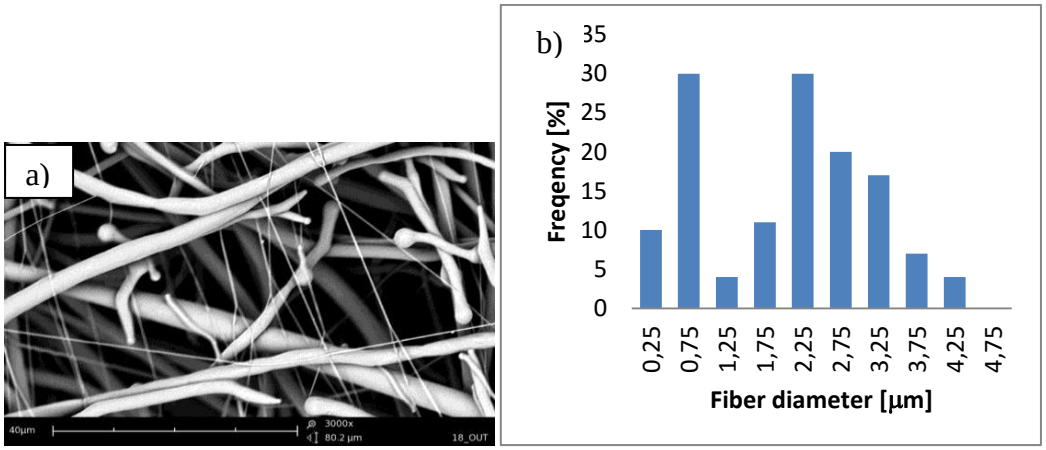

Figure 13: The morphology of the fibers obtained from electrospinning of 20 wt % PCL containing nanofibers and microfibers, scale bar 40 µm (a). The graph shows the frequency of fiber diameter with two peaks corresponding with 2 types of fibers occurred in the structure (b).

The morphology of prepared tubular grafts was analyzed on the inner and outer side. It was found that the fibers in the inner layer were deformed probably because of collector impact (see figure 14). Several experiments (exchange of collector material, different methods of graft removal from the mandrel) were performed to minimize or better to eliminate occurrence of these deformed fibers but with no reproducible solution.

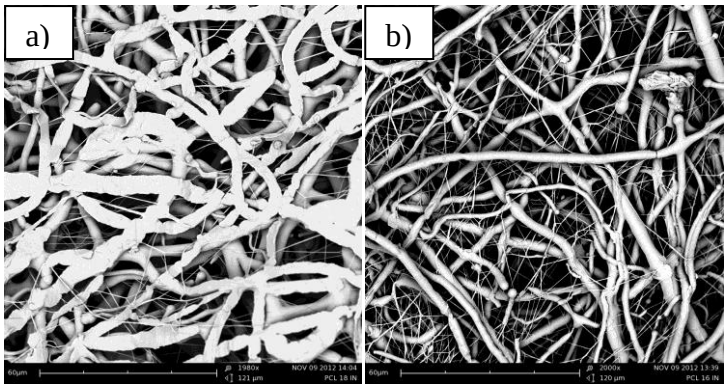

Figure 14: SEM pictures of inner (a) and outer layer (b) of electrospun vascular graft having inner diameter of 6 mm made from 18 wt % PCL. Scale bars 60 µm.

3.3.2 Fiber orientation

Preferential fiber orientation in radial direction is required for mimicking of medial layer of prepared vascular graft as described previously in subchapter 3.1. This orientation could be achieved by increasing of mandrel rotational speed (250 rpm, 5 000 rpm, 10 000 rpm and 15 000 rpm). Orientation of fibers was measured manually using NIS Elements software from 100 fibers from at least 5 pictures. The direction of radial axis of the tube was determined as 0° and the fiber angle with the axis was recorded. The data were translated in the graph as the dependence of frequency on the angle of orientation.

Oriented fibers in the vascular graft with 6 mm inner diameter were obtained using rotation speed of 5 000 rpm and higher. The structure of resulting fibers obtained by increasing rotational speed (250 rpm, 5 000 rpm, 10 000 rpm and 15 000 rpm) is depicted in SEM picture below in figure 15.

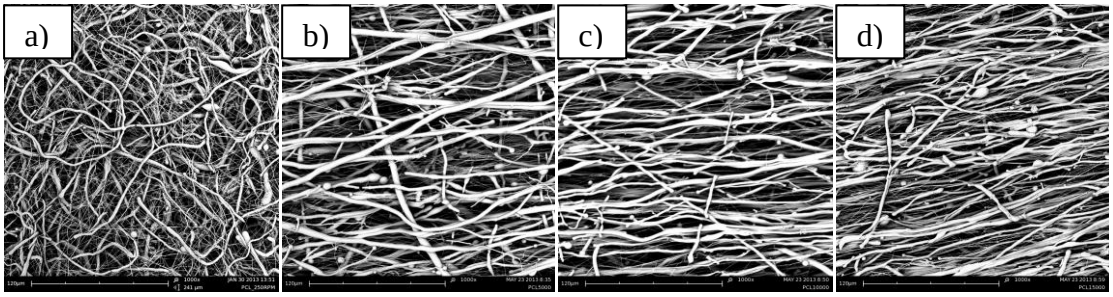

Figure 15: SEM photos of fibers collected on mandrel (6 mm inner diameter) with various rotational speed: 250 rpm (a), 5 000 rpm (b), 10 000 rpm (c) and 15 000 rpm (d). Scale bars 120 µm.

Increasing in rotational speed led to more accurate orientation as shown in the graph in figure 16). In Additional properties of these layers were studied and the results were published in *Journal of Industrial Textiles (Yalcin, 2014).*

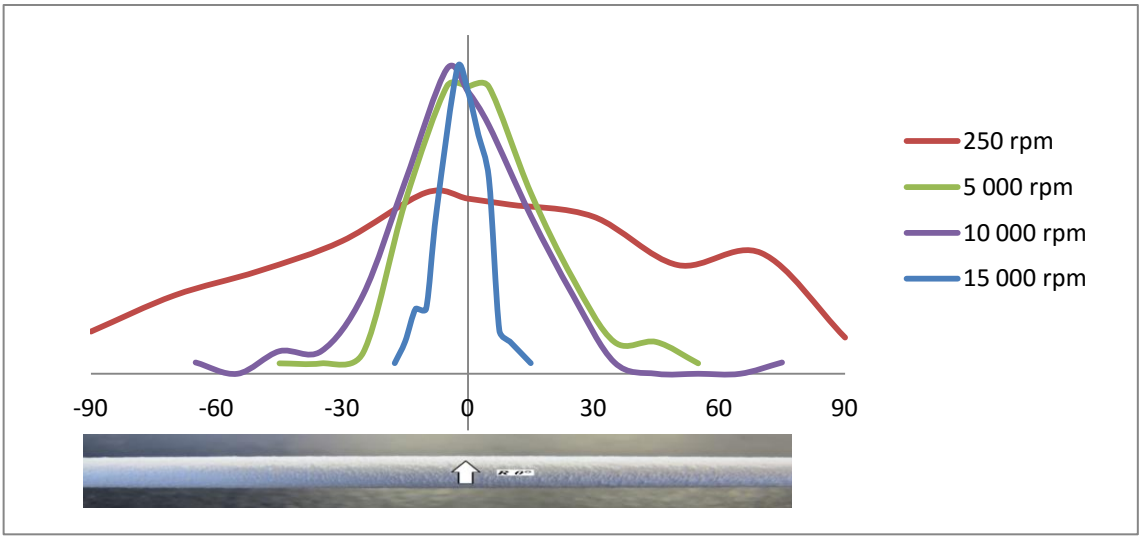

Figure 16: The graph showing fiber orientation distribution: the dependence of frequency on fiber orientation angle. Radial direction marked by the white arrow in the tubular sample under the graph is considered as 0°. Red line reflects the orientation of fibers obtained by 250 rpm, green line 5 000 rpm, violet line 10 000 rpm and blue line the highest rpm of 15 000.

3.3.3 Preparation of double layered vascular graft

One of the goals of the thesis was mimicking of structure of native blood vessel that is naturally composed of 3 layers. The idea was to mimic only 2 layers (inner and medial) assuming that the third outer layer will create naturally after implantation into the body (see figure 8). The inner layer supports the endothelial cells that are crucial for vascular graft function within the body. Endothelialization of the graft lumen will ensure the antithrombotic surface. The inner layer was composed of nanofibrous structure made from 16 wt % PCL. It has been found out that the addition of acetic acid into electrospinning solution decrease the fiber diameter therefore PCL for inner layer was dissolved in chloroform/ethanol/acetic acid 8/1/1 (v/v/v). The solution led mostly to the fibers having about 150 nm diameter with a few deformed fibers and beads (figure 17 a). Nanofibrous structure also serves as a barrier for migration of other cell types into this layer that could lead to severe complications. The thickness of the layer

was adjusted by the time of electrospinning that was set to 5-10 minutes for the thin inner layer giving the thickness of tens of micrometers. There was no requirement for fiber orientation therefore the rotation speed was set between 3 000 and 5 000 rpm.

The middle layer has to ensure the mechanical strength and support for smooth muscle cells that are radially oriented in many layers. The infiltration of the smooth muscle cells is supported by microfibrous structure allowing cells to penetrate the middle part of the graft. The middle layer was prepared by electrospinning of 18 wt % PCL dissolved in chloroform/ethanol 9/1 (v/v) having diameter of around 1 μm (figure 17 b). The layer was thicker (250-300 μm set by the time of electrospinning that was about 1 hour) in order to ensure the mechanical strength of the graft. The speed of collector rotation was adjusted to 10 000 rpm in order to obtain fiber orientation. The electrospinning parameters were the same for both layers: temperature 22-23°C, relative humidity 50-60%, voltage 15 kV, distance 20 cm, feed rate 3 ml/h. Morphology of separate layers are depicted in figure 17. Cross section of double layered PCL graft is seen in figure 18.

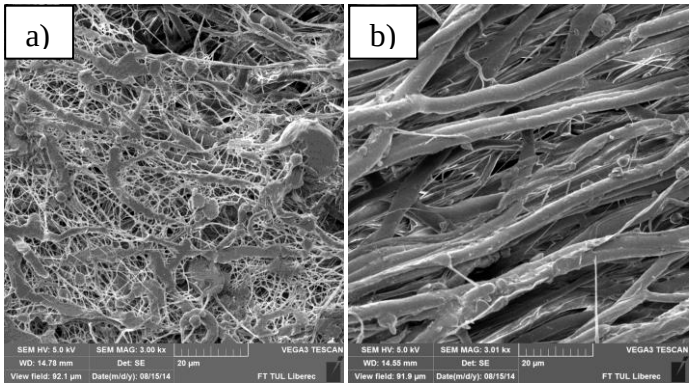

Figure 17: Inner layer of the graft composed of nanofibers with a few deformed fibers and beads (a) and outer layer composed of oriented microfibers (b). Scale bars 20 μm.

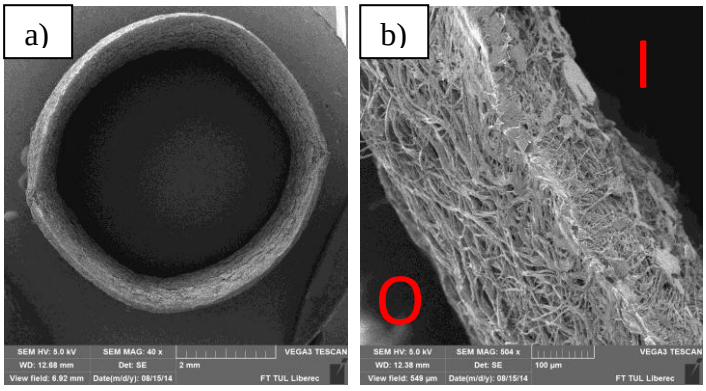

Figure 18: Cross section of double layered PCL graft composed of nanofibers in the inner side (I) and microfibers in the outer side (O). Scale bars 2 mm (a), 100 μm (b).

3.4 Electrospinning of copolymer polylactide and polycaprolactone

Copolymer PLC was tested for the first time in the Department of Nonwovens and Nanofibrous Materials. Therefore the optimization of electrospinning parameters as well as solution composition had started using needle electrospinning with planar collector. Copolymer PLC is very sensitive to the temperature and relative humidity. These parameters strongly affected spinability of polymeric solutions therefore standard conditions were strictly kept during production of fibrous layers in range of 23-25°C and 50-55% relative humidity.

3.4.1 Optimization of polymeric concentration

Firstly, the optimization of electrospinning solution composition was done. Various concentrations of copolymer PLC were electrospun using a needle. The pictures in figure 19 show that concentrations below 5 wt% were not sufficient for fiber formation. Capsules with the diameter of about 4 μm were created (figure 20 a). When 7,5 wt% was used, beaded structure composed of capsules together with fibers was obtained (Figure 19 d). Concentration above 8 wt% led to uniform fibrous structure.

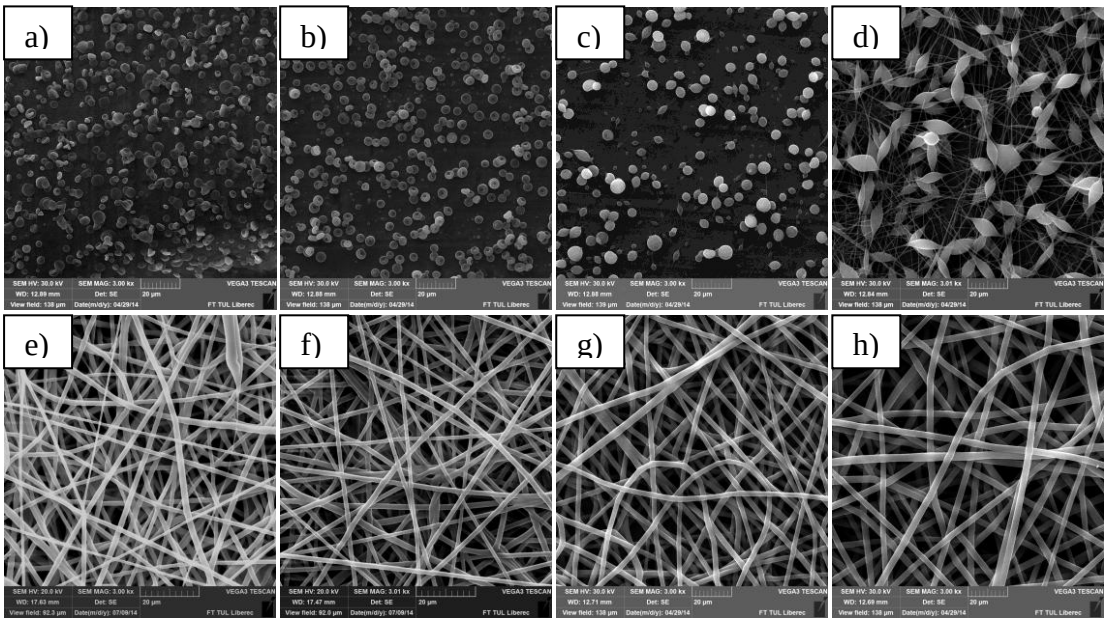

Figure 19: SEM photos of electrospun PLC in different concentrations: 2 wt% (a); 3 wt% (b); 5 wt% (c); 7,5 wt% (d); 8 wt% (e); 9 wt% (f); 10 wt% (g) and 12,5 wt% (h). Scale bars 20 μm.

Fiber diameter of fibrous structure is described in the graph in figure 20 b. Electrospinning of copolymer PLC resulted in the structure composed mostly of microfibers with no significant change in structure with different solution with concentration higher than 8 wt% or electrospinning parameters.

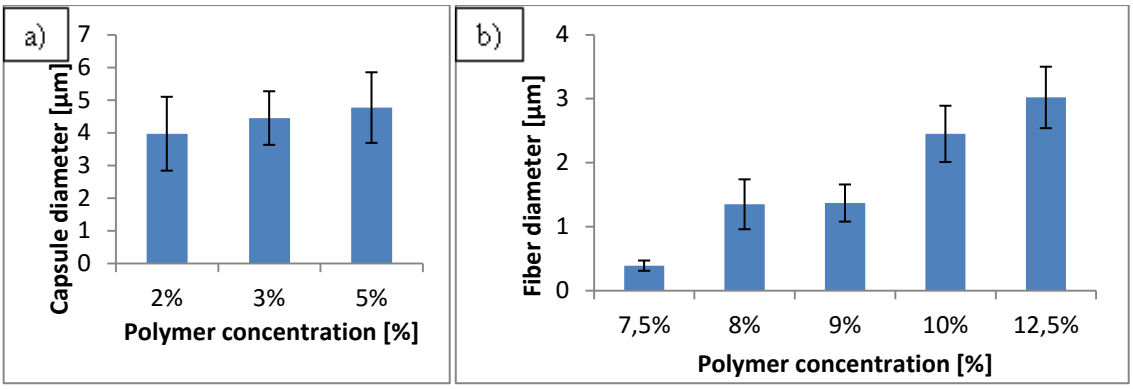

Figure 20: Morphology evaluation of electrospun PLC: comparison of capsule diameter formed after electrospinning of solutions with low PLC content (a) and fiber diameter formed after electrospinning of 7,5 wt% PLC and higher (b).

3.4.2 Tubular scaffolds made from PLC

For further experiments, ideal electrospinning solution composed of 10 wt % PLC dissolved in chloroform/ethanol/acetic acid 8/1/1 (v/v/v) was chosen for production of tubular scaffolds. Electrospinning parameters were set as follows: needle diameter 0,6 mm, voltage 15 kV, distance between the tip of the needle and collector 20 cm, rotational speed of the mandrel 5 000 rpm, feed rate 3 ml/h. As seen from the pictures in figure 21 there were not observed differences between the inner and outer side of the graft as previously in case of PCL electrospinning depicted in figure 14.

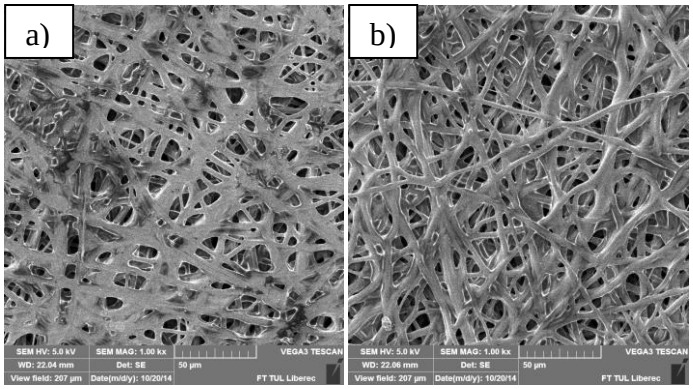

Figure 21: SEM pictures of inner (a) and outer layer (b) of electrospun vascular graft having inner diameter of 6 mm made from 10 wt % PLC. Scale bars 50 µm.

Cross section of PLC vascular grafts were performed with more satisfactory results. The cross section of PCL graft was not sharp-edged to enable detailed characterization of single fiber cross section. The cross section of PLC was straight with no defects such as glued fibers in figure 18. The difference in cross section could be explained by different thermal characteristics of polymers used (more in chapter 3.5.2.). Glass transition temperature (T_g) of PCL is much lower (-60°C) than PLA (60-65°C) that creates 70 % of copolymer PLC. It is assumed that successful cross section has to be carried out in the temperature under T_g. On the contrary, successful cross sections of PCL were not achieved even when working in the liquid nitrogen.

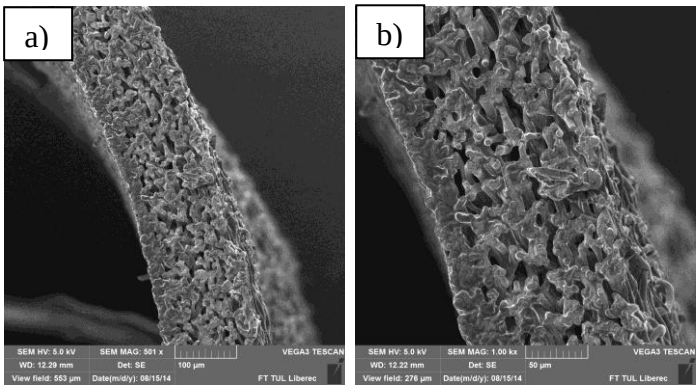

Figure 22: Cross section of vascular graft made from PLC. Scale bars 100 µm (a), 50 µm (b).

Copolymer PLC did not enable the creation a double layered vascular graft with morphology resembling native ECM. Electrospinning of PLC on rotating mandrel led to the structure composed of uniform microfibers. Changing of neither electrospinning solution composition nor electrospinning conditions did not enable the creation of nanofibers from this copolymer.

3.5 Characterization of electrospun polymeric layers

Additional properties of polymers used were investigated. Some of the methods require planar samples for evaluation therefore needleless electrospinning utilizing Nanospider were employed to prepare sufficient amount of planar material available for further testing.

3.5.1 Surface wettability

Surface wettability of microfibrous PCL (22 wt %) and PLC (10 wt %) layers prepared by needleless electrospinning (structure is depicted in figure 10) was assessed by contact angle measurement. Due to the difficulties of wettability evaluation of fibrous structures, polymeric foils were prepared for testing. Both tested polymers (PCL and PLC) in the total concentration of 2 wt% were dissolved in chloroform, placed to a microscopic slide and let evaporated. Foils were measured in the same way as fibrous layers to characterize the surface wettability of polymers without affect of nonhomogenities within electrospun layers. A water droplet was placed on dried electrospun layers attached to a glass slide. The droplet was captured and analyzed by Digital Contact Angle Measurement System with a camera. The measurements were carried out in triplicates and water contact angle was plotted as mean ± standard deviation. Tests for significant differences used a two-tailed Student's t-test and required $p < 0.05$ to claim significance.

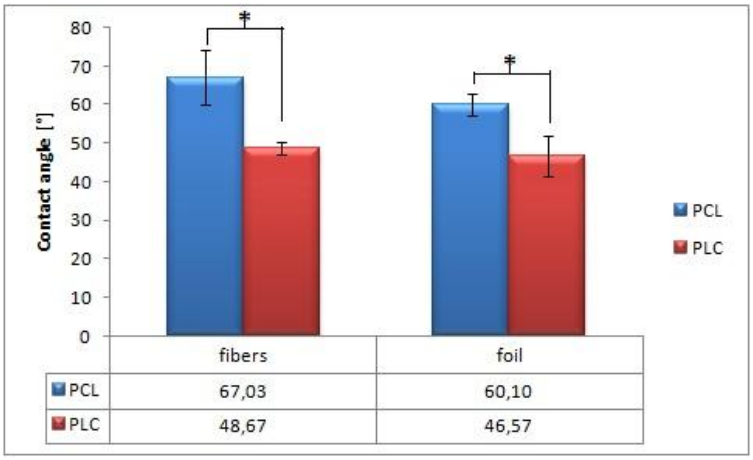

Figure 23: Surface wettability of electrospun fibers and foils made from PCL and copolymer PLC (indicates $p < 0.05$).*

The results depicted in graph in figure 23 showed that PCL possess higher contact angle of water droplet than copolymer PLC when foils or fibrous layers were tested. The outcome corresponds within the expectations based on the chemical structure of tested polymers; polycaprolactone is more hydrophobic than polylactide that creates 70% of copolymer PLC. PCL fibers as well as foils had significantly higher contact angle (between 60° and 70°C) compared to PLC layers (45-50°).

3.5.2 Differential scanning calorimetry (DSC)

Thermal analysis was carried out in order to measure the thermic curves of both polyesters PCL and copolymer PLC. The difference in thermal behavior could have influence on mechanical properties of the grafts described later, on the processing conditions like cross sections, sterilization method as well as on cellular response. The measurements were done in cooperation with L. Běhálek from the Department of Engineering Technology, Technical University of Liberec. For measurement of thermal curves, original polymer in the form of granules from suppliers as well as needleless electrospun polymeric layers (structure is depicted in figure 10) was used. Thermal analysis was done using DSC 1/700 Mettler-Toledo instrument calibrated against indium and zinc. Accurately weighed samples were sealed in aluminum pans. The heating rate was 5°C /min and the nitrogen purge rate was 40 ml/min. The range of temperatures were set from -20°C to 100°C for PCL and maximum of 180°C for PLC. Characteristic temperatures (melting, crystallization and glass temperatures) were calculated by integration of measured peaks of heat flow.

Thermal curves of both polymers (PCL and PLC in the form of granules as well as fibers) are depicted in figures 24 and 25. Polycaprolactone showed standard thermal curves during both cycles of heating with melting temperature of 57°C and crystallization temperature of 29°C (derived from the second cycle). The first cycle of heating is influenced by the technology used. There was a slight difference between electrospun fibers and original granules of PCL in the first peak (during the first heating cycle) that has not appeared during the second cycle of heating (third peak in the graph in the figure 24).

Thermal characteristics of copolymer PLC were measured in the same way. Similarly, there is a difference in the first measured peak that corresponds to melting temperature that reflects the technology used. Further crystallization phase during cooling of the system had to change the polymeric structure since no peaks are presented afterwards in graph in figure 25. Melting point of PLC was about 110°C and glass transition temperature about 19°C.

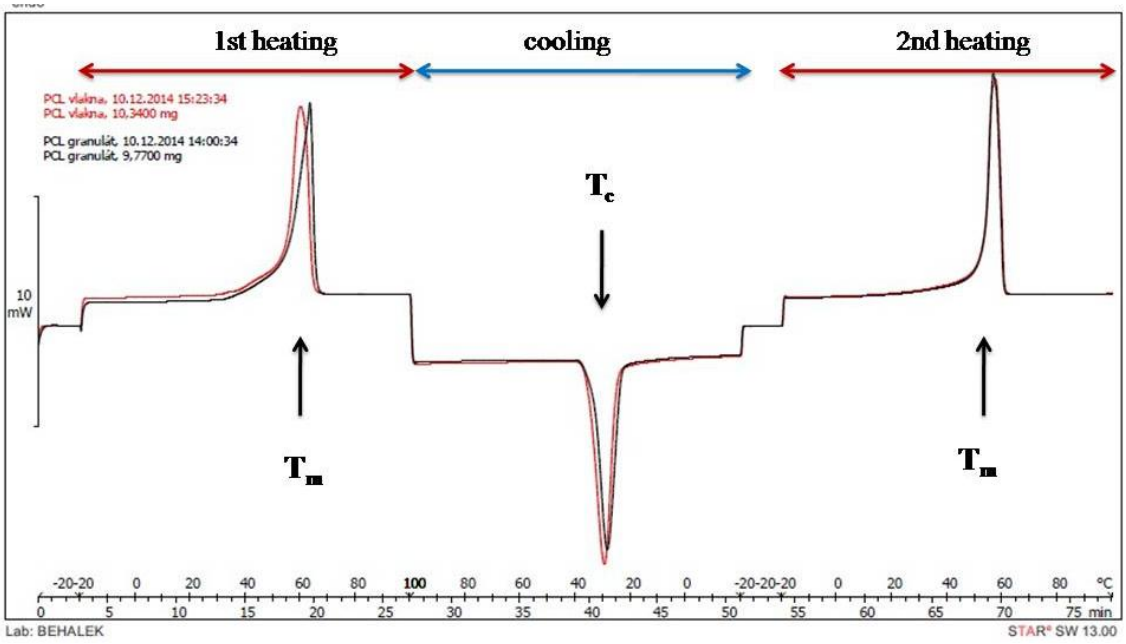

Figure 24: Thermal curves of PCL (black line – granules, red line – electrospun fibers). X axis depicts temperature and time, y axis shows heat flow. The first peak in the graph corresponds with melting temperature (T_m=57°C), the second peak reflects crystallization temperature (T_c=29°C), and the third peak represents melting temperature during the second cycle of heating (T_m=57°C).

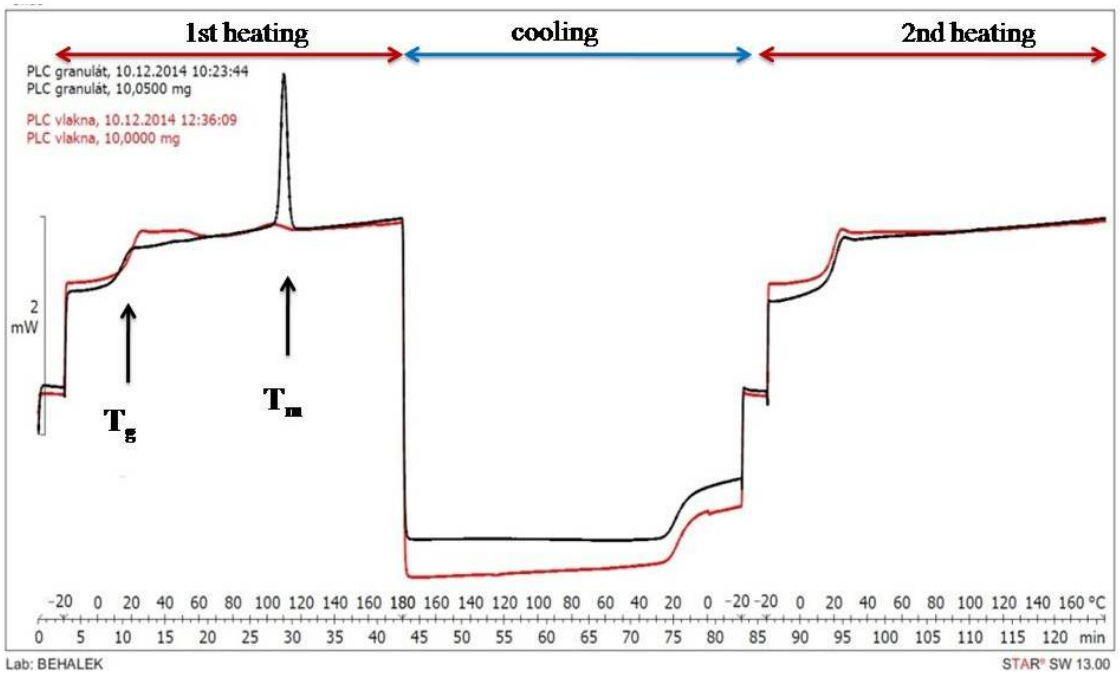

Figure 25: Thermal curves of copolymer PLC (black line – granules, red line – electrospun fibers). X axis depicts temperature and time, y axis shows heat flow. Glass transition temperature (T_g) as well as melting temperature (T_m) was derived from the first cycle of heating.

Data obtained from measurement of PCL thermal curves corresponds to the data obtained from the supplier (Sigma Aldrich) in case of melting temperature. There was no change between melting temperature in PCL between granules and fibers in the second heating cycle that is frequently used for thermal characterization. Copolymer PLC had higher melting point of 110°C that corresponds to the fact that the copolymer is composed from 70% from PLA with melting temperature about 150-160°C. The electrospinning process affects the thermal behavior of PLC. There is a difference in heat flow when granules and electrospun layers were measured. Therefore melting temperature was calculated from measurement of granules were the area under the peak can be evaluated. After cooling cycle, the polymer probably degraded and the second cycle could not be measured. This outcome could be explained by the fact that PLC is a copolymer that could not been crystalline. It is known that PCL is partially crystalline polymer depending on its molecular weight *(Jenkins, 2006).* Statistic copolymers like PLC due to its irregular structure are not able to create crystals during the cooling cycle therefore no crystallization temperature was detected.

The difference in thermal behavior has an impact on many aspects of vascular grafts such as cross section of tubular scaffold that was successfully done with copolymer PLC only. It was hypothesized that fibers could be cross sectioned closed to the value of glass transition of the polymer. Certain sterilization technique requires resistance to heat. Copolymer PLC is stable up to melting temperature of 110°C compared to PCL that is stable only to 57°C. Thermal curves also reflect the crystallinity of polymers. Polycaprolactone as a semicrystalline polymer underwent crystallization process at about 29°C during cooling phase. On the other hand, copolymer PLC as a representative of statistical copolymer is mostly amorphous and no crystallization was detected during cooling cycle. Presence of crystalline and amorphous phases within the polymer affect the degradation rate of polymers as described in the theoretical part (figure 2). Thermal analysis showed that PCL contained crystalline regions suggesting slower degradation rate compared to statistical copolymer PLC. The amorphous phase will be probably degraded faster but degradation studies have to be carried out.

3.5.3 Mechanical testing

Mechanical performance belongs to important parameters of tissue engineering scaffolds. It is hypothesized that mechanical properties could mimic the environmental behavior of native tissues. Vascular grafts have to possess sufficient strength as well as elasticity. Mechanical testing was carried out in cooperation with M. Ackermann from the Department of Applied Mechanics, Faculty of Mechanical Engineering, Technical University of Liberec.

In order to compare the mechanical properties of electrospun polymers, stress-strain curves were measured using a universal tensile testing machine TIRA Test 2810. Firstly, planar materials made from 22% wt PCL and 10% wt PLC prepared by Nanospider were measured (structure is depicted in figure 10). Planar materials were cut into rectangular shapes with constant width of 20 mm and length of 50 mm. The thickness of the electrospun layer was measured using micrometer screw gauge before each experiment. The samples were clamped into jaws and stretched using loading rate of 100 mm/min until break. Measurement was repeated three times for each material. The active length of measured sample was 30 mm. During the tensile test, force F and elongation Δl_0 of the scaffold were recorded to obtain stress-strain curves of each tested material. The relationship for engineering tension calculation was related to the measured sample thickness t and standard width of the samples d (20 mm). Engineering tension σ was then calculated for current strength as:

$$\sigma = \frac{F}{d * t}$$

Relative deformation ε was calculated as a quotient of sample elongation Δl and its original length l_o (30 mm) $\varepsilon = \Delta l / l_o$. The directly measured values of force F and elongation Δl_0 were recalculated to the dependence of engineering tension [MPa] on relative deformation [%] that were depicted into graphs below in figures 26-28 describing mechanical behavior of electrospun layers.

Stress-strain curve of electrospun PCL mat is depicted in figure 26. There is a noticeable increase of stress with slight increase of strain followed by a change in the response that continues until break. The maximum strength of PCL layers was between 10,4 and 17 MPa depending on the materials thickness (the highest strength was noticed in the thickest sample). The elongation of the samples was also dependent on the thickness of materials with the values ranging from 27% to 71%. The average

values of engineering tension for PCL reached values of 13,0 ± 3,6 MPa a elongation of 44,3 ± 23,6 % (n=3).

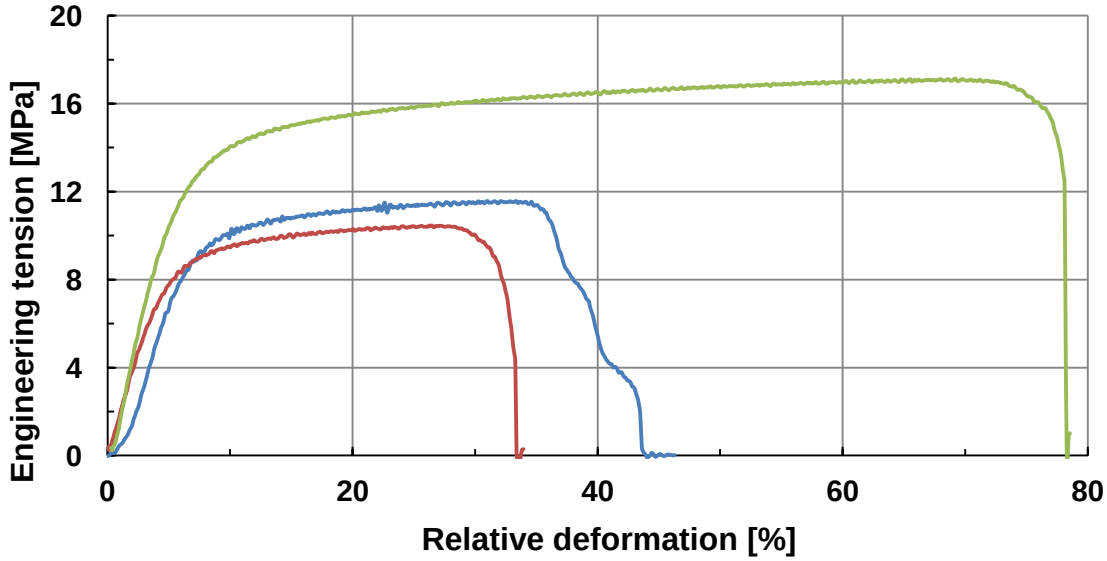

Figure 26: Stress-strain curve of electrospun PCL layers having the thickness of 24 µm (red line), 24,5 µm (blue line) and 32 µm (green line).

Electrospun copolymer PLC showed different shapes of stress-strain curves with linear response of stress to strain as depicted in figure 27. Tested samples gave more homogeneous results with the maximal strength between 30 to 40 MPa and elongation between 128 and 144% of its original length. Even if there were differences in the thickness of the samples, similar trend of mechanical response could be seen from the graphs. Electrospun layers made from copolymer PLC possess higher value of mechanical strength (average value of 33,7 ± 6,1 MPa) and elongation with the average value of 135,4 ± 6,3 % (n=3).

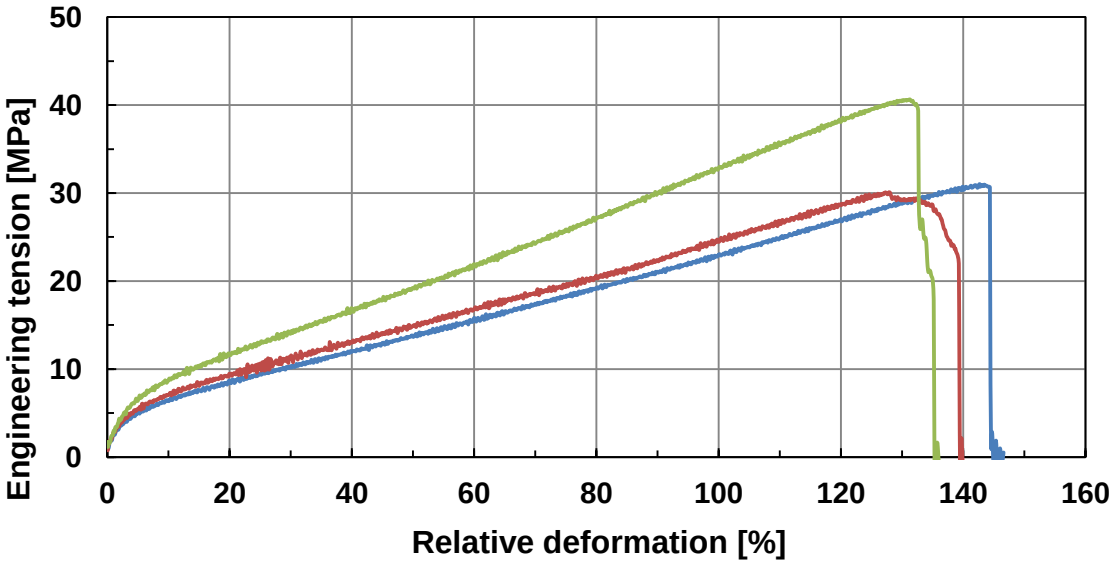

Figure 27: Stress-strain curve of electrospun PLC layers having the thickness of 8,5 µm (red line), 6,5 µm (blue line) and 7 µm (green line).

For mechanical performance comparison of electrospun PCL and PLC on planar collector, representative stress-strain curves were placed in the graph in figure 28. Obviously, PLC reached about three times higher values of engineering and elongation. Samples were tested in a triplicate that is not sufficient for statistical evaluation. However, the outcomes provided obviously different mechanical properties of semicrystalline PCL and amorphous copolymer PLC in the form of planar microfibrous layers.

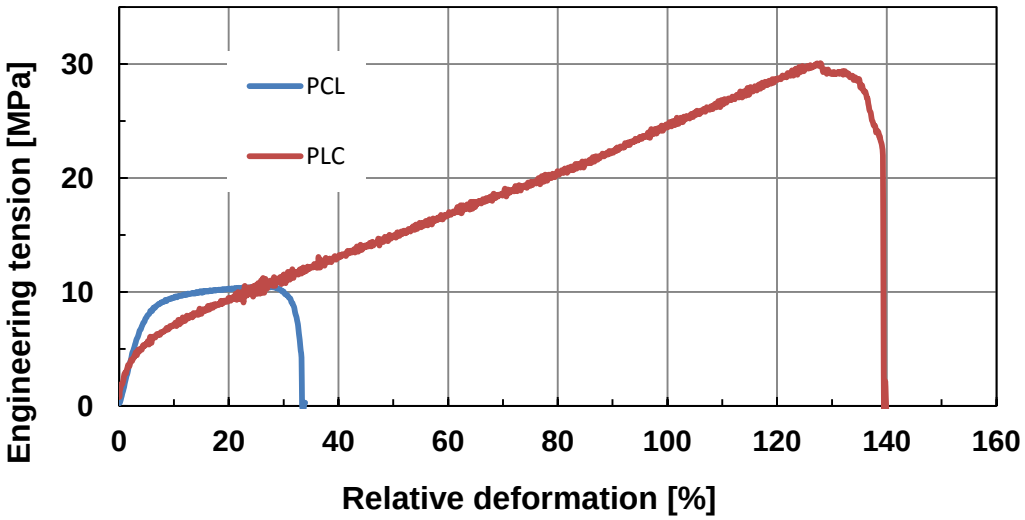

Figure 28: Comparison of stress-strain curves of PCL planar fibrous layer (blue line, 24 µm thickness) and PLC layer (red line, 7 µm thickness).

Further tests were performed in a tubular form in order to investigate the effect of rotating mandrel collector on produced layers and its mechanical performance. Microfibrous samples with similar morphology were prepared by electrospinning of 18% wt PCL and 10 % wt PLC on rotating mandrel having the inner diameter of 6 mm. Single layered tubular scaffolds were tested based on the hypothesis that middle layer of final vascular graft is responsible for mechanical properties. These tubular samples were cut into rectangular shapes with a constant width of 10 mm (n=3). The thickness of the graft wall was measured using micrometer screw gauge before each experiment. The samples were clamped into jaws and stretched using loading rate of 50 mm/min until break. The active length of measured sample was 50 mm. During the tensile test, force and elongation of the scaffold were recorded and further recalculated in the same way as previously mentioned to the engineering tension and relative elongation that is depicted in the graphs.

Mechanical behavior of tubular samples reflected different mechanical behavior between PCL and PLC fibrous layers. In case of PCL, there was no significant change in a response between stress and strain as observed in planar form (compare figure 26 and 29). The maximum strength was lower than in case of planar samples giving the values between 2,3 and 4,4 MPa (the average engineering tension of 3,3 ± 1,1 MPa). The elongation of tubular samples ranged between 32 and 48% with the average value of 37,5 ± 8,8 % that is comparable to planar samples (44,3 ± 23,6 %).

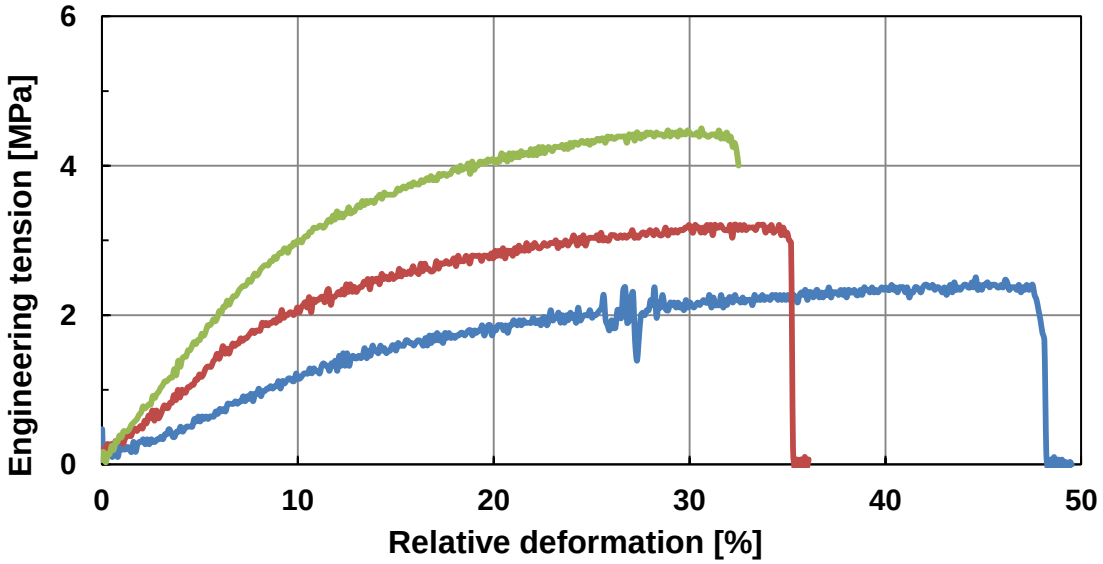

Figure 29: Stress-strain curves of electrospun tubular PCL scaffolds having the thickness of 29,5 µm (red line), 29 µm (blue line) and 32 µm (green line).

The scaffolds made from copolymer PLC showed similar shape of measured stress-strain curves reaching the maximum strength between 26 and 43 MPa and elongation of 230-450% as depicted in figure 30. The average maximum strength of 37,2 ± 9,2 MPa was similar as previously measured in planar form (33,7 ± 6,1 MPa) but the elongation of tubular form with average values of 377,4 ± 157,4 % was significantly higher than in planar scaffolds (135,4 ± 6,3 %). This difference could be explained by different fibrous morphology of electrospun layers on planar collector and into tubular forms and by different thickness of tested layers that were about three times higher in tubular scaffolds (average thickness of 25 μm) compared to planar samples having average thickness of 7 μm. Tubular scaffolds made from PLC have excellent mechanical properties making them ideal choice in terms of mechanical performance for utilization in vascular tissue engineering.

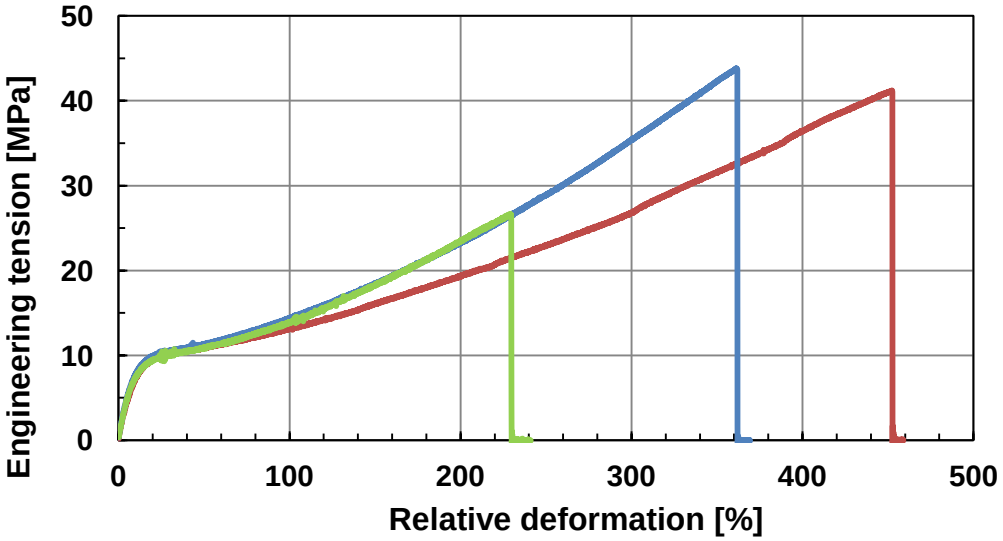

Figure 30: Stress-strain curves of electrospun tubular PLC scaffolds having the thickness of 27 μm (red line), 29 μm (blue line) and 20 μm (green line).

The comparison of representative stress-strain curves is depicted in figure 31. Copolymer PLC is capable to withstand higher engineering tension and elongation that are considered to be important aspects of functional vascular grafts. As previously mentioned, the population of tested samples has not been sufficient for statistical evaluation. Deeper analysis with more samples will have to be carried out in order to fully characterize the mechanical features of tubular scaffolds.

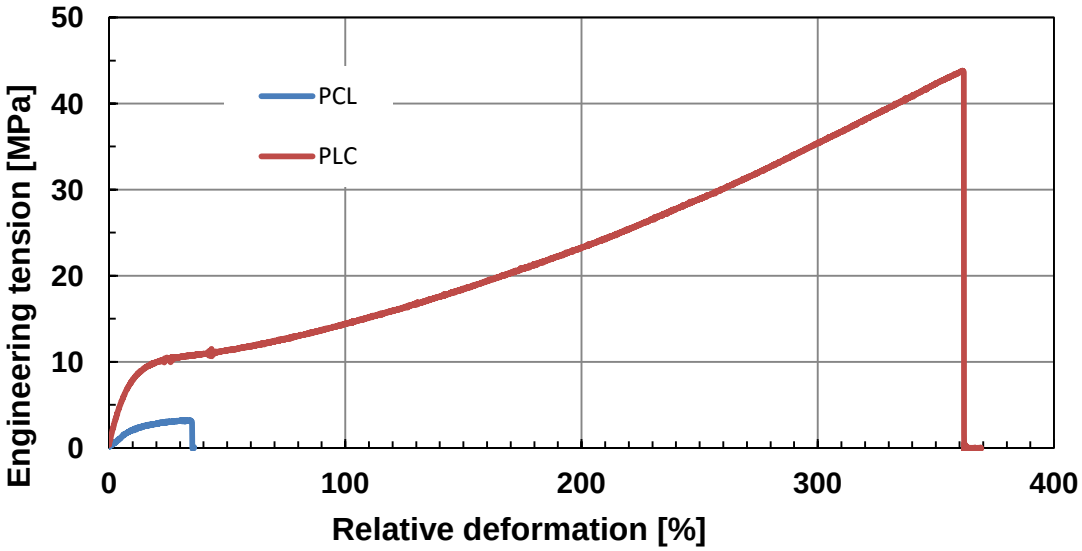

Figure 31: Comparison of stress-strain curves of PCL tubular fibrous layer (blue line, 29 µm thickness) and PLC layer (red line, 29,5 µm thickness).

3.6 Conclusion of synthetic vascular grafts fabrication and testing

The first experimental part of the thesis was focused on understanding of native blood vessels structure that was subsequently mimicked by electrospinning of 2 chosen biodegradable polymers: PCL and copolymer PLC. An ideal model of vascular graft morphology was designed as double layered graft with defined morphologies of certain layers. In case of PCL, the proposed model was created and the double layered graft was produced. When PLC was used for production of tubular scaffolds, only single layered graft was prepared.

The second tested hypothesis was the mechanical performance of vascular grafts. Copolymer PLC created tubular scaffolds possessing excellent elongation properties of 377,4 ± 157,4 % of elongation until break compared to only 37,5 ± 8,8 % achieved with tubular scaffolds made from PCL. Mechanical strength of PLC was also higher than PCL (37,2 ± 9,2 MPa in case of PLC compared to 3,3 ± 1,1 MPa for PCL). Based on the mechanical behavior, copolymer PLC seems to be more appropriate candidate for production of vascular grafts even if double layered structure has not been achieved. Copolymer PLC also excels by higher contact angle suggesting increased cell attachment *in vitro*. The last hypothesis was tested in the following experimental chapter.

The thesis is focused on comparison two chosen biodegradable polymers for small diameter vascular grafts. However, the combination of these 2 polymers could bring improvements of final vascular prosthesis. Inner layer of vascular graft could be created from nanofibrous polycaprolactone and the middle layer could be created by electrospinning of copolymer PLC ensuring sufficient mechanical properties.

4 Biological testing of vascular grafts

The function of vascular grafts has to be evaluated *in vitro* as well as *in vivo* before translation to clinical use. Endothelialization of graft lumen is crucial to ensure non-thrombogenic surface. Otherwise thrombocytes became activated and aggregate making the graft occluded. In order to ensure sufficient mechanical properties, the graft has to be infiltrated with smooth muscle cells that will enable contraction of the vessel. Only the cooperation between endothelial cells and smooth muscle cells allow the vascular graft normal function. Therefore biological testing of produced grafts was performed. At first, fibroblast cell line was used for overall evaluation of cytocompatibility of materials introduced in the first section (PCL and PLC). Following tests were carried out using endothelial cells in order to investigate whether the fibrous materials supports endothelialization. Because of the delay of complete endothelial cell coverage of the lumen, the thrombogenicity of the graft was also evaluated by incubation the scaffold with trombocyte rich solution in static and dynamic conditions using bioreactor.

4.1 *In vitro* tests with 3T3 mouse fibroblasts

Prepared electrospun layers made from 22 wt% PCL and 10 wt% PLC as described previously (see the morphology in the figure 10) were analyzed *in vitro*. Firstly, 3T3 mouse fibroblasts (ATCC) were used to assess the overall cell behavior when cultured on prepared layers.

4.1.1 Materials and methods used for biocompatibility testing with fibroblast cell line

To test cell adhesion and proliferation, MTT test was used for measurement of cell viability during the cultivation time. Fluorescence microscopy and SEM was used for an analysis of cellular morphology on the fibrous layers.

Prior to cell seeding, scaffolds were cut into round patches of 6 mm in diameter and sterilized by immersion in 70% ethanol for 30 minutes followed by double washing in phosphated buffer saline (PBS, Lonza).

Mouse 3T3 fibroblasts were cultivated in Dulbecco´s Modified Eagle Medium (DMEM, Lonza) supplemented by 10% fetal bovine serum (FBS, Lonza) and 1% penicillin/streptomycin/amfotericin B (Lonza). The cells were placed in a humidified incubator at an atmosphere of 5% CO_2 at 37°C. When cells became confluent, they were suspended using trypsin-EDTA solution (Lonza), centrifuged (200 x g) and resuspended in fresh complete medium. Number of cells was determined by Luna^{TM} cell counter (Logos Biosystems). Fibroblasts (passage 19) were seeded on the scaffolds placed in 96-well plate at density of $5x10^3$ per well plate.

Viability of the cells seeded on the scaffolds was analyzed by ***MTT test*** after 1, 3, 7 and 14 days of culturing. MTT [3-(4,5-dimethylthiazol-2-yl)-2,5-diphenyl-2*H*-tetrazolium bromide] has been reduced to purple formazan by mitochondrial dehydrogenase in cells indicating normal metabolism. MTT solution (Sigma Aldrich) in amount of 50 µl was added to 150 µl of complete medium and samples were incubated at 37°C for 4 hours. Formed violet crystals of formazan were solubilised with acidic isopropanol. Optical density of suspension was measured (λ_{sample} 570 nm, $\lambda_{reference}$ 690 nm) using Absorbance Reader ELx808 (BioTek). Each testing day, 4 samples of each material were incubated with MTT solution and average absorbance was calculated as the difference between absorbance measured by 570 nm and by reference wavelength 690 nm. The data were expressed as mean ± standard deviation. Tests for significant differences used a two-tailed Student's t-test and required $p < 0,05$ to claim significance.

The samples for ***fluorescence microscopy*** were washed twice in PBS and fixed in frozen methanol for 10 minutes followed by double washing with PBS and staining with propidium iodide (PI dilution 2 g/l PBS, Sigma Aldrich) for 10 minutes in the dark. Propidium iodide binds to nucleic acids (DNA and RNA) therefore it enables the visualization of the cells. For observation of cellular shape, indirect immunostaining with phalloidin-fluorescein isothiocyanate (FITC) conjugated antibody was performed. Phalloidin binds to F-actin therefore it enables the visualization of actin filaments within the cells. Briefly, scaffolds seeded with cells were washed twice with PBS and fixed using 2,5% glutaraldehyde (Sigma Aldrich) in PBS. Then, scaffolds were washed twice in PBS and incubated in 0,2% Triton X-100 (Sigma Aldrich) in PBS at room temperature for 30 minutes. Antigen blocking was done by incubation with 1% bovine serum albumin (BSA, Prolabo) in Triton solution for 30 minutes at room temperature. Then, incubation with phalloidin-FITC antibody (Sigma Aldrich, dilution 1:1000) was

done for 30 minutes in the dark. After double washing in PBS, counterstaining of cell nuclei was done with 2-(4-amidinophenyl)-1H-indole-6-carboxamidine (DAPI 1 mg/ml, dilution 1:1000, Sigma Aldrich) that binds to double stranded DNA in cell nuclei. Stained cells were observed by inverted microscope Nikon ECLIPSE Ti-E/B.

Cell counting on the scaffolds was done manually using NIS Elements software from PI stained scaffolds after 1, 3, 7 and 14 days of testing. Testing probe (cell counting frame) in the size of 200 x 200 μm was placed on fluorescence picture with magnification 100 x. For each testing day, 4 pictures were randomly chosen and 6 testing probe were placed on the picture (total 24 measurements). Average cell number ± standard deviation per area of 1 mm^2 was calculated and plotted into graph.

The samples for ***SEM*** analyses were washed twice in PBS and fixed in 2,5% glutaraldehyde in PBS for 10 minutes (4°C). The samples were dehydrated by treating with a series of graded ethanol solutions (60%, 70%, 80%, 90%, 96% and 100%). After water removing, the scaffolds were transferred to SEM holder, coated with gold and analyze using SEM VEGA3 SB - Easy Probe (TESCAN, Czech Republic) or SEM from Phenom-World (FEI Company, USA).

4.1.2 Results of culturing 3T3 mouse fibroblasts with electrospun scaffolds

Cultivation of 3T3 mouse fibroblasts with electrospun PCL and PLC was evaluated using complex methods that reflect the response of cells in terms of the adhesion and proliferation rate on both tested microfibrous materials.

Cell viability seeded on PCL and PLC microfibrous scaffold was measured by MTT test during the time of cultivation in days 1, 3, 7 and 14 as depicted in figure 32. After the first and the third day of cultivation, the adhesion of fibroblasts did not show statistically significant difference between both tested materials. After a week of cultivation, higher proliferation rate was found in PLC layer. After 7 and 14 days of cell culture, the viability of fibroblasts on copolymer PLC was significantly higher compared to PCL fibers ($p<0,05$).

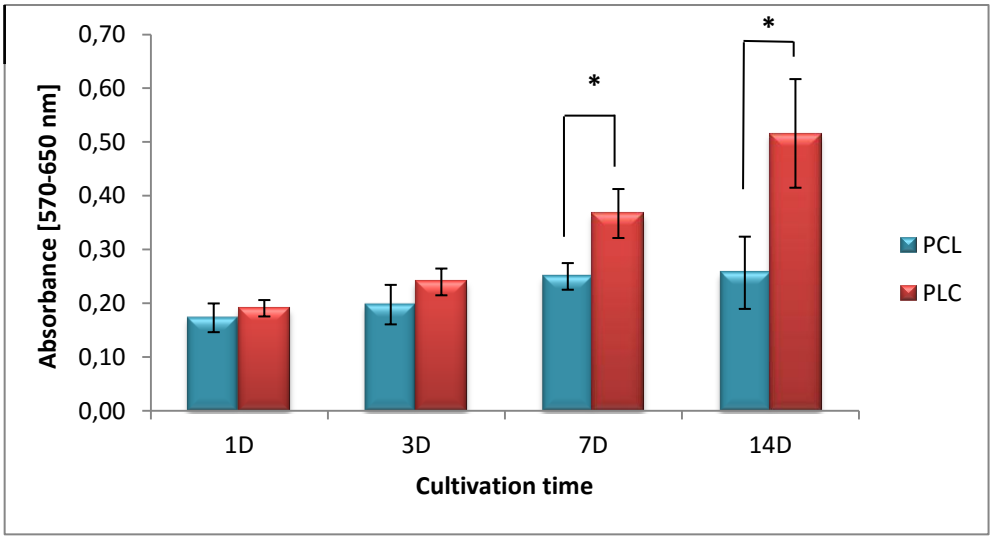

Figure 32: Cell viability measured by MTT test after 1, 3, 7 and 14 days of scaffold cultivation with 3T3 mouse fibroblasts (indicates $p < 0,05$).*

Fluorescence microscopy pictures show cellular adhesion after 1 day that was followed by proliferation of fibroblasts through the scaffold surface (figure 33, magnification 100 x). Cells adhered well on PCL as well as PLC layers. Both microfibrous structures support uniform cell distribution within the scaffold surface during proliferation on these tested layers.

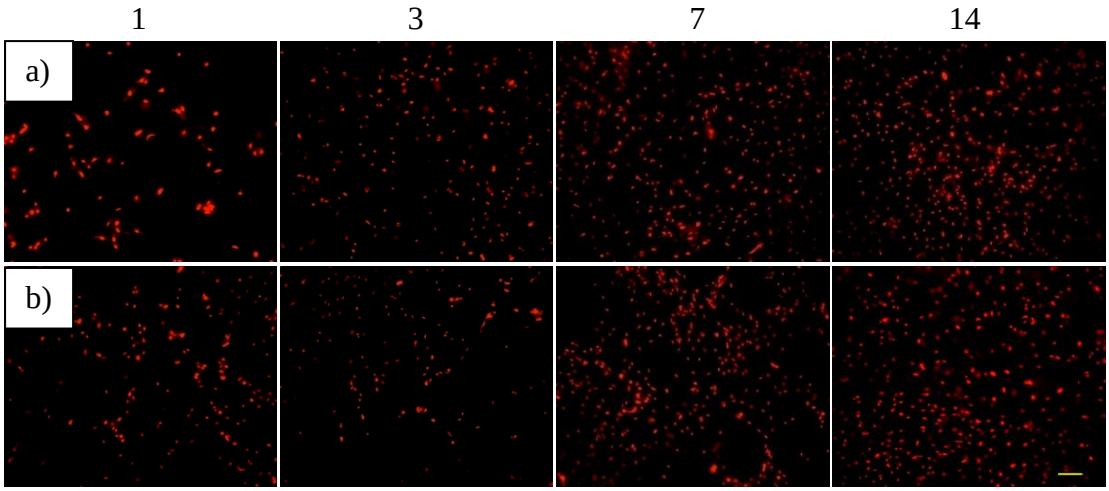

Figure 33: Fluorescence microscopy pictures of propidium iodide-stained cell nuclei of 3T3 mouse fibroblasts during cell culture (1, 3, 7 and 14 days): a) PCL, b) PLC. Scale bar 100 µm.

In order to evaluate the homogeneicity of cellular spreading through the scaffold surface, the tested samples were captured using 40 x magnification.

Subsequently, those pictures were folded up to a single picture showing the colonization of the cells within the scaffold surface (figure 34).

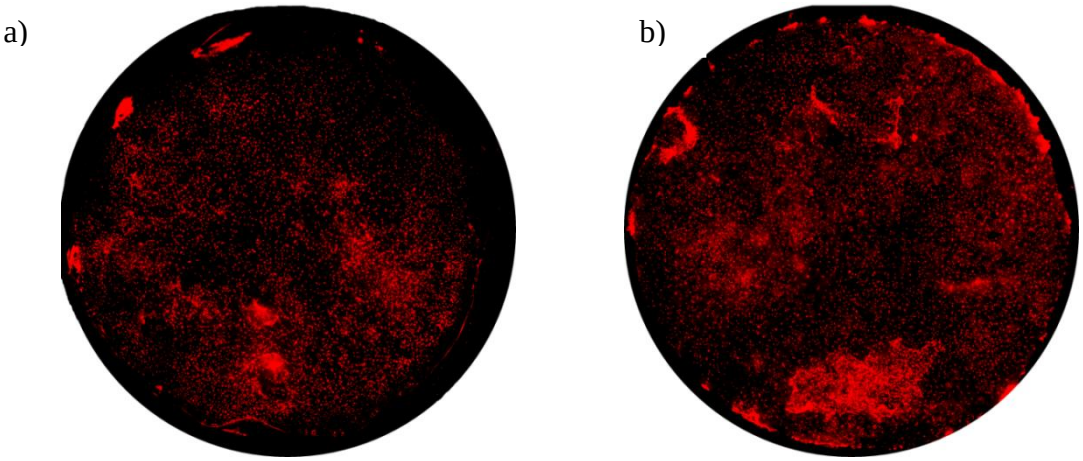

Figure 34: Propidium iodide- stained 3T3 mouse fibroblasts cultured on PCL (a) and PLC (b) scaffolds after 14 days of incubation.

Cell counting using counting frames showed that more cells were present in PLC scaffold compared to PCL layer (figure 35). The difference is statistically significant only the third testing day because of high standard deviations in this type of evaluation. There were efforts for automatic cell counting with the whole scaffold surface but the quality of pictures does not allow such a measurement (see figure 33). The cells are on both sides of the scaffold and they can penetrate into the structure making the proper counting impossible. Therefore the usage of counting frames was employed in order to obtain an estimate of cell number per area. The standard deviations of cell numbers reflect the homogeneicity of the cell deposition within scaffold surface.

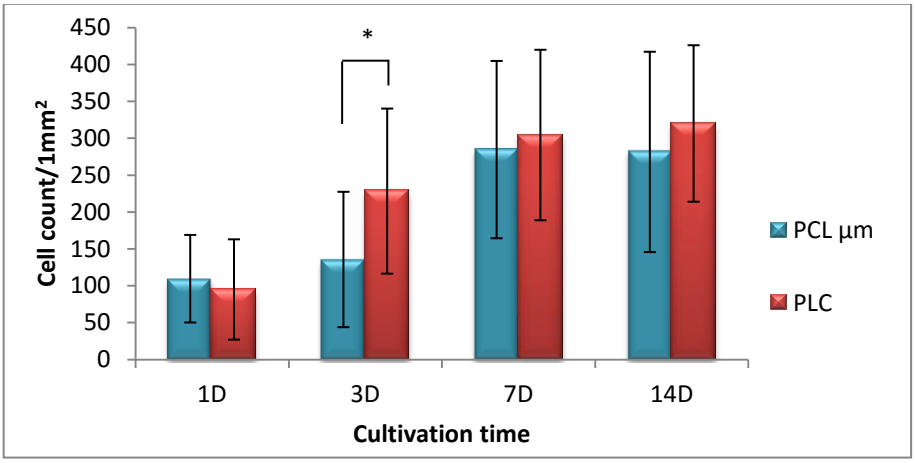

Figure 35: Estimation of cell count per 1 mm^2 in scaffolds after 1, 3, 7 and 14 days of cultivation (indicates $p < 0,05$).*

Cell morphology of fibroblasts attached to tested scaffolds was evaluated from phalloidin-DAPI staining. Actin filaments stained by phalloidin (green color in figure 36) show promising adhesion and spreading of the cells on the microfibrous scaffolds facilitating its colonization. Counterstaining of cell nuclei using DAPI (blue color in figure 36) depicted that more cells were found on PLC scaffold (figure 36 b) but the quantification has already been done from PI staining.

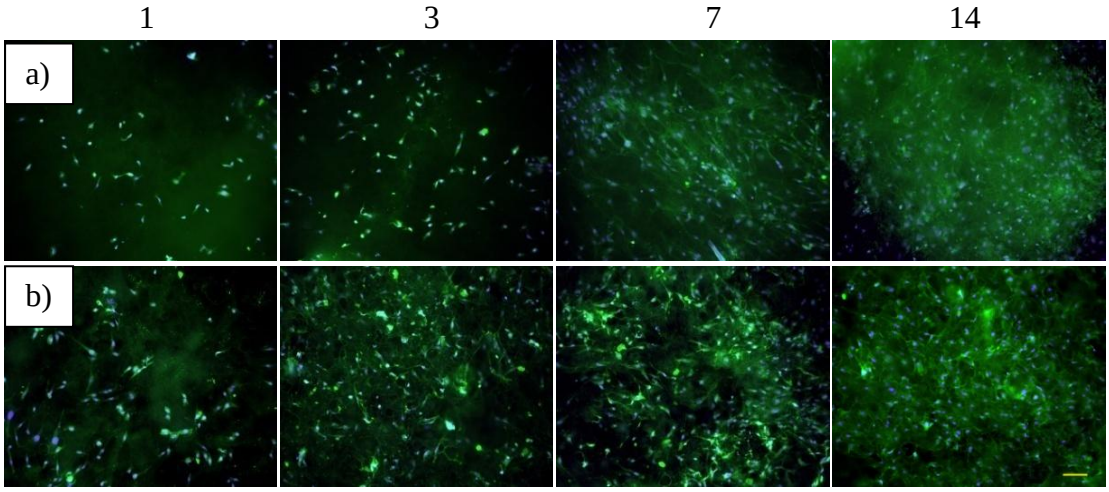

Figure 36: Fluorescence microscopy pictures of 3T3 mouse fibroblasts stained with phalloidin-FITC (green) and DAPI (blue) during cell culture (1, 3, 7 and 14 days): a) PCL, b) PLC. Scale bar 100 µm.

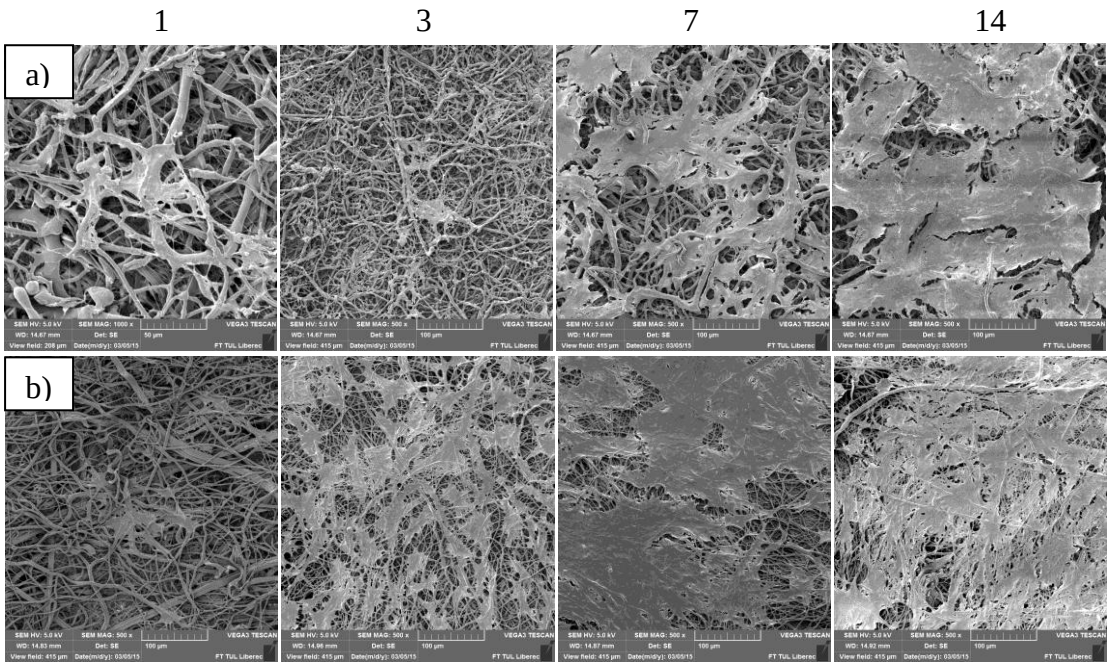

Figure 37: Scanning electrone microscopy pictures of 3T3 mouse fibroblasts during cell culture (1, 3, 7 and 14 days): a) PCL, b) PLC. Scale bar 100 µm.

Pictures from scanning electrone microscopy shows cellular spreading during 2 weeks of cell culture (figure 37). After 14 days, the surface was almost covered with cells in both tested materials. Copolymer PLC was colonized by cells more than PCL as shown in SEM pictures after 3 and 7 days of cultivation. More area of PLC fibrous structure is covered by fibroblasts compared to PCL.

4.1.3 Assessment of material biocompatibility with fibroblasts

In vitro tests with 3T3 mouse fibroblasts proved biocompatibility of both tested materials with 3T3 mouse fibroblasts. Microscopic techniques showed sufficient cell adhesion after 1 day of cell culture followed by proliferation through the scaffold surface during 2 weeks of cell culture. Microfibrous structures also enable uniform cell spreading through the scaffold surface. Cell viability was supported mostly by PLC fibrous structure where absorbance measured by MTT test was higher at each testing day (1, 3, 7 and 14). Cell viability was probably influenced by surface wettability properties that are more beneficial in PLC since the fiber morphology was equal in both tested electrospun layers.

4.2 *In vitro* tests with endothelial cells

In order to test the biological performance of PCL and PLC for vascular tissue engineering, endothelial cells were seeded onto the layers to test their adhesion and proliferation to the material using similar methods described in the previous section. *In vitro* tests were performed with endothelial cells to evaluate the effect of material itself by testing similar fiber morphologies made from different polymers (PCL and PLC) and to assess the effect of fiber diameter on endothelialization of scaffold (nanofibers versus microfibers). The proposed structure of ideal vascular graft was composed of nanofibers that were assumed to promote endothelialization. Since only polymer PCL was able to create nanofibrous structure as described in paragraph 3.3.3, PCL with different fiber diameters (nano- and microfibrous) was tested together with copolymer PLC (microfibrous).

4.2.1 Materials and methods used for assessment of scaffolds culturing with endothelial cell line

Electrospun layers made from PCL and PLC were tested as in the previous experiment with fibroblasts. PCL was also prepared by needleless electrospinning technique utilizing Nanospider to obtain fibrous layer having fiber diameters in nanoscale. Such a structure was achieved by electrospinning of 18 wt% PCL dissolved in chloroform/ethanol/acetic acid 8/1/1 v/v/v. The average fiber diameter of electrospun "PCL nm" was 230 ± 190 nm. The structure is depicted later in figure 41 a. This experiment was design to compare PCL and PLC with similar morphologies (1) and to assess the effect of PCL fiber diameter on endothelial cell adhesion and proliferation (2). Three materials were tested to prove this hypothesis marked as PLC, PCL μm and PCL nm.

The materials were prepared in the same way as described in previous section. Before endothelial cell seeding, the scaffolds were pre-incubated for 2 hours with complete medium in order to facilitate cell adhesion by protein adsorption.

Human umbilical vein endothelial cells (HUVEC, Lonza) were cultivated in Endothelial Basal Medium (EBM-2, Lonza) supplemented by EGM-2 Single Quots (Lonza) containing Human Epidermal Growth Factor, Hydrocortisone, Bovine Brain Extract, Ascorbic Acid, Fetal Bovine Serum, and Gentamicin/Amphotericin-B. The cells were placed in humidified incubator at an atmosphere of 5% CO_2 at 37°C. When cells became confluent, they were suspended using trypsin-EDTA solution, centrifuged (200 x g) and resuspended in fresh complete medium. Endothelial cells (passage 6) were seeded on the scaffolds placed in 96-well plate at density of $7{,}5x10^3$ per well plate.

Evaluation of endothelialization was carried out using MTT test, fluorescence microscopy and SEM after 1, 3, 7 and 14 days of incubation.

4.2.2 Results of endothelial cells cultured with electrospun scaffolds

Endothelial cell viability was detected by MTT test during 14 days of experiment. Cells adhered to the scaffold and started to proliferate through the surface. The proliferation rate was delayed in comparison with the results obtained with 3T3 mouse fibroblasts. Measured values of absorbance obtained during the first week of testing were in low levels (about 0,1). Even if the seeding density was three times

higher than in case of fibroblasts, it seems that even higher cell number needs to be seeded or longer cultivation time should be performed.

However, the highest proliferation rate of the cells was found in PLC fibers as previously with fibroblast cell line. After 7 days of cell culture, the viability of endothelial cells on PLC was significantly higher compared to PCL microfibrous layer ($p<0,05$). After 2 weeks of cell culture, higher cellular viability was also measured in scaffolds made from PLC but this difference did not claim significance.

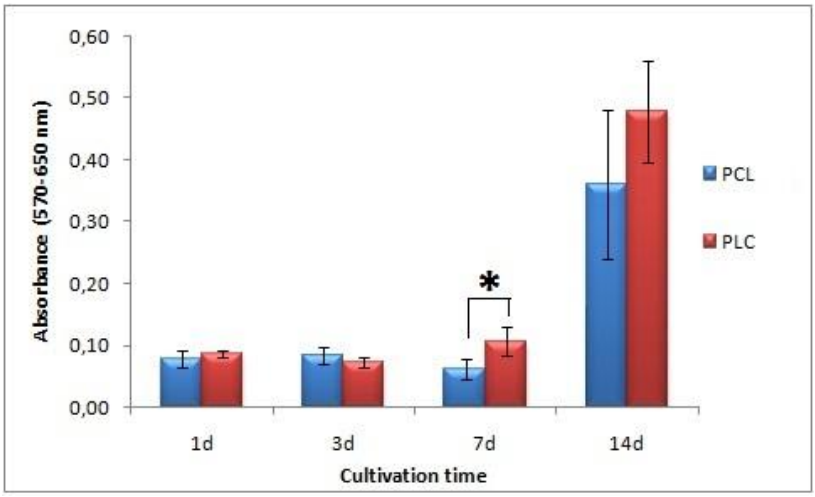

Figure 38: Comparison of cellular viability on PCL and PLC microfibrous scaffold measured by MTT test after 1, 3, 7 and 14 days of scaffold cultivation with human umbilical vein endothelial cells (indicates $p < 0,05$).*

When morphology of PCL fibers was compared, contrary to the assumptions, microfibers supported endothelialization of the surface more than nanofibers as seen in figure 39.

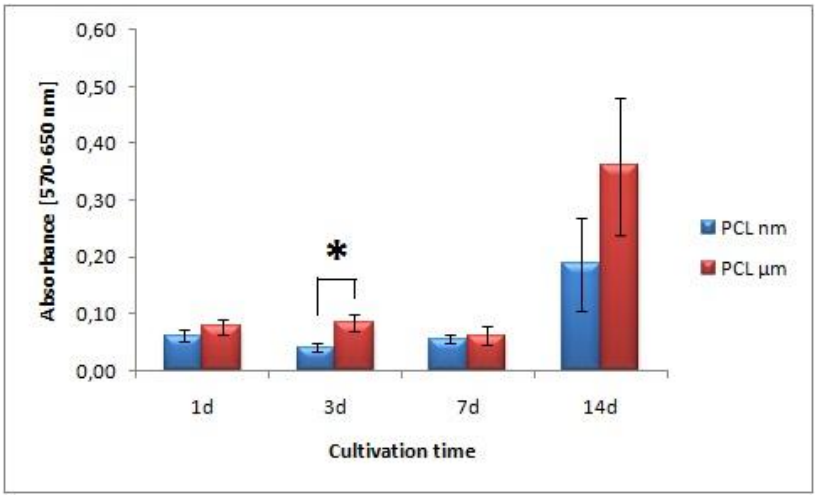

Figure 39: Comparison of cellular viability on PCL nano- and microfibrous scaffolds measured by MTT test after 1, 3, 7 and 14 days of scaffold cultivation with human umbilical vein endothelial cells (indicates $p < 0,05$).*

Fluorescence microscopy pictures show endothelial cell adhesion and proliferation on PCL nano- and microfibrous and PLC layers (figure 40). Surprisingly, the cell adhesion was not enhanced by the nanofibrous structure (figure 40a). Cells proliferated on the scaffold surface during 2 weeks of cell culturing. In agreement with MTT test results, PLC microfibers were populated more than PCL layers after 7 and 14 days of culturing.

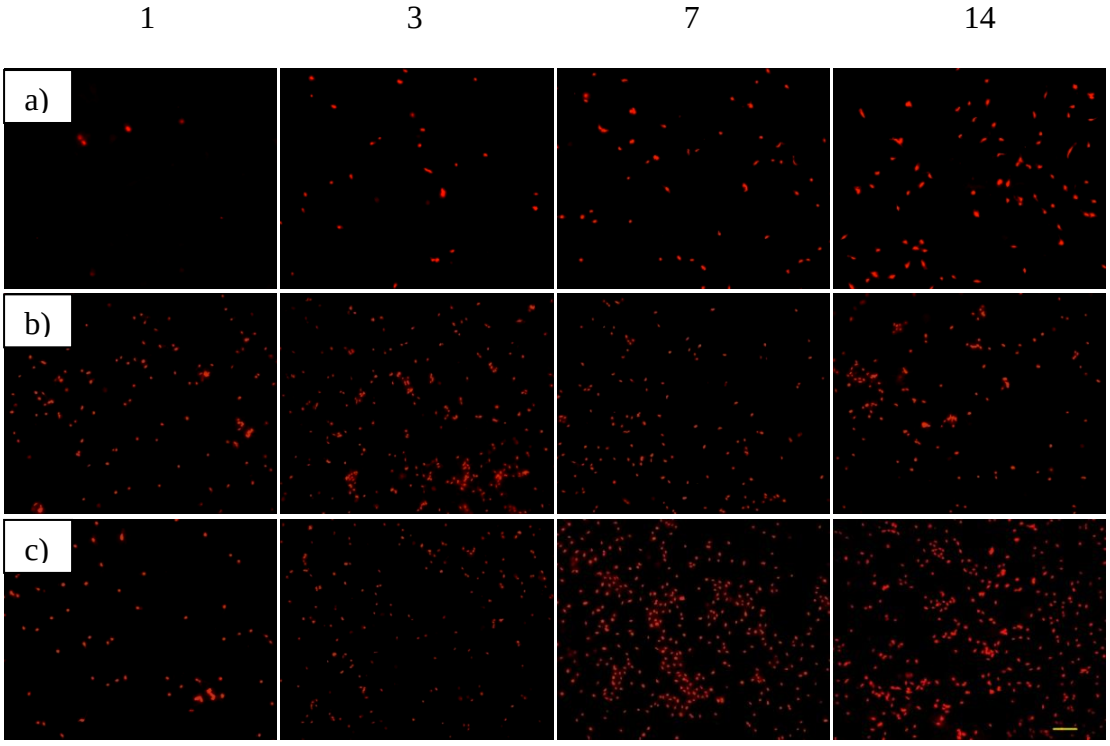

Figure 40: Fluorescence microscopy pictures of propidium iodide-stained cell nuclei of human umbilical vein endothelial cells during cell culture (1, 3, 7 and 14 days): a) PCL nm, b) PCL µm, c) PLC. Scale bar 100 µm.

Cell counting using counting frame could not be done by using the same approach as previously with fibroblasts. Endothelial cells did not grow homogeneously in the surface. On the other hand, endothelial cell amount is reflected by their metabolic activity measured by MTT test that is a reliable method for measurement of cellular viability that corresponds to the cell number on tested materials.

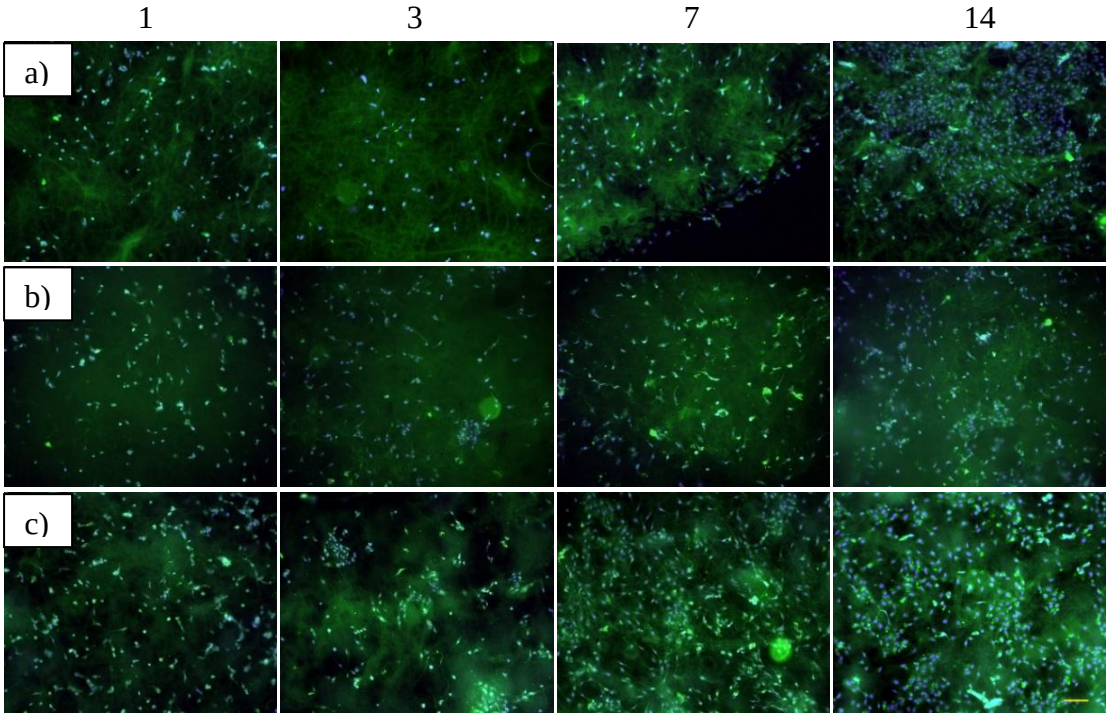

Figure 41: Fluorescence microscopy pictures of human umbilical vein endothelial cells stained with phalloidin-FITC (green) and DAPI (blue) during cell culture (1, 3, 7 and 14 days): a) PCL nm, b) PCL µm, c) PLC. Scale bar 100 µm.

Pictures from scanning electrone microscopy depict similar trend as fluorescence microscopy. In the pictures below cellular spreading during 2 weeks of cell culture (figure 41) is shown. The nanofibrous PCL layers did not enhance endothelial cell adhesion that had been assumed, only a few cells adhered to the nanofibers. Even after 2 weeks of culturing, cells did not start to create monolayer as seen in microfibrous PCL and PLC (figure 41 b, c). The tests were carried out in the static conditions. It is necessary to verify the results in dynamic conditions using bioreactor before final conclusion of appropriate fiber diameter for successful endothelialization.

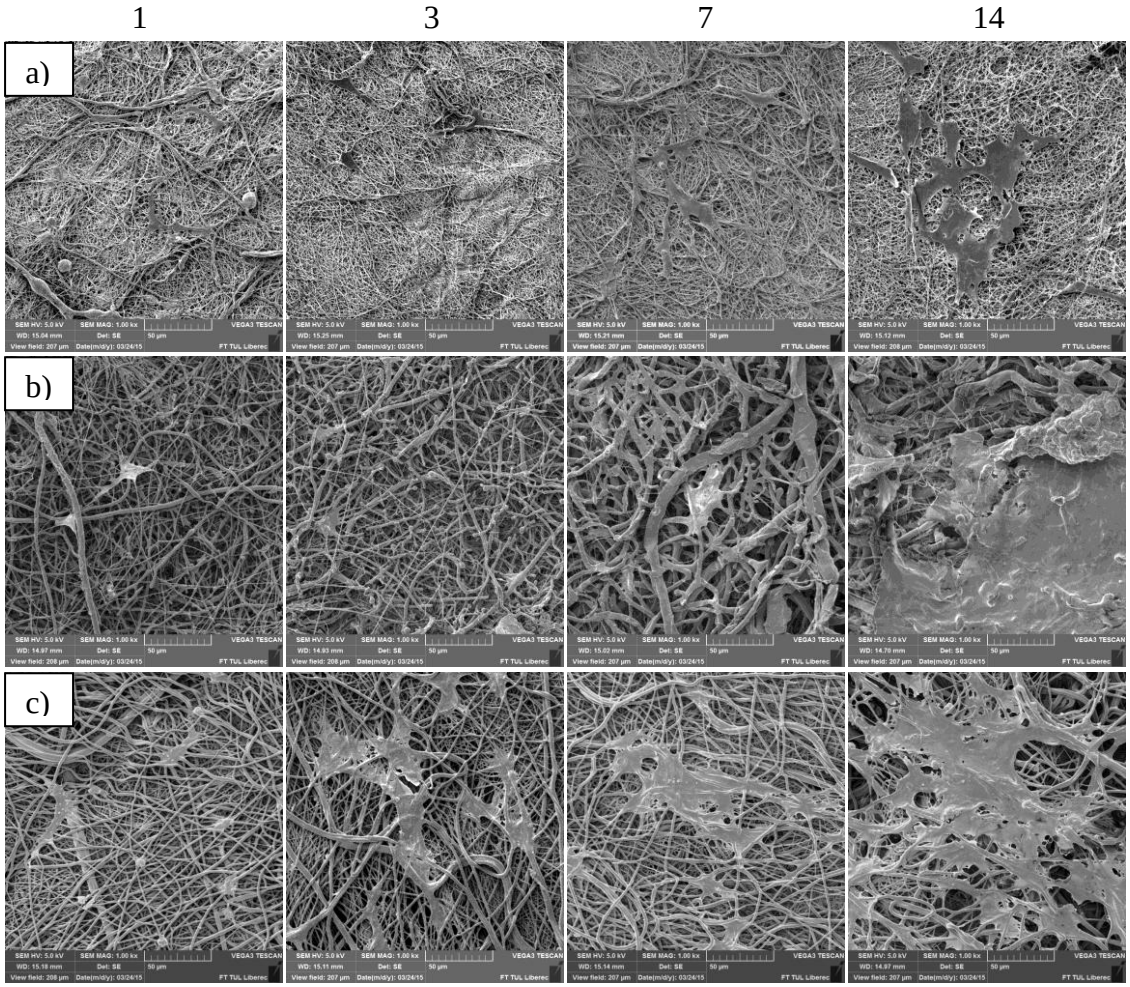

Figure 41: Scanning electrone microscopy pictures of human umbilical vein endothelial cells during cell culture (1, 3, 7 and 14 days): a) PCL nm, b) PCL µm, c) PLC. Scale bars 50 µm.

4.2.3 Biocompatibility of electrospun biodegradable polyesters with endothelial cells

All three tested materials (microfibrous PCL, nanofibrous PCL and microfibrous copolymer PLC) supported human umbilical vein endothelial cell adhesion and proliferation. Microscopic techniques as well as viability measurement using MTT test showed satisfying cell adhesion after 1 day of cell culture followed by proliferation through the scaffold surface during 2 weeks of cell culture. Even though the cell seeding density was too low for comparison of cellular viability during the first days of culturing, after 7 days the difference between tested materials appeared to be significant. Copolymer PLC supported endothelial cell proliferation more than PCL. In case of PCL, nanofibers did not fasten the endothelialization of the scaffold surface. The effect seemed to be in the opposite way - microfibers were more beneficial

for endothelialization than nanofibers. Based on these results, endothelialization is dependent on fiber diameter and chemical structure; however nanofibers did not show the enhanced endothelialization as expected when cultured under static conditions.

4.3 Thrombogenicity

The main failure of vascular grafts after implantation is the acute thrombogenicity that is affected by chemical composition of surface, morphology of exposed surface and other factors. In order to characterize an extent of thrombogenicity of the electrospun layers, samples were tested with thrombocyte rich solution (TRS) under in static and dynamic conditions.

Thrombocyte rich solution was obtained from Liberec Regional Hospital, blood transfusion centre. The solution was prepared from mixed buffy coats obtained from 4 blood donors. After centrifugation using a deleucotization filter (CompoStop® Flex 3F T&B, Fresenius Kabi), thrombocyte rich solution was obtained.

4.3.1 Thrombogenicity testing in static conditions

Firstly, the thrombogenicity of electrospun layers made from PCL and PLC was assessed by incubation of scaffolds in TRS containing $914x10^6$ thrombocytes/ml up to a week. The analysis of platelet activation was carried out after 2 hours, 1, 4 and 7 days by MTT test, fluorescence microscopy and SEM. Secondly, the comparison of different roughness of the samples was carried out. Foils made from the PCL and PLC were prepared similarly as described in subchapter 3.5.1 Surface wettability. The extent of thrombogenicity was compared between samples with the same chemical composition but different surface roughness (smooth foils vs. fibrous layers).

Materials and methods used for assessment of thrombogenic potential of scaffolds tested in static conditions

For static conditions, the ethanol sterilized samples (PCL μm, PCL nm and PLC) with the diameter of 6 mm after double washing in PBS were placed in 96-well plate and incubated with 200 μl TRS (~$183x10^6$ thrombocytes/well) for 2 hours and then the solution was replaced with Composol PS solution (Fresenius Kabi) that is frequently used for platelet storage. MTT test and SEM was carried out after 2 hours, 1,

4 and 7 days of incubation as described above in subchapter 4.1.1 Materials and methods used for biocompatibility testing with fibroblast cell line.

Indirect immunofluorescence staining of thrombocytes was done using FITC-conjugated antibody against integrin αIIb/β3 (CD 41) (dilution 1:50, Santa Cruz Biotechnology) that is considered as a marker of thrombocyte activation. In resting platelets, integrin αIIb/β3 is normally in a low activation state. Stimulation of thrombocytes will induce a conformational change called inside-out signaling and the marker could be abundantly found in the membrane of platelets. After the incubation with TRS, tested scaffolds were washed twice in PBS, fixed in 2,5% glutaraldehyde and blocked in 0,1% bovine serum albumine. Primary antibody anti CD41-FITC was added for 30 minutes followed by triple washing in 0,1% BSA solution.

In order to compare different surface morphology, samples made from PCL (foils and nanofibrous electrospun layer) and PLC (foil and microfibrous electrospun layer) were prepared in the same way as in previous experiment and incubated with TRS containing $1046x10^6$ thrombocytes/ml for 2 hours (~$209x10^6$ thrombocytes/well). After the incubation period, MTT test was measured and platelet morphology was observed by scanning electrone microscopy.

Results of thrombogenicity assessment in static condition

Figure 42 shows metabolic activity of thrombocytes after incubation with TRS for certain period (2 hours, 1 day, 4 and 7 days). The highest metabolic activity of adhered thrombocytes after 2 hours of incubation measured by MTT test was found in nanofibrous layer made from PCL but the difference did not claim significance ($p>0,05$). Platelets lost their viability during the incubation time. After 4 and 7 days of incubation the metabolic activity was very low that is in agreement with the life-time of thrombocytes.

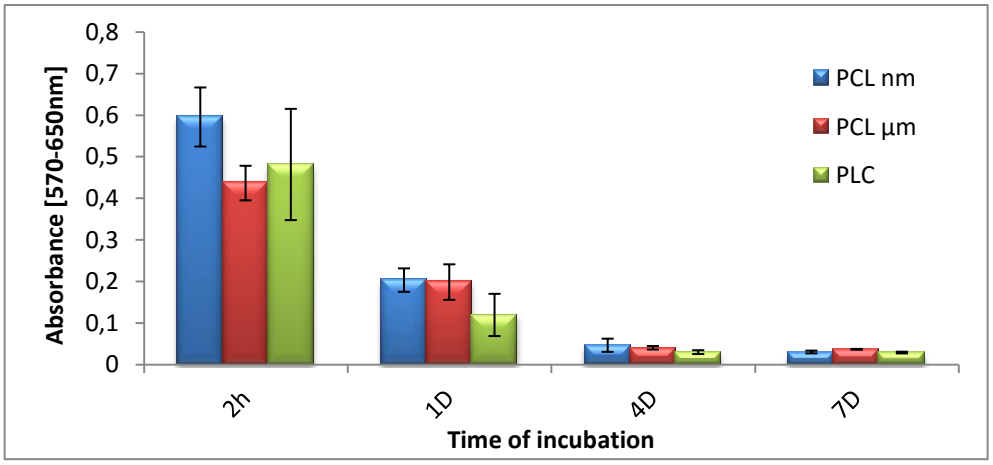

Figure 42: Metabolic activity of thrombocytes adhered to electrospun layers measured by MTT test after 2 hours, 1, 4 and 7 days.

Fluorescence microscopic pictures showed the aggregates formation. Firstly, the thrombocytes adhered to the surface of the fibrous layers, became activated and aggregated. The biggest aggregates were found in PLC microfibrous structures (indicated by an arrow in figure 43) due to the pore sizes that enable creation of such aggregates. In the figure 43 there are fluorescence images of 3 tested materials incubated with TRS for 2 hours (first row) and for 4 days (second row). Number of adhered platelets is very high therefore cell counting could not be performed.

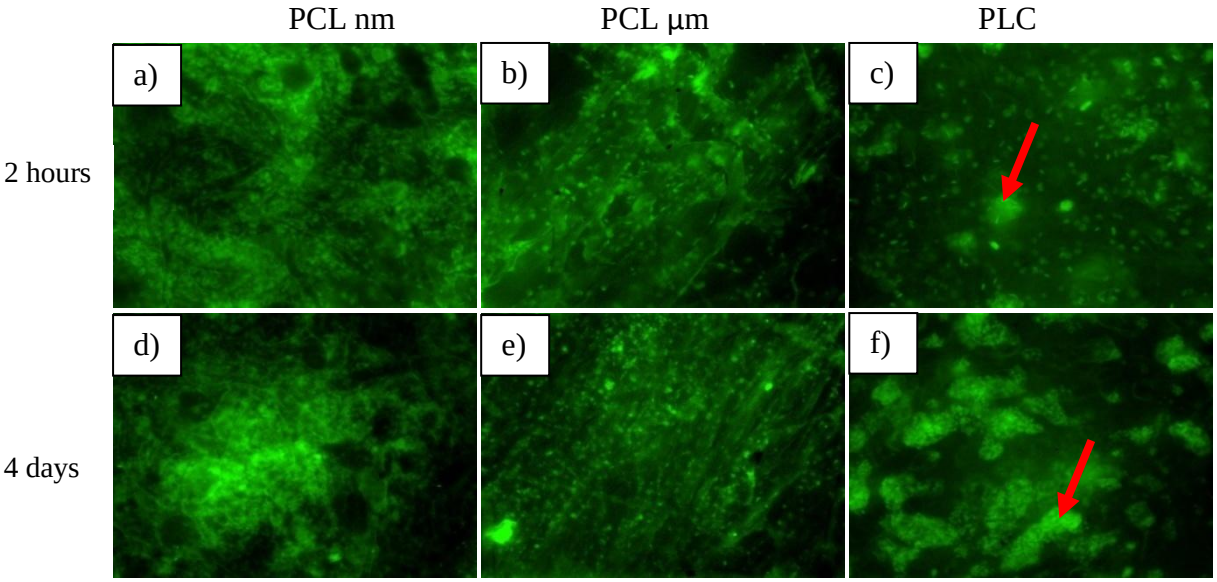

Figure 43: Fluorescence microscopic pictures of adhered thrombocytes to fibrous layers: PCL nm (a), PCL µm (b) and PLC (c) after 2 hours and after 4 days (d, e, f). Red arrows mark platelet aggregates formation found in PLC microfibrous layer.

The scaffolds incubated with thrombocytes were also evaluated by scanning electrone microscopy to see their morphology (figure 44). After 2 hours the nanofibrous PCL layer (PCL nm) contained the highest number of thrombocytes that corresponds with the result of MTT test. The surface of nanofibrous layer was fully covered with adhered thrombocytes. On the other hand, microfibrous structures allowed platelets to penetrate the layer and they were found not only on the surface as in case of nanofibrous structure. This could be an explanation of similar metabolic activity measured by MTT test.

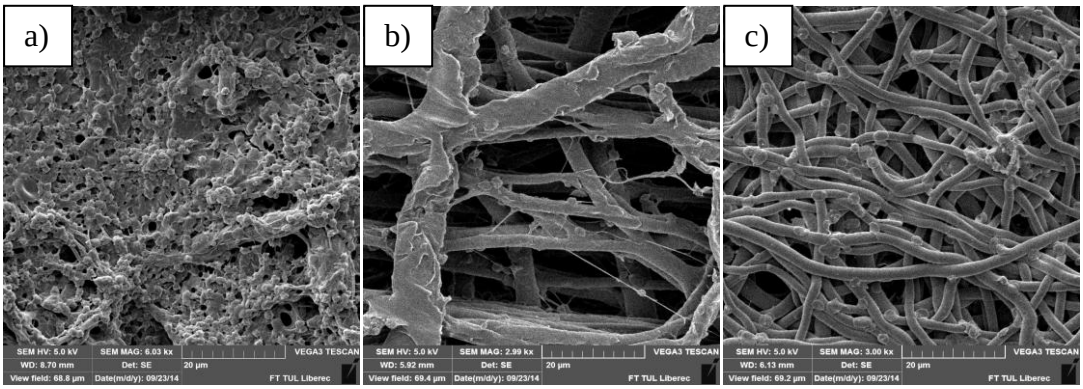

Figure 44: SEM pictures of adhered thrombocytes after 2 hours of incubation in thrombocyte rich solution on PCL nm (a), PCL µm (b) and PLC (c). Scale bars 20 µm.

The structure of adhered thrombocytes changed during the time of incubation. The following SEM pictures in figure 45 show the structure of platelets after 1 day and after 7 days of incubation. The platelets lost their viability after adhesion and activation during the incubation therefore their structure had changed.

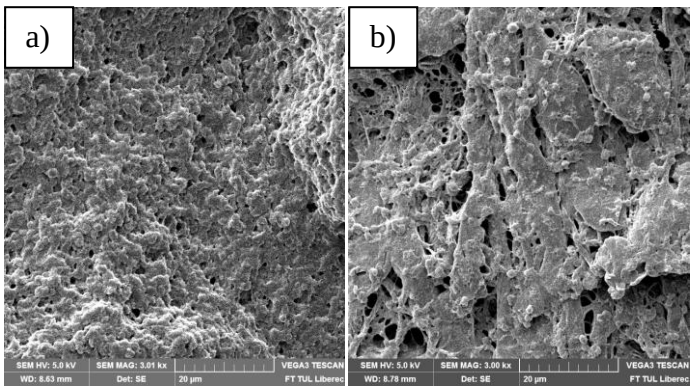

Figure 45: SEM pictures of adhered thrombocytes on nanofibrous PCL layer during the incubation: after 1 day (a) and after 7 days (b). Scale bars 20 µm.

The fibrous surface of tested polymers caused the activation of thrombocytes that is seen from SEM pictures below in figure 46. The structure of platelets changed from circular shape to the structure with many pseudopodia. The microfibrous structures also promote the creation of platelet aggregates that is also visible from fluorescence picture in figure 43 f.

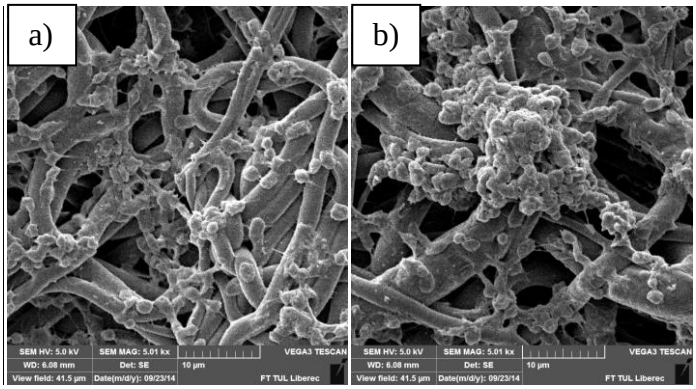

Figure 46: SEM pictures of activated platelets with many pseudopodia (a) and aggregated platelets (b) on microfibrous PLC layer after 1 day of incubation. Scale bars 10 µm.

In order to examine the influence of surface roughness, foils and electrospun layers were tested in similar way. The MTT results showed that fibrous layers activated more thrombocytes than foils prepared from the same materials as depicted in graph in figure 47.

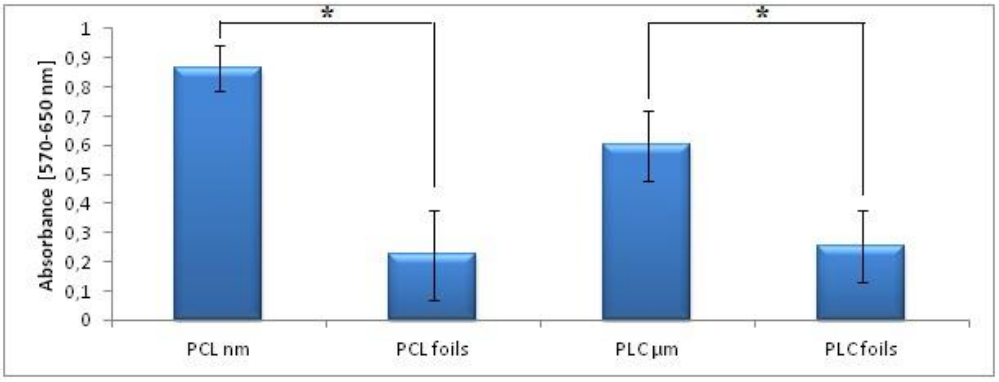

Figure 47: MTT test of thrombocytes incubated with electrospun layers (PCL nanofibrous and PLC microfibrous) and with foils with smooth surface (indicates $p < 0,05$).*

The rate of platelet activation was also visible in scanning electrone microscopic pictures. While fibrous layers were fully covered with spread thrombocytes as shown in previous pictures (Figures 44-46), smooth surfaces of foils were covered

by individual platelets in different stages of their activation. Circular resting platelets (indicated by blue arrows) as well as irregular shapes of thrombocytes with pseudopodia (indicated by red arrows) were found as seen in figure 48.

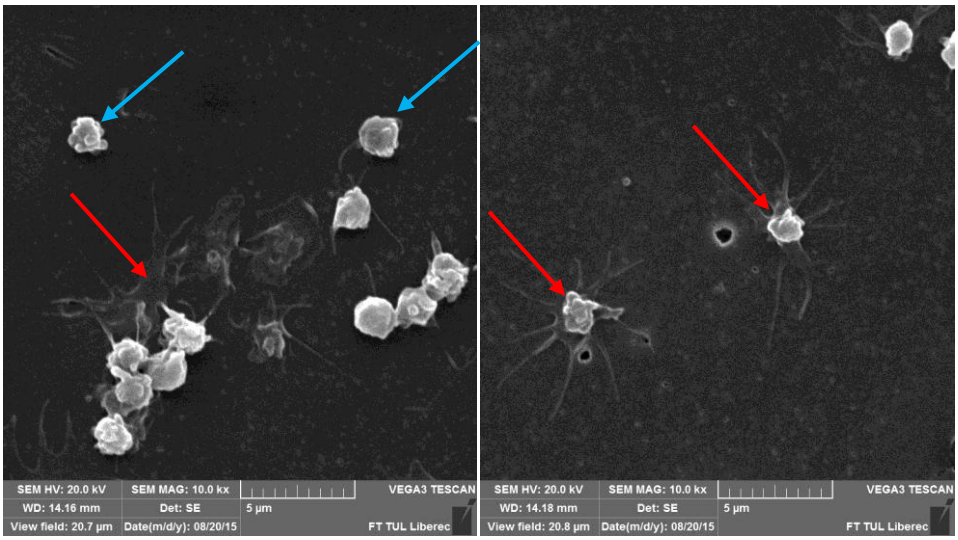

Figure 48: SEM pictures of platelets incubated in PLC foils. Red arrows mark activated spread platelets, blue arrows sign resting circular platelets. Scale bars 5 µm.

Conclusion of scaffold thrombogenic potential in static conditions

Incubation of nanofibrous and microfibrous scaffolds with thrombocytes did not show significant difference between PCL and PLC nor between nanofibrous and microfibrous layer made from PCL in terms of measured thrombocyte viability. There was a difference in platelet colonization of the scaffold. Nanofibrous layers did not allow the penetration to the inner structure therefore platelets were abundantly found on the surface. On the contrary, platelets incubated with microfibrous structures made from PCL and PLC were poorly spread over the surface but the platelets reached the inner parts of the scaffolds due to bigger pore sizes. Thrombocyte aggregate formation was typical in these pores.

Roughness of fibrous structure contributes to thrombocytes activation that was manifested by testing the same materials in 2 forms - electrospun fibers and smooth foils. It was found that smooth surface with the same chemical composition is less thrombogenic than corresponding fibrous surface. Electrospun layers were fully covered with thrombocytes whereas foils were covered by single platelets in different stage of their activation that was clearly visible from SEM pictures in figure 48.

4.3.2 Dynamic conditions for thrombogenicity assessment

Static incubation does not fully simulate conditions *in vivo* therefore bioreactor was employed to simulate platelet circulation. Blood flow is an important aspect that contributes to thrombocytes activation. The first prototype of bioreactor was designed and constructed in the Technical University of Liberec.

Materials and methods used for assessment of thrombogenic potential of scaffolds tested in dynamic conditions

The experiments were conducted in bioreactor that has been constructed in cooperation with M. Ackermann from the Department Applied Mechanics, Faculty of Technical Engineering, Technical University of Liberec. The device is depicted in figure 49. The bioreactor consisted of a transparent polymethylmethacrylate (PMMA) pipe with a core that allows testing of 4 tubular samples with inner diameter 6 mm and length of 10 cm. The system was placed in CO_2 incubator to maintain appropriate cell culture conditions as depicted in figure 50.

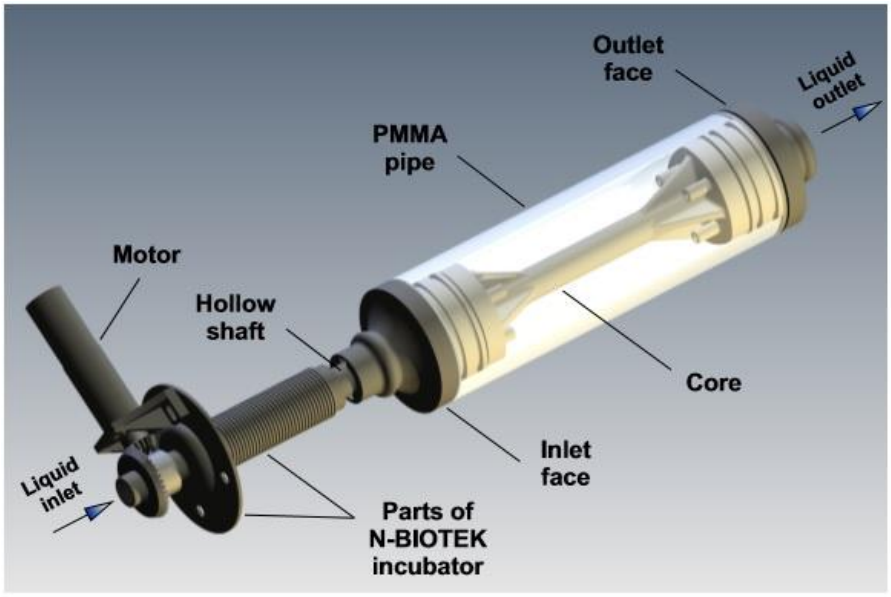

Figure 49: Description of bioreactor used for thrombogenicity assessment in dynamic conditions.

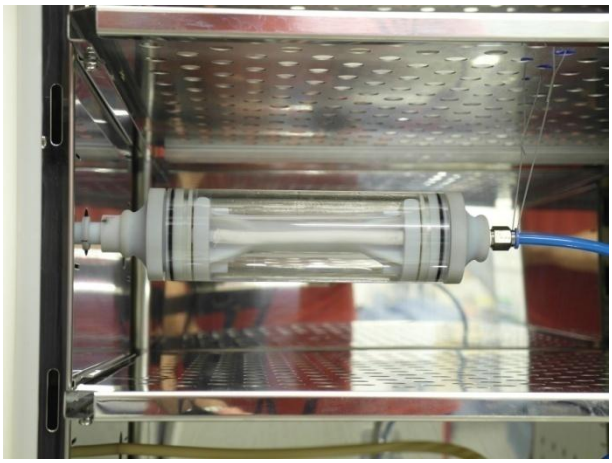

Figure 50: Photograph of bioreactor placed in CO_2 incubator used for dynamic thrombogenicity testing.

During dynamic conditions, two double layered PCL vascular graft (inner layer interacting with thrombocytes was composed of nanofibers, the SEM structure is depicted in figure 18) and two single layered microfibrous PLC grafts (SEM structure could be seen in figures 21 and 22) were attached in bioreactor and sterilized by 70% ethanol and washed with PBS. Subsequently, thrombocyte rich solution containing $914x10^6$ thrombocytes/ml was circulated through each tested graft for 2 hours (10 ml/min). The analysis of adhered thrombocytes was done by SEM only.

Results of thrombogenicity testing in dynamic conditions

After 2 hours of thrombocytes rich solution flow through the vascular grafts made from double layered PCL and microfibrous PLC, different morphology of adhered thrombocytes were found in SEM pictures. Thrombocytes adhered to nanofibrous structures and became activated and almost no circular platelet was found such as in the picture in figure 44 after static incubation. The nanofibrous PCL structure was covered by completely spread thrombocytes. In case of microfibrous PLC graft, the platelets were also spread but some of the circular platelets with pseudopodia were found. Nanofibers have high surface to volume ratio therefore it was assumed that the activation of thrombocytes will be higher. No quantitative data were obtained from this experiment but different morphology of platelets was found. The flow of thrombocytes rich solution contributed to higher platelet activation compared to static conditions.

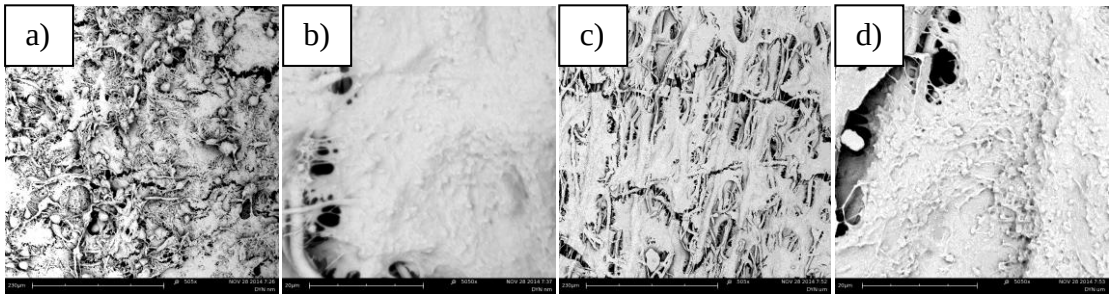

Figure 51: SEM pictures of vascular graft thrombogenicity tests under flow conditions: inner nanofibrous layer of PCL vascular graft in low (a) and high magnification (b) and microfibrous PLC vascular graft in low (c) and high magnification (d). Scale bars 230 μm (low magnification), 20 μm (high magnification).

Conclusion of thrombogenicity evaluation in dynamic conditions

The difference found in thrombocytes morphology after static and dynamic conditions pointed the necessity of working as close as possible to natural environment of cells. Nanofibrous PCL layer attracted more thrombocytes during static and dynamic conditions. When tested in bioreactor, thrombocytes in nanofibrous PCL layer possessed completely spread structure compared to microfibrous PLC layer. However, these preliminary qualitative results have to be supported by further studies focused on experimental design and evaluation of thrombogenicity testing.

4.4 Evaluation of tested materials

Electrospun layers made from biodegradable polymers that were described in the previous chapter were tested *in vitro*. The first test compared electrospun PCL and PLC layers having similar fiber diameter around 1 μm (PCL 0,96 ± 0,76 μm; PLC 1,03 ± 0,71 μm). Copolymer PLC significantly supported fibroblast proliferation on those scaffolds compared to PCL one probably due to the lower hydrophobicity of the surface that corresponds with the assumption that slightly hydrophilic surfaces supports cellular adhesion due to the adhesion of proteins in right conformation. Similar results were obtained by using endothelial cells. Copolymer PLC was endothelialized faster than PCL. Another tested hypothesis was whether nanofibers support endothelial cell adhesion but this assumption has not been proved. The design of ideal vascular graft has to be remake according to these findings. Nanofibers also activated more thrombocytes than microfibrous layers.

Taken together, even if copolymer PLC was not able to create previously designed double layered graft, it seems that other materials properties in general are more important when considering ideal material for usage in vascular tissue engineering applications. Copolymer PLC has excellent mechanical properties, it is less hydrophobic than PCL and it supports cell adhesion and proliferation. Based on the copolymer PLC properties besides its microfibrous morphology it could be stated that the material is more beneficial for vascular tissue engineering in terms of better surface wettability properties, higher elongation, mechanical strength, cytocompatibility with both tested cell lines (fibroblasts and endothelial cells) and lower thrombogenicity compared to PCL. Another important property of polyesters is their degradation rate that strongly influenced *in vivo* performance. The degradation studies will be carried out as well in order to fully characterize suitability of presented materials. However, the results are not a part of the thesis.

5 Vascular grafts releasing nitric oxide

The third experimental section of the thesis was done during my Fulbright-Masaryk fellowship at Michigan Technological University (MTU), Department of Biomedical Engineering. The aim of the research was the development of a long-term nitric oxide (NO) releasing polymeric vascular graft by blending different NO releasing compound from the group of S-Nitrosothiols with PCL by the way of electrospinning. The section describes synthesis of NO donors, NO release measurement, *in vitro* testing of modified scaffolds using endothelial cell line and *in vivo* testing of control and NO releasing vascular grafts. All experiments except of *in vitro* tests were done in MTU.

5.1 Modification of PCL vascular grafts by NO releasing compounds

In this section, preparation of selected NO donors from the group of S-Nitrosothiols is described together with its incorporation into vascular grafts made from PCL. The fibrous morphology and NO release kinetics are described. Produced grafts were tested *in vitro* and *in vivo* in order to confirm long term NO release and its consequences on vascular functions mentioned in theoretical part of the thesis.

5.1.1 Synthesis of nitric oxide releasing compound

Firstly, representative NO donors from the group of S-Nitrosothiols were chosen. At the beginning, variety of substances weas tested for NO release such as spermine, spermidine, and fumed silica nanoparticles capable of NO release etc. However, the best results were achieved using 2 NO releasing compounds - S-Nitrosoacetyl-D-penicillamine (SNAPs) and S-Nitrosoacetyl-D-penicillamine derivatized cyclam (SNAP-cyclam). Representative compound SNAP was chosen as a model substance that has already been published *(Gierka, 2011)*. Newly synthesized compound, SNAP-cyclam, was studied for long term NO release. This compound was discovered in MTU and its characterization was carried out by C. McCarthy, Department of Biomedical Engineering, MTU.

Materials used were purchased from Sigma Aldrich except of 1, 4, 8, 11-tetraazacyclotetradecane (cyclam) and tert-butyl nitrite that were obtained from Acros Organics.

S-Nitrosoacetyl-D-penicillamine

The chemical structure of NO releasing compoung, S-Nitrosoacetyl-D-penicillamine (SNAP), is depicted in figure 52. SNAPs were prepared by dissolving of 200 mg N-acetyl-D-penicillamine (NAP) in 5 ml of methanol. After short sonication, acids were added in amount of 1,5 ml of 1M HCl and 100 µl 17,8M H_2SO_4. Afterwards, sodium nitrite (144,9 mg) was added. The mixture was vortexed and let react for at least 30 minutes until a pale green color has developed. Subsequently the solution was cooled on ice for 45 minutes until crystals begin to precipitate and a dark green/red color developed. Finally, methanol was removed using rotary evaporator (40°C water bath) and green crystals were collected after complete evaporation of solvents. After SNAPs synthesis, the crystals were stored in 4°C protected from light.

For modification of PCL vascular grafts, electrospinning solutions containing 16 wt% PCL and 0,2 wt% of SNAPs were prepared after a series of optimization experiments. Maximum amount of SNAPs (M_w=220,25 g/mol) dissolvable in the electrospinning solution was about 0,6 wt%. Higher amount of SNAPs added to the electrospinning solution led to increased initial burst of NO, not to prolonged NO release in time as expected. Therefore this low concentration was chosen for further experiments otherwise the initial burst was too high when higher amount of SNAPs was added to the electrospinning solutions.

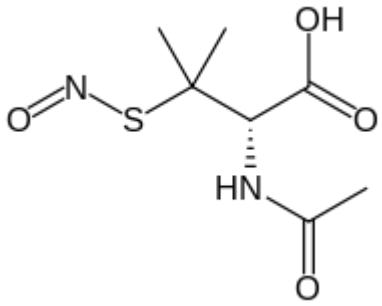

Figure 52: Structure of S-nitroso-N-acetylpenicillamine (SNAP).

S-Nitrosoacetyl-D-penicillamine derivatized cyclam

N-acetyl-D-penicillamine-thiolactone was prepared according to a previously published method by *Riccio et al., 2012*. Briefly, N-acetyl-D-penicillamine was

dissolved in pyridine and cooled on ice for 1 hour. This solution was mixed with equal volumes of ice chilled acetic anhydride dissolved in pyridine. The mixture was stirred for 24 hours until the solution turned light red. The solvents were removed using a rotary evaporator at 45-60°C. The remaining liquid was re-dissolved in chloroform, followed by three extractions with 1M HCl. The organic layer containing NAP-thiolactone was dried using magnesium sulfate. The remaining chloroform was removed with the rotary evaporator. Solid particles were resuspended in hexanes, and crystals were collected using vacuum filtration.

NAP-cyclam was prepared by dissolving two components: NAP-thiolactone and cyclam in chloroform in a stoichiometric ratio of 2:1. The solutions were combined and allowed to react for 2 hours. Chloroform was removed by flash evaporation using a rotary evaporator (200 rpm, 35°C). The resulting crystals were vacuum dried for 2 hours.

Tert-butyl nitrite was prepared for use by cleaning with an aqueous 30 mM cyclam solution to chelate copper ions. Copper ions are used to stabilize the tert-butyl nitrite.

NAP-cyclam was converted to its nitrosated form—SNAP-cyclam—by the addition of clean tert-butyl nitrite immediately prior to electrospinning. Firstly, NAP-cyclam was dissolved in concentration that should be theoretically capable of releasing of 10mM NO (0,2734 wt %) in chloroform/ethanol/acetic acid (8/1/1 v/v/v). Secondly, 150 μl of clean tert-butyl nitrite was added to this solution. The solution was allowed to react for 24 hours until the solution turned green in color. Samples were protected from light until electrospinning commenced. The proposed structure of newly synthesized compound, SNAP-cyclam (M_w=546,794 g/mol), is depicted in figure 53.

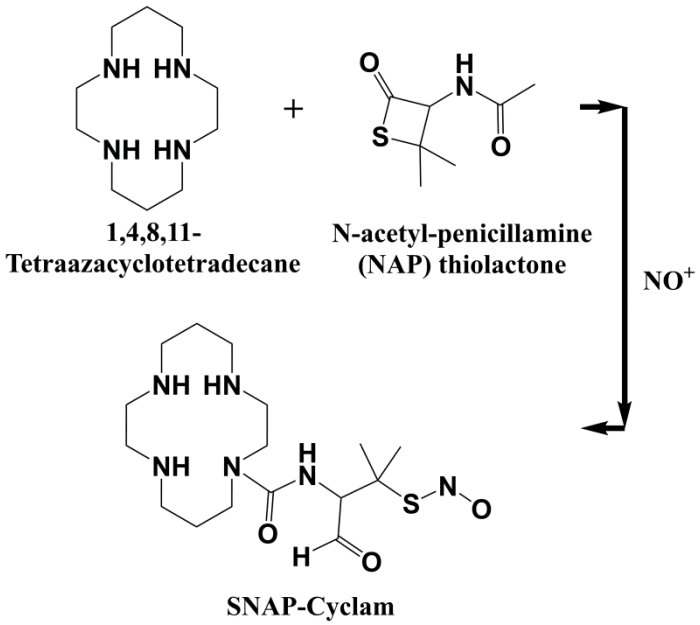

Figure 53: Chemical structure of SNAP-cyclam that is produced from 1,4,8,11-tetraazacyclotetradecane (cyclam) and NAP-thiolactone.

5.2 Vascular graft preparation and characterization

Vascular grafts made from poly-ε-caprolactone (PCL, Sigma Aldrich, M_n=45,000) were obtained by electrospinning a 16 wt% of PCL dissolved in chloroform/ethanol/acetic acid (8/1/1 v/v/v) using similar device as described in chapter 3 Synthetic vascular grafts preparation and testing (figure 9). Vascular grafts with long-term NO release were prepared by mixing the SNAPs (0,2 wt%) or SNAP-cyclam (0,2734 wt%) into the PCL electrospinning solution. The final concentration of NO releasing compounds was optimized by: the amount of compounds added to the electrospinning solution (a), the way of preparation of electrospinning solution (b), the release kinetics of produced grafts (c). After a series of optimization procedure of electrospinning solution preparation, the electrospinning parameters were set as follows: the solution was charged at 20 kV and ejected through a 22 G needle at a constant rate of 2,54 ml/h. The fibers were collected on a rotating stainless steel mandrel at a rotational speed of 250 rpm. The mandrel with 1,65 mm inner diameter was placed 15 cm from the needle tip. After electrospinning, the tubes were easily removed from the collector and placed under vacuum for 2 hours to evaporate any residual solvent.

Fiber morphology was evaluated by field emission scanning electrone microscopy (FESEM) on a Hitachi S-4700. The samples were sputter coated

with platinum/palladium to a thickness of 5 nm and observed at low and high magnification to compare the inner and outer surface of each graft. Fiber diameter was measured based on FESEM images at 15 000x magnification. For each sample, five images were analyzed, and 50 fibers were manually measured and analyzed on each image using NIH Image J software *(Rasband, 1997-2014).*

Produced scaffolds were about 5 cm in length, 1,65 mm inner diameter with a wall thickness between 500 and 700 μm. Fiber morphology can be seen in figure 56. The layers have not shown any difference in morphology when NO releasing compounds were added. Tubular scaffold made from PCL had average fiber diameter of 143 ± 80 nm, PCL modified by SNAPs 154 ± 61 and PCL modified by SNAP-cyclam 179 ± 182 nm.

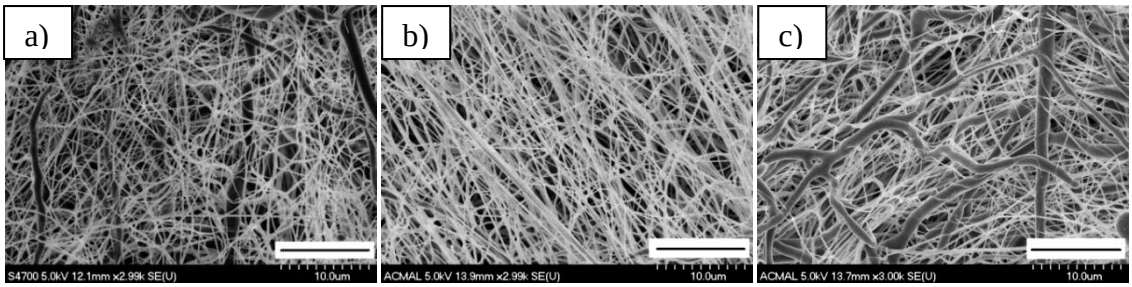

Figure 54: Scanning electrone microscopy pictures of electrospun 16 wt % PCL (a), 16 wt % PCL+SNAPs (b), 16 wt % PCL+SNAP-cyclam (c). Scale bars 10 μm.

Further morphological evaluation was carried out with vascular grafts made from 16 wt% PCL (control graft) and PCL graft modified by SNAP-cyclam. Measurement of fiber diameters was performed on the inner and outer graft surfaces showing no difference between the two graft types or between their respective inner and outer surfaces. The morphology of produced grafts is depicted in figure 55. In addition to fibers, polymeric beads are seen in the structures of both control and NO-releasing PCL grafts. The summary of fiber diameter measurement is summarized in the figures 55 and 56 where average fiber diameters measured in inner and outer side of the grafts are plotted.

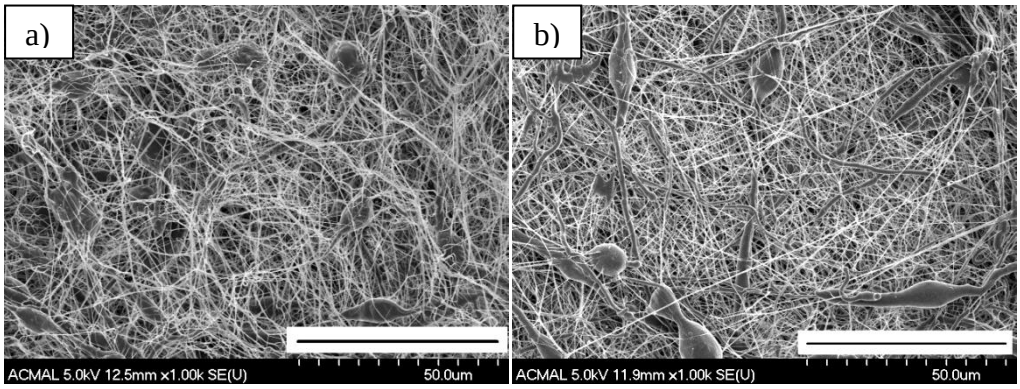

Figure 55: SEM images of a PCL control (a) and NO releasing vascular graft made from PCL+SNAP-cyclam (b). Scale bars 50µm.

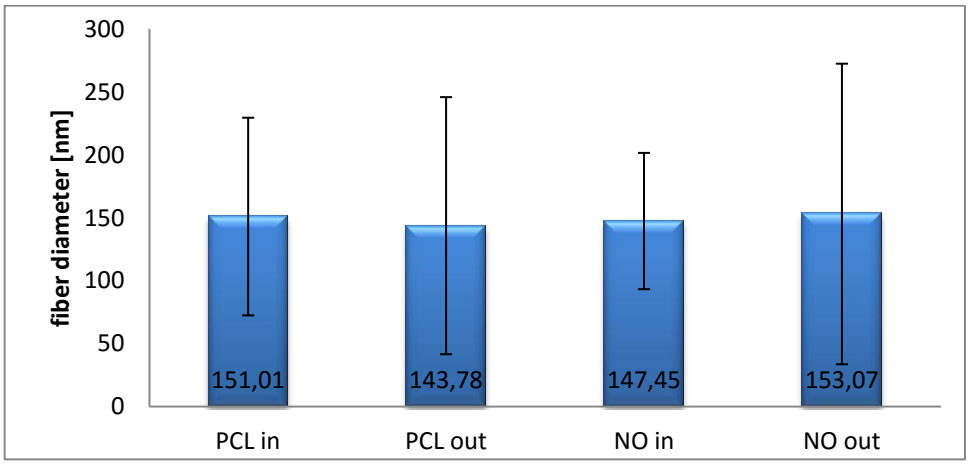

Figure 56: Fiber diameter of produced vascular grafts: "in" signifies inner surface, "out" marks outer surface (p<0,05).

The similarity of inner and outer side of the tubular grafts was in contrast to the previous experiments provided in Technical University Liberec even if the material of the collector and polymeric solution were similar (see figure 14). Possibly the collector diameter (1,65 mm) could play an important role.

5.3 NO release measurement

Measurement of NO release was carried out using a Siever's Nitric Oxide Analyzer (NOA) that is based on chemiluminiscence reaction of NO with ozone yielding to nitrogen dioxide in its activated state (NO_2^*) that is relaxed by photon emission (hν) to nitrogen dioxide:

$$NO + O_3 \rightarrow NO_2^* + O_2$$

$$NO_2^* \rightarrow NO_2 + h\nu$$

The device offers the most versatile detection system for NO analysis. Samples releasing NO were measured immersed in PBS at 37°C to imitate conditions in the body. As mentioned in the theoretical part (section 2.2.6), S-Nitrosothiols release NO group in the presence of copper ions and ascorbic acid. Therefore when NO release declined, these agents were added to PBS and further NO release was detected.

Data from NOA measurement were collected in parts per billion NO released (ppb) that were further recalculated by known constant of calibrated NOA to NO Surface Flux with the unit of moles/(min x cm^2). The calibration constant was 1,25799 x 10^{-13} mol/s ppb. Commonly, the data are represented in units of moles/(min x cm^2) but nanofibers possess high surface to volume ration, its surface is impossible to calculate. Therefore the data from NOA were related to the mass weight of measured sample in units of mg/cm^2. When a single evaluation of NO release was carried out, the unit in the graph is represented as moles/(min x cm^2 x mg). When two samples were compared for NO release kinetics, the weight of the samples was omitted and standard units of moles/(min x cm^2) were used. Samples of the same size and similar weight were always measured in order to avoid any data misinterpretations.

5.3.1 Comparison of NO release between SNAPs and SNAP- cyclam

Two NO releasing vascular grafts containing either SNAPs or SNAP-cyclam were tested for NO release using a Siever's Nitric Oxide Analyzer (Boulder, CO). One centimeter PCL vascular graft modified by NO releasing compounds was weighted and put into PBS to measure NO release. A dry nitrogen sweep gas (200 ml/min) was used to carry the generated NO to the analyzer. After an initial burst of NO measured for 60 minutes, 200 μl of 0.1M aqueous $CuCl_2$ and 0.1M ascorbic acid were added to the PBS solution containing the sample and additional NO release was observed. The samples were put to PBS and NO release measurement was repeated after 24, 48 and 72 hours with shortened period (5 minutes) of NO release measured in PBS only. The third day, UV light (RX Firefly; 400 nm, Phoseon Technology) was used to photolytically release NO from the material. The lamp was placed against the clear glass sampling tube containing the sample and activated for 1 minute in order to determine if a further reservoir of NO was available. Due to the presence of NO donors after 3 days, the samples were kept at 37°C for total of 42 days when measurement of NO release using NOA was repeated.

At the beginning of a 42 days long experiment, the initial burst of NO was about $1x10^{-8}$ moles/(min*cm^2*mg) in case of SNAPs and $2x10^{-8}$ moles/(min*cm^2*mg) when SNAP-cyclam was incorporated in PCL. The NO release was diminished during 60 minutes of measurement until external $CuCl_2$ and ascorbic acid were added. Higher NO flux the addition of NO release initiates was observed with SNAP-cyclam modification of PCL (see figure 57).

a) b)

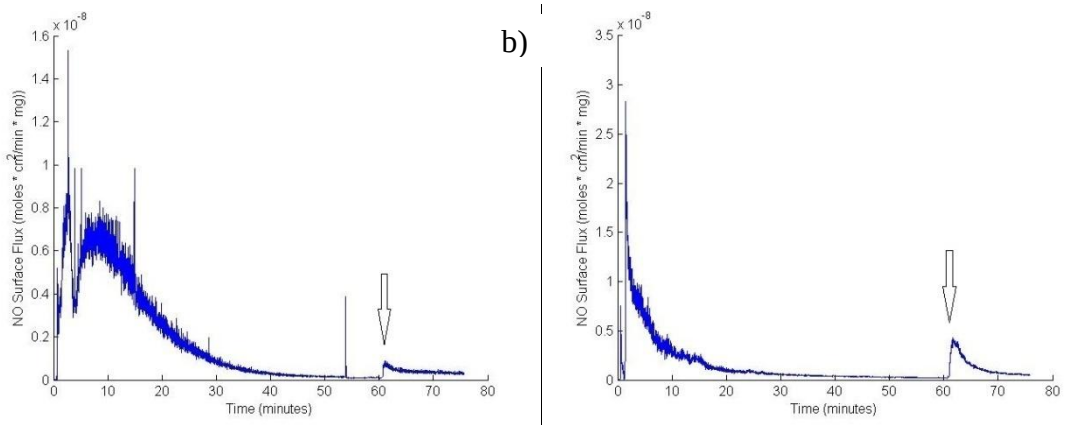

Figure 57: NO release profile of PCL+SNAPs (a) and PCL+SNAP-cyclam (b) measured in PBS solution. After 60 minutes, $CuCl_2$ and ascorbic acid were added to PBS solution (indicated by an arrow).

The measurement of NO release was repeated after 24 and 48 hours of incubation in PBS at 37°C. Because of the decrease of spontaneous NO release in PBS only, the external $CuCl_2$ and ascorbic acids were added in minute 6 (corresponds to peaks indicated by arrows in figure 58). The level of released NO was in the same order of 10^{-11} moles/(min x cm^2) but there was a difference between the releasing kinetics. SNAP-cyclam showed more stable NO release for 15 minutes whereas modification with SNAPs lead to fast consumption and decreasing of released NO.

a)

b)

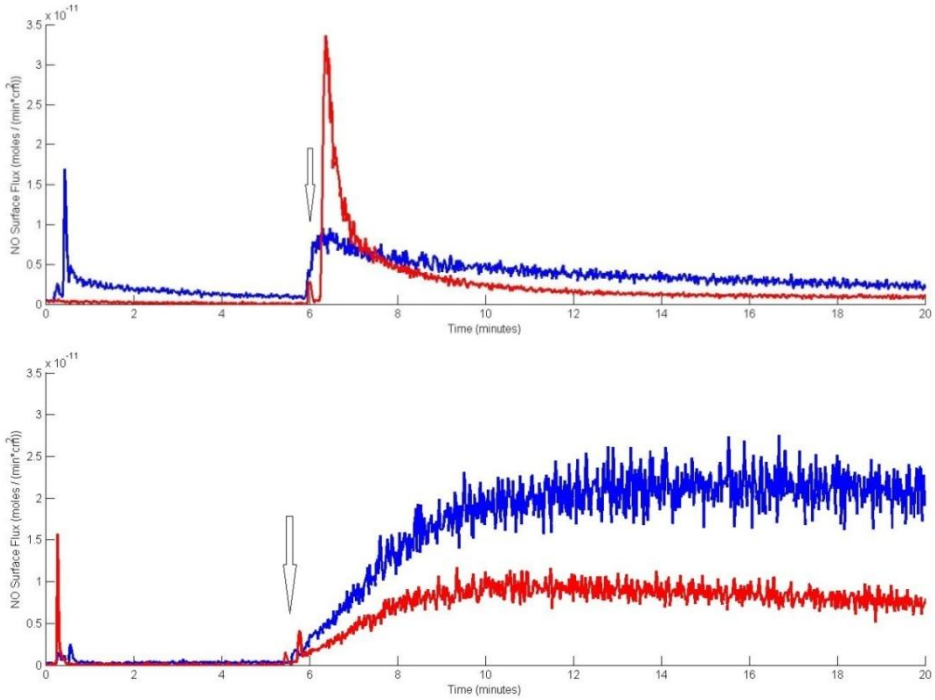

Figure 58: NO release profile of PCL+SNAPs (a) and PCL+SNAP-cyclam (b). Blue line shows NO release after 24 hours of incubation, red line after 48 hours of incubation in PBS at 37°C. The increase in minutes 6 refers to addition of $CuCl_2$ and ascorbic acid to the solution indicated by an arrow.

The vascular grafts after 72 hours of incubation were illuminated by UV for 1 minute showing the presence of NO reservoir within the fibers. Due to the fact that another mechanism of S-NO cleavage is used, the NO fluxes reached higher values than in PBS with addition of $CuCl_2$ and ascorbic acid. As previously, the SNAP-cyclam within PCL fibers proved one order higher NO release (surface flux about $4x10^{-9}$ moles/(min*cm^2*mg)) compared to SNAPs modification with surface flux about $4x10^{-10}$ moles/(min*cm^2*mg) as shown in figure 59.

a)

b)

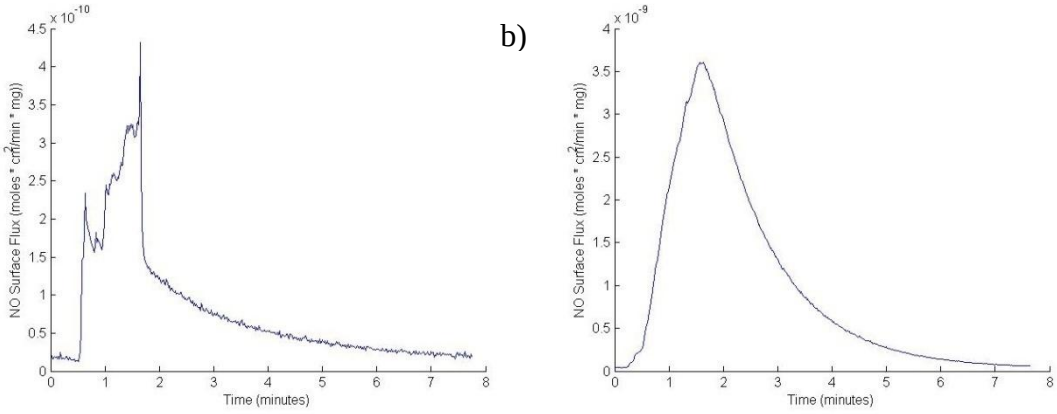

Figure 59: NO release of PCL+SNAPs (a) and PCL+SNAP-cyclam (b) after illumination of the samples using UV light for 1 minute after 72 hours of incubation.

Tubular scaffolds were placed again in PBS at 37°C and the NO release measurement was repeated after 42 days of incubation. In figure 60 there is depicted the comparison of NO release from PCL containing SNAPs and SNAP-cyclam after 3 days (blue line) and 42 days (red line). After 42 days the vascular graft made from PCL + SNAPs showed NO surface flux of $6*10^{-12}$ moles/(min*cm^2) compared to PCL + SNAP-cyclam with NO surface flux of an order higher ($6*10^{-11}$ moles/(min*cm^2)). Modification of vascular grafts by incorporation of SNAP-cyclam led to physiological NO flux (50-400 pmol/min*cm^2) when reducing agents were present as depicted in figure 60 b. Vascular grafts modified by SNAPs produced one order lower levels of NO flux after 42 days in PBS at 37°C compared to physiological levels released from endothelial cells.

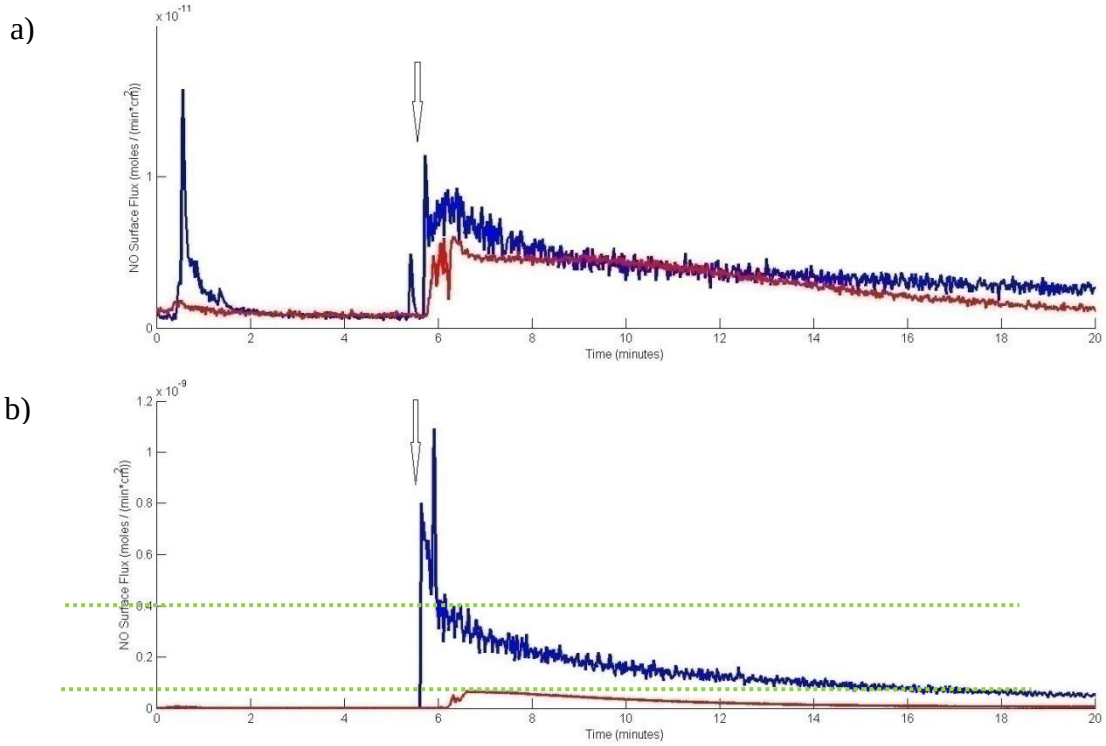

Figure 60: NO release profile of PCL+SNAPs (a) and PCL+SNAP-cyclam (b). Blue line shows NO release after 3 days of incubation, red line after 42 days of incubation in PBS at 37°C. The peak in minute 6 refers to addition of $CuCl_2$ and ascorbic acid to the solution indicated by an arrow. Green lines displays physiological NO release by endothelial cells that is achieved only by using SNAP-cyclam (b).

These complex measurements of NO release showed that newly synthesized compound, SNAP-cyclam, is capable of stable and long term NO release

in physiological levels therefore further characterization was performed with this compound only.

5.3.2 NO release from SNAP-cyclam in PCL vascular grafts

It was shown in previous experiments that incorporation of newly synthesized compound SNAP-cyclam is capable of NO release in physiological levels up to 42 days of incubation in PBS at 37°C. However, it is known that NO release is influenced by chemical composition of the environment. In order to simulate body conditions, vascular grafts were incubated in PBS and in complete medium between NO release measurements. Vascular grafts made from PCL modified by SNAP-cyclam (length 1 cm) were weighted and incubated in PBS as well as complete medium consisting of Dulbecco's Modified Eagle's Medium (DMEM), 10% fetal bovine serum and 1% penicillin/streptomycin. The data obtained by incubation in PBS/complete medium should simulate the environment *in vivo* where the same vascular grafts were further implanted for time period of 10 days. Nitric oxide release from the samples immersed in PBS and complete DMEM was assessed at time points of 1 hour, 3 days and 10 days after washing twice in PBS. All samples were immersed in PBS at 37°C during analysis. After an initial burst of NO measured for 60 minutes, 200 µl of 0,1M aqueous $CuCl_2$ and 0,1M ascorbic acid were added to the PBS solution containing the sample to stimulate NO release. At 1 hour time point, $CuCl_2$ and ascorbic acid solutions were added after 60 minutes of measurement in PBS because of high level initial burst of NO. At later time points (3 days and 10 days), the release in PBS was diminished, so the initial measurement in PBS was shortened to 5 minutes followed by 15 minutes of measurement after the introduction of $CuCl_2$ and ascorbic acid solutions. Cumulative NO release was determined by plotting the release data and determining the area under the curve using a calibration constant specific to the machine. After 10 days of incubation, UV light was used as previously described to measure remaining NO-releasing groups within the fibers.

Nitric oxide releasing PCL grafts were evaluated for NO release after 1 hour incubation period bathed in PBS (figure 61, blue line) and in complete DMEM (figure 61, red line) which are conditions that are known to promote NO release from the polymer composite. The grafts display an initial burst of NO immediately after soaking in PBS between $2x10^{-10}$ moles/(min*cm^2) and $4,5x10^{-10}$ moles/(min*cm^2)

that is similar to physiological levels released from endothelial cells. NO release decreased with time until $CuCl_2$ and ascorbic acid were added after 60 minutes. Addition of exogenous solutions caused an increased NO release to comparable levels as measured during the initial burst in PBS.

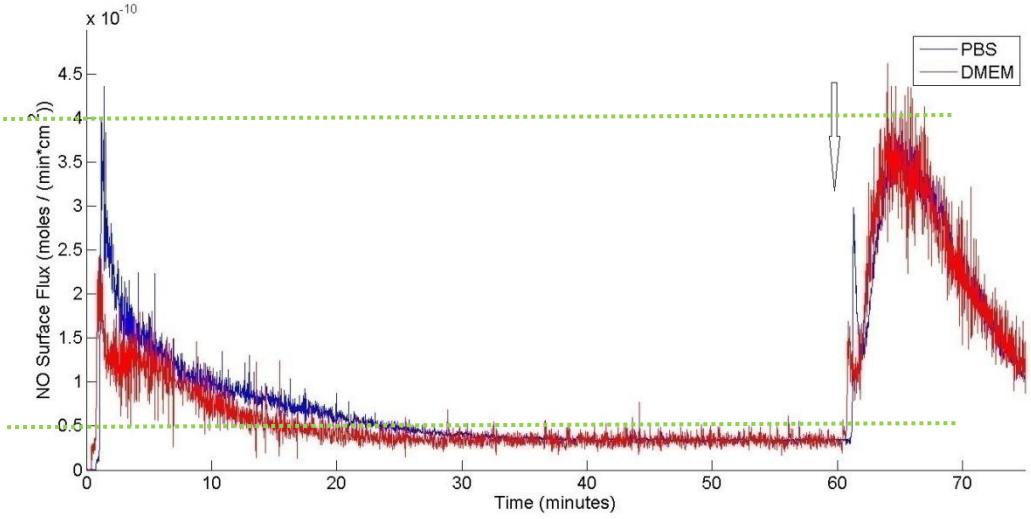

Figure 61: NO release from a SNAP-cyclam PCL graft after 1 hour bathing in PBS (blue line) and in complete DMEM (red line). After 60 minutes, $CuCl_2$ and ascorbic acid were added to the PBS solution, stimulating the further release of NO (indicated by an arrow). Green lines displays physiological NO release by endothelial cells.

After measurements were taken at the one hour time point, the grafts were incubated at 37°C in PBS and complete DMEM for 3 and 10 days. The surface flux was reduced after 3 and 10 days of incubation when measured in PBS but after the addition of $CuCl_2$ and ascorbic acid, NO release increased to $1x10^{-11}$ moles/(min*cm^2) when incubated in PBS and $3x10^{-11}$ moles/(min*cm^2) when incubated in complete DMEM (data not shown). To compare the total NO release during 10 days of incubation in PBS solution containing $CuCl_2$ and ascorbic acid, cumulative NO release after the addition of $CuCl_2$ and ascorbic acid was plotted in figure 62.

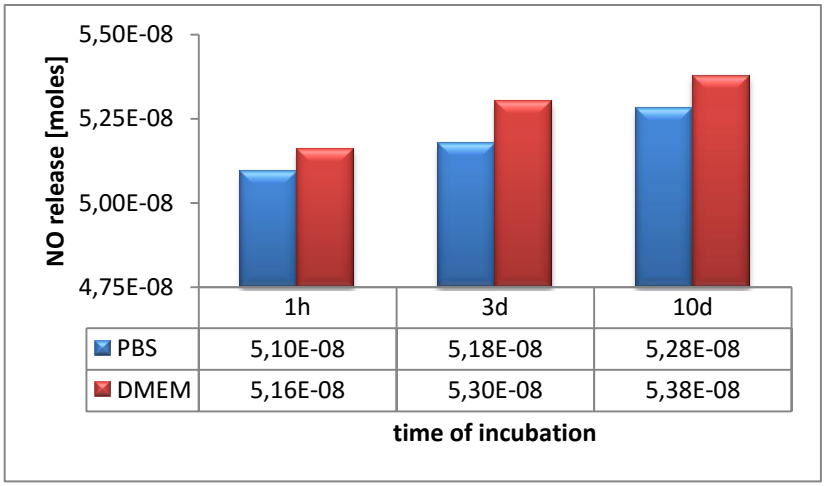

Figure 62: Cumulative NO release measured from vascular graft for 15 minutes in PBS with the addition of $CuCl_2$ and ascorbic acid after incubation in PBS/complete DMEM for 1 hour, 3 days and 10 days. N=1 for each sample type.

After 10 days of incubation, the NO releasing samples were exposed to UV light (400 nm) for 1 minute to demonstrate continued control of NO release from the grafts. The results indicate that after 10 days of storage in PBS and complete DMEM, a physiologically relevant reservoir of NO remains available for further NO release. UV light exposure was limited to 1 minute. However, this provoked NO release from the grafts for more than 20 minutes (figure 63).

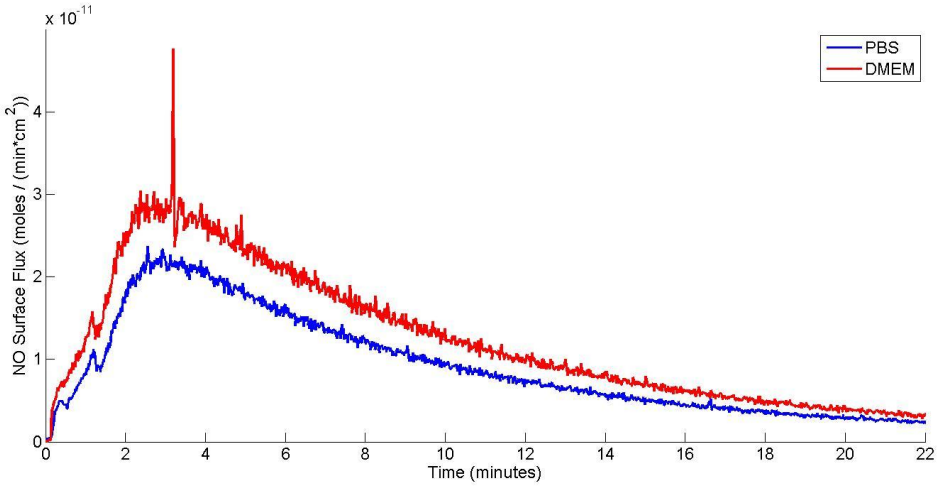

Figure 63: NO release measured after exposure to a 400 nm UV light for 1 minute, N=1 for each sample type.

5.3.3 Evaluation of NO releasing materials

Modification of PCL vascular graft was carried out by choosing appropriate substances capable of nitric oxide release. Representative compounds from the group

of S-Nitrosothiols - SNAPs and SNAP-cyclam were blended with PCL electrospinning solution and modified vascular grafts were produced. NO release kinetics was studied for 42 days *in vitro* showing that incorporation of SNAP-cyclam enables the NO release in physiological levels up to 42 days in *in vitro* conditions. Further assessment of NO release from SNAP-cyclam modified PCL vascular graft was carried out in 2 mediums - buffer PBS and complete medium. It was confirmed that vascular graft containing SNAP-cyclam is capable of NO release in physiological conditions such as endothelial cells when incubated in PBS or complete medium (see Figure 61). Therefore, this type of graft was chosen as an ideal candidate for further *in vitro* and *in vivo* tests.

5.4 Seeding of endothelial cells

Electrospun layers made from 16 wt% PCL and 16 wt% PCL containing 0,2 wt% nitrosated SNAP-cyclam (synthesized and delivered from Michigan Technological University) were prepared by needle electrospinning using flat collector. Previously, slightly higher amount of the compound was added but the nitrosation had taken place within the electrospinning solution. MTU prepared nitrosated form of SNAP-cyclam therefore lower concentration (similar to SNAPs concentration) was used for electrospinning in Technical University of Liberec. The electrospinning conditions were set as follows: 18 cm distance between the needle and the planar aluminium foil collector, 15 kV voltage, speed of polymeric solution dosage 3 ml/h, temperature 23°C, relative humidity 40%. Evaluation of affect of NO for endothelial cells was done by seeding the samples(0,6 mm in diameter) with human umbilical vein endothelial cells (HUVEC, passage 6) as described previously in chapter 4 Biological testing of vascular grafts, subchapter 4.2 (*In vitro* tests with endothelial cells). The analysis was done by MTT test and SEM.

Cell viability was measured during the time of cultivation in days 1, 3, 7 and 14. Cells adhered to the scaffold and start to proliferate through the surface. Statistically significant difference in cell viability was found within cells cultured on PCL layer modified by SNAP- cyclam at day 1, 3 and 7.

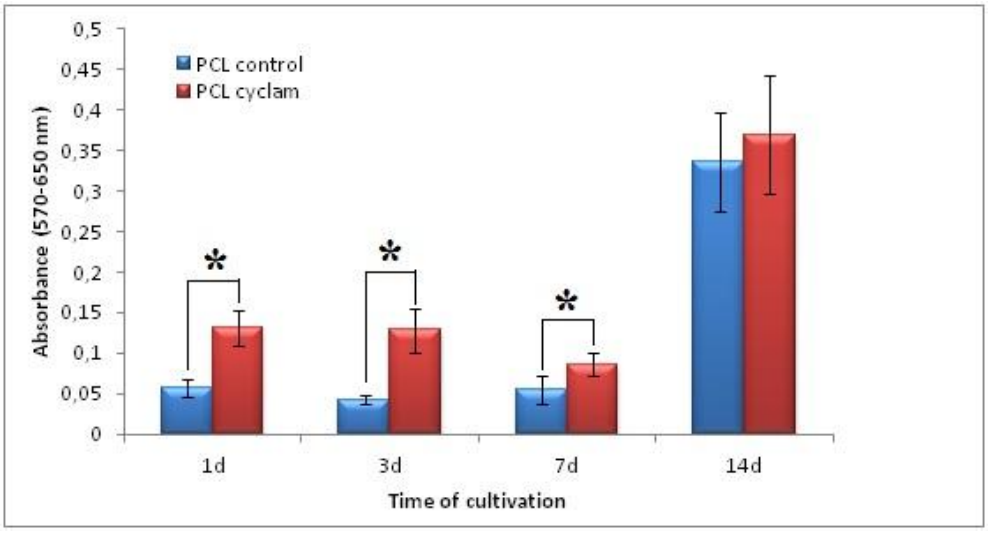

*Figure 64: Cell viability measured by MTT test after 1, 3, 7 and 14 days of scaffold cultivation with human umbilical vein endothelial cells on control PCL scaffold and on modified scaffold by SNAP-cyclam (PCL cyclam) (*indicates $p < 0,05$).*

Scanning electrone microscopy pictures (figure 65) show endothelial cells after 2 weeks of culturing. Endothelial cells started to create a monolayer on the scaffold surface, especially on PCL modified by SNAP-cyclam (figure 65 b).

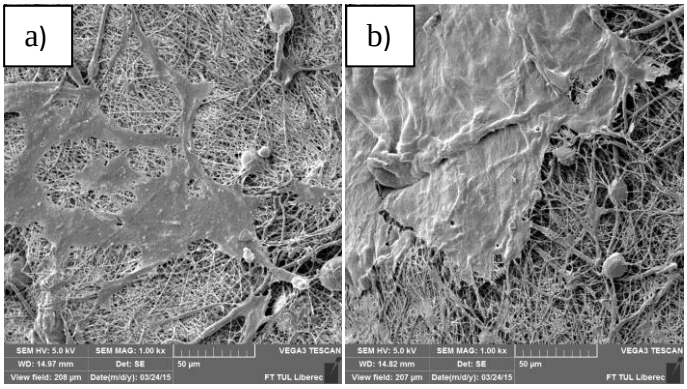

Figure 65: Scanning electrone microscopy pictures of human umbilical vein endothelial cells after 14 days of culturing on: a) PCL control, b) PCL modified by SNAP-cyclam. Scale bars 50 µm.

The viability of human umbilical vein endothelial cells was supported by NO release during the first week of cell culture. The NO release could be diminished by the way of sterilization. Previous experiments of NO release measurement described above were carried out with non-sterile samples in contrary to *in vitro* tests that were made with samples after 30 minutes soaking in ethanol followed by double washing

in PBS. The duration of NO release could be also accelerated in endothelial basal medium that contains ascorbic acid known as NO releasing promoter.

5.5 In vivo implantation

The *in vivo* experimental protocol was approved by the Michigan Technological University Institutional Animal Care and Use Committee. Six Sprague Dawley rats received an abdominal aorta replacement graft with an inside diameter of 1,65 mm and wall thickness of 685,5 ± 53,3 μm, of which three were pure electrospun PCL controls, and three were experimental NO releasing, electrospun vascular grafts containing 10 mM SNAP-cyclam that was fully characterized by NO releasing measurement described in chapter 5.3.2. Samples for *in vivo* implantation were sterilized by immersion in 70% ethanol for 10 minutes. Rats were anesthetized with 2,1% inhaled isoflurane in oxygen. A midline laparotomy incision was performed and the abdominal aorta was isolated. Side branches from a 10 mm long segment of the artery between the renal and femoral bifurcations were tied off to prevent collateral blood flow from within the segment. The proximal and distal ends of the segment were clamped and the artery was severed near the midpoint of the 10 mm segment. A microdose (~10 μL) of 200 units/mL heparin was administered to the exposed ends of the artery. The polymeric grafts were sutured to the exposed ends of the artery using an end-to-end anastomotic technique with 10-0 nylon sutures (15–20 stitches at each end). After suturing both ends of the graft to the native vessel, blood flow was re-established and pulsation of the distal artery was observed, demonstrating blood flow. The abdomen was closed using sutures for muscle and staples for skin. Rats recovered from anesthesia and were kept with food and water *ad libitum*. No anticoagulation treatment was administered to the rats.

After 10 days, the rats were sacrificed by increasing the inhaled isoflurane concentration from 2,1 to 5,0% and then puncturing the diaphragm followed by the removal of the heart after the rats were deeply anesthetized. The graft was collected with the host distal and proximal ends of the artery. The samples were embedded in freezing medium (Neg 50; Thermo Scientific), snap frozen in liquid nitrogen, and stored at -80°C until cryo-sectioning.

Both PCL and NO-releasing PCL vascular grafts exhibited excellent surgical handling and suture retention properties during implantation. No significant blood

leakage was observed after restoration of blood flow and pressure (see figure 66). It could be caused by microthrombi formation in the vessel wall. It was reported by thrombogenicity testing in chapter 4.3 that platelets are activated by fibrous structures in dynamic conditions. A beneficial effect of coagulation was observed. Since normally the graft is permeable, there were concerns about the leakage after suturing. The thrombogenic potential in this case was beneficial since no graft occlusion was observed inside the graft and simultaneously the grafts did not leak after restoration of blood flow. After 10 days *in vivo,* none of the six implanted grafts demonstrated thrombosis or aneurysm formation.

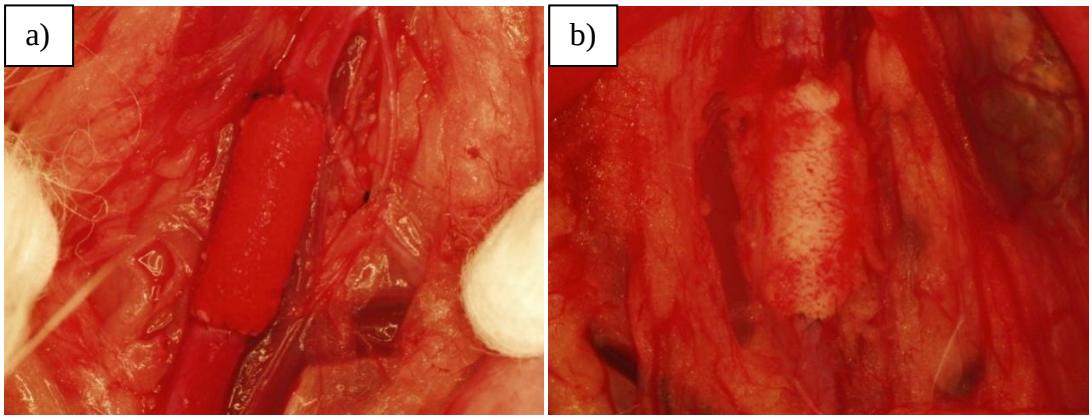

Figure 66: Stereomicroscopic picture of implanted vascular graft made from PCL immediately after suturing (a) and after 10 days of implantation (b).

5.5.1 Morphological and quantitative analysis of explanted vascular grafts

Grafts were cut longitudinally (10 µm thickness) using a Microm HM550 cryostat (Microm International GmbH; Walldorf, Germany) and stained with Hematoxylin and Eosin (H&E) for later bright-field examination. All staining reagents were obtained from Sigma Aldrich with the exception of the Gill's #3 (Leica Biosystems). Briefly, the sections were fixed in chilled ethanol for 1 min followed by triple-washing in PBS. After rinsing in tap water, the slides were stained in Gill's #3 solution for 3 minutes. After that, the sections were dipped in an acidic solution (pH 1.8) to differentiate the Gill's staining. The slides were then rinsed in deionized water and washed twice in 95% ethanol. Subsequently, the sections were counter-stained with 0.25% eosin Y for 30 s and immediately dehydrated in ethanol. The slides were cleared in xylene substitute and mounted in resinous mounting medium.

Slides for fluorescence analysis were fixed in chilled ethanol followed by double washing in PBS. Sections were stained for 10 min using 4',6-diamidino-2-phenylindole (DAPI 5 mg/ml, dilution 3 μL in 1 mL PBS) followed by two washes in PBS. The slides were dehydrated in ethanol, cleared in xylene substitute and mounted.

The evaluation of the stained slides was carried out on an Olympus BX51 microscope. Image analysis was performed using NIH Image J software *(Rasband, 1997-2014).*

Cell density inside the implanted graft was quantified from DAPI staining. At first, cell density was counted through the whole graft thickness. Cells were counted from 6 randomly selected images (nominal magnification 100×) per specimen. The area of the vascular graft was measured and the cell number was normalized to a 100×100 μm area.

Cell density was also quantified in the mid-section of the graft. Images stained with DAPI (nominal magnification 600×) were cropped to display the middle part of the graft with the area of 100×100 μm. The middle part is between the lumen of the graft and adventitial part depicted by red square in figure 67. The cells were counted manually in 30 randomly selected images per specimen.

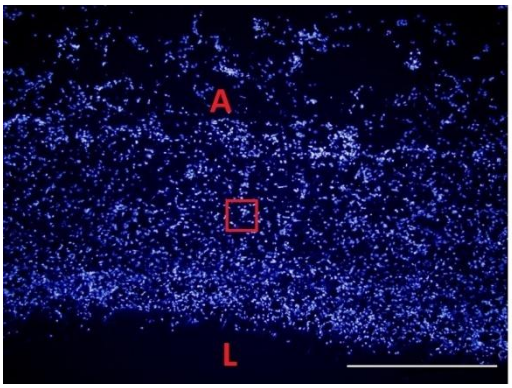

Figure 67: Image of vascular graft infiltrated by cells with marked mid section where cell density was counted. Adventitial side of the graft (A) as well as luminal side (L) is marked by red letters, scale bar 500 μm.

In NO-releasing grafts, respective cellular infiltration from the adventitial and luminal sides was calculated from H&E-stained images (nominal magnification 100×). The wall thickness of each graft was measured from H&E stained images, as well as cellular penetration depth from both sides. The cellular infiltration was expressed as a percentage of cellular infiltration depth from the luminal and adventitial

sides. The cellular ingrowth was evaluated from 6 random images by measuring adventitial and luminal ingrowth in 5 randomly selected locations (30 measurements per specimen). The analysis could not be performed in PCL grafts due to their complete cellular infiltration through the graft thickness (see figure 68 B, C)

Data are expressed herein as mean ± standard deviation. Tests for significant differences used a two-tailed Student's t-test and required $p < 0,05$ to claim significance.

Longitudinal cross sections revealed extensive cellular infiltration within the wall of the grafts (figure 68, 69). However, the presence and distribution of cells in the control graft differed from that of the NO-releasing grafts. The PCL control graft was homogeneously infiltrated with cells. In contrast, a high density of cells was present in the luminal and adventitial margins of the NO-releasing graft, but cells were nearly absent from the central region. Cells had penetrated the NO-releasing graft largely from the adventitial side, with only a relatively thin band of cells observed along the luminal side of the graft. No evidence of cell injury or necrosis was detected in the NO-releasing graft cross sections (figure 69 D, E, and F).

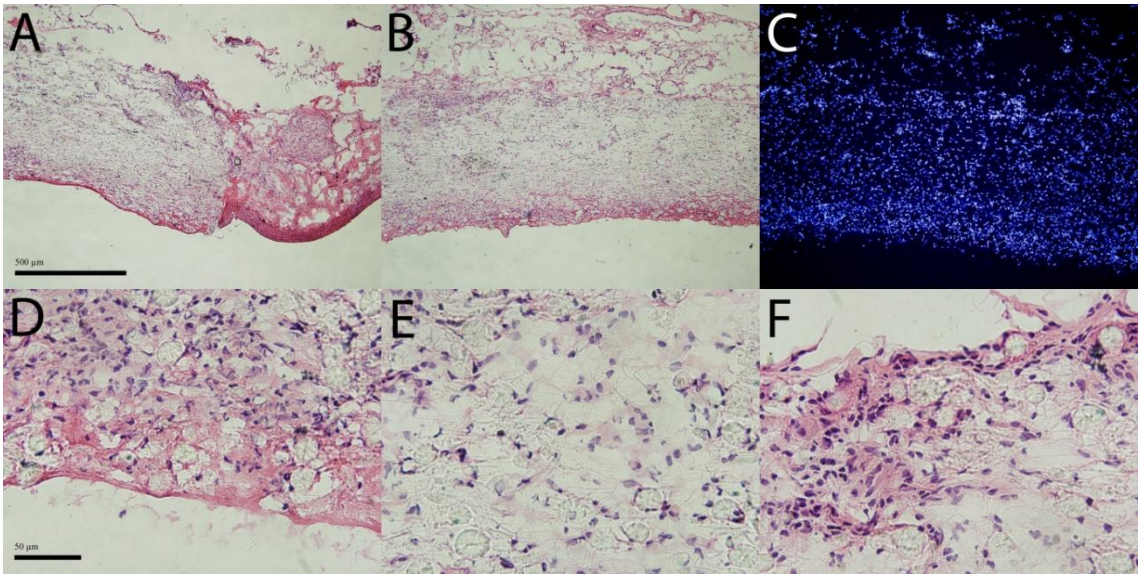

Figure 68: H&E and DAPI staining of PCL vascular graft after 10 days of implantation: Graft-artery junction showing host artery to the right (A), transverse cross section of graft's wall H&E stained (B) and DAPI stained (C); scale bars 500 µm. Detailed images of luminal side of the graft (D), middle part (E) and adventitial part (F); scale bars 50 µm.

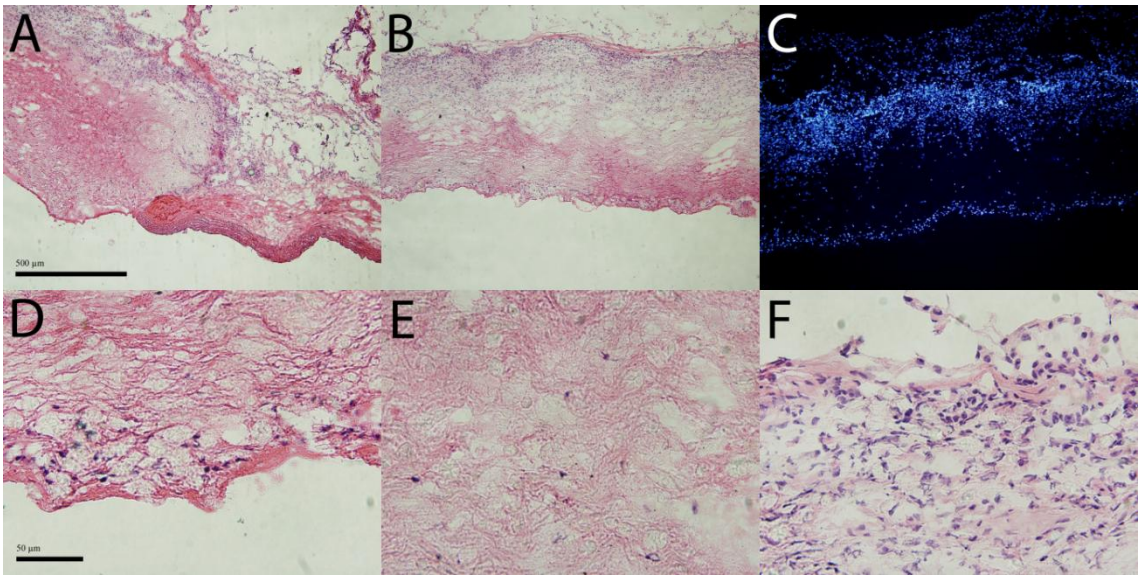

Figure 69: H&E and DAPI staining of a NO-releasing vascular graft after 10 days of implantation: Graft-artery junction showing host artery to the right (A), transverse cross section of graft's wall H&E stained (B) and DAPI stained (C); scale bars 500 µm. Detailed images of luminal side of the graft (D), middle part (E), and adventitial part (F); scale bars 50 µm.

Quantification of the cells present in each graft confirmed that the PCL control was homogeneously infiltrated by cells. The mean cellular density for the PCL control graft was similar throughout the entire graft (23,5 ± 0,8 cells/100×100 µm) relative to the middle region (24,2 ± 0,6 cells/100×100 µm). In contrast, the NO-releasing graft exhibited an average cell density of 18,1± 1,0 cells/100×100 µm compared to 6,5 ± 0,5 cells/100×100 µm in the middle region of the graft. Both the average cell density and the density of cells from the middle of the graft were significantly reduced in the NO-releasing graft relative to the control PCL grafts ($p = 0,039$ and 0,003, respectively). The results are summarized in figure 70. Specific cell staining in order to distinguish different cell phenotype has not been carried out. However, after 10 days of implantation it is expected that most of the cells were immune cells. This suggestion was also noticeable from morphology of cells when observed with higher magnification objective. The majority of the cells belonged to macrophages and neutrophils.

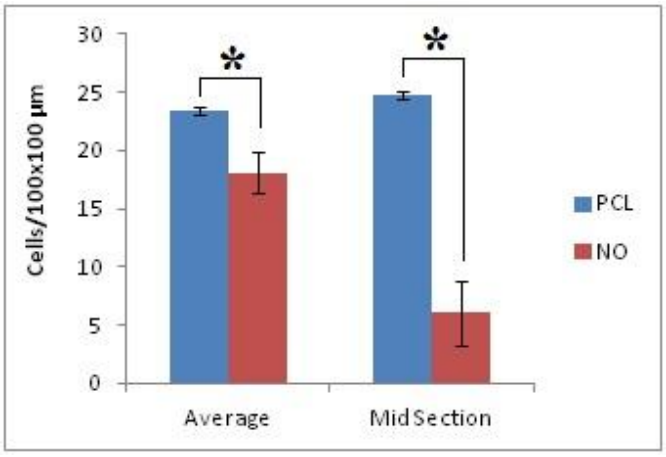

*Figure 70: The density of cells within the control PCL and NO-releasing vascular graft calculated based on DAPI staining (*indicates p < 0,05; n=3). Average value over the whole graft thickness as well as cellular density in only the middle part of the grafts are depicted (P=0,0386 average; P=0,0026 in the Mid Section).*

In order to characterize cellular ingrowth into the NO-releasing graft, cellular infiltration depth from the luminal and adventitial sides was measured. The NO-releasing graft was found to have been infiltrated from the adventitial side up to 38,4 ± 11,1% of its nominal thickness. This stands in stark contrast to cellular infiltration from the luminal side, which was measured at 14,8 ± 9,7% of the nominal graft thickness (figure 71). The PCL graft was uniformly infiltrated throughout the graft (see figure 68 B and C) therefore a comparable analysis could not be performed. Surprisingly, the primary source of infiltrating cells in this abdominal aortic graft is therefore the surrounding microcirculation, rather than the arterial blood or the host artery.

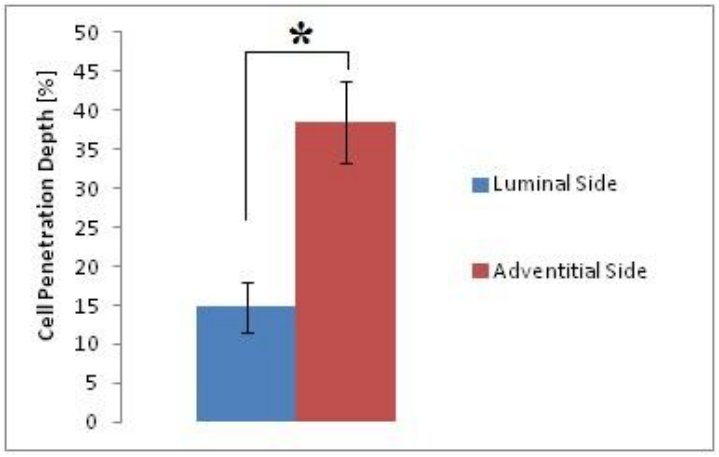

*Figure 71: Cell infiltration distances in the NO-releasing graft from luminal side and from adventitial side (*indicates p < 0,05). The depth of cellular penetration is expressed as a percentage of the total graft thickness (P=0,0189).*

5.6 Conclusion of vascular grafts modified by NO-releasing compounds

The third section of the thesis was focused on modification of polymeric vascular grafts made from PCL. Nitric oxide donors were added to electrospinning solution and release kinetics was studied *in vitro*. Newly synthesized compound, SNAP-cyclam, was able to release NO in a long term that was proved in *in vitro* as well as *in vivo* conditions. Newly synthesized compound, SNAP-cyclam, was able to release NO at physiological levels up to 42 days measured in PBS after blending with PCL by the way of electrospinning. Similar results were achieved when vascular grafts were incubated in complete medium that more closely simulate conditions within the body. Seeding of endothelial cells confirmed higher proliferation rate of cells in the first week of culturing. After implantation *in vivo*, vascular grafts were patent after 10 days of implantation. There were differences between control PCL grafts and NO releasing grafts, especially in the way of cellular distribution within the graft thickness. The NO release strongly inhibits the harmful infiltration of inflammatory cells into the middle and inner regions of the vascular grafts. Additional long-term studies should be conducted to confirm a reduced intimal hyperplasia relative to control grafts and measure the rate of re-endothelialization.

6 Discussion

Achieved results presented in previous experimental parts are discussed in a broad context within the field of vascular tissue engineering. The advantages and limitations of the results are presented towards further studies in the development of ideal small diameter vascular graft.

6.1 The design of vascular graft

The design of vascular graft has to start with a smart choice of appropriate materials. Biodegradable polyesters are commonly used for tissue engineering applications including vascular grafts (*Watanabe, 2001; Vaz, 2005; Wu, 2010; Du, 2012; Hu, 2012; Diban, 2013).* In the thesis, comparison of 2 chosen polymers from the group of biodegradable polyesters was carried out. Polycaprolactone obtained from Sigma Aldrich and copolymer composed of polylactide and polycaprolactone obtained from PURASORB were used for tubular scaffold fabrication. It was found that both polymers are biocompatible when tested *in vitro* using fibroblast cell line (subchapter 4.1) and endothelial cell line (subchapter 4.2).

Since the hypothesis was based on mimicking the extracellular matrix, electrospinning technique was employed in order to produce structure that resembles this cellular natural environment. Electrospinning is versatile technique enabling creation of fibrous structures with various morphologies. For fabrication of small diameter vascular graft, rotating mandrel was used as a collector and tubular scaffolds with defined morphology were produced. The device is depicted in chapter 2 in the figure 9. Depending on polymer properties, composition of electrospinning solution and electrospinning parameters, different fibrous morphology could be obtained. In case of polycaprolactone, fibers were created when 16-22 wt% was electrospun in solvent system composed of chloroform/ethanol 9/1 (v/v) as shown in figure 11. The resulting fibers could be oriented in radial direction by increasing the rotational speed (see figure 15). Copolymer PLC gave rise to fibrous structure when 9-12,5 wt% was dissolved in solvent system composed of chloroform/ethanol/acetic acid 8/1/1 (v/v/v) as depicted in figure 19. Lower polymeric concentration led to beaded structure.

Histological assessment of vessel wall composition was carried out in order to visualize the structure of native blood vessel, especially the native extracellular

matrix that is thought to be mimicked by electrospinning. There are 3 layers in native blood vessels with special arrangement that is shown in figure 7. The inner layer called *tunica intima* is composed of single layer endothelial cells that are crucial for maintaining non-thrombogenic surface of the lumen besides many other properties. Therefore it is necessary to provide a structure that will enable fast endothelialization of the scaffold after implantation. The middle layer of vessel wall is called *tunica media* and it is composed of radially oriented collagen fibers and smooth muscle cells. Similar structure was designed for vascular graft production in the thesis. The structure of proposed ideal vascular graft is depicted in figure 8. The outermost layer was not considered to be important to mimic since it is composed mostly of fibroblast cells that are believed to colonize the scaffold spontaneously after implantation. The proposed structure of double layered graft was achieved by electrospinning of PCL (see figures 17, 18) with different parameters of solution composition and electrospinning conditions. The inner layer was composed of thin nanofibers that had been assumed to support endothelialization. The outer layer was created by oriented microfibers with sufficient pore size for further smooth muscle cell infiltration. Copolymer PLC was electrospun in a single layered tubular scaffold. Its fibrous morphology is depicted in figures 21 and 22. This vascular graft did not resemble native ECM by layering approach but its properties seemed to surpass the material performance in other qualities discussed later. Ideal vascular graft has to be designed not just morphologically but mechanical properties, surface wettability and biocompatibility have to be complexly evaluated. Morphology of the graft is not the only one aspect that has to be considered when appropriate tissue engineering scaffolds is being developed.

6.2 Surface wettability

Appropriate surface wettability enables protein adsorption in a right conformation followed by cell attachment to the substrate. Surface properties in terms of their wettability were tested using contact angle measurement. Surface wettability is influenced by surface roughness, testing of wettability of fibrous structures could provide misleading outcomes. Therefore foils made from PCL and copolymer PLC were tested. The results showed that copolymer PLC in both tested forms (foils and electrospun fibers) was more hydrophilic than PCL (PLC contact angle between 46 and 49°compared to PCL with contact angle in range of 60-67°). This outcome

corresponds with the chemical structure of tested polymers. Copolymer PLC is composed from 70% of monomer lactide units that are more hydrophilic than caprolactone units. It was reported that slightly hydrophilic materials are preferred for tissue engineering scaffolds *(Bacakova, 2011).* Polycaprolactone is known to be hydrophobic and there were attempts to increase its hydrophilicity for example using plasma treatment. Electrospun PCL without modification had the contact angle 127,6°± 0,88°. The value of measured contact angle decreased with increasing time of plasma treatment. After 60 seconds of plasma treatment the PCL surface reached complete wetting (contact angle 0°) *(Valence, 2013).*

6.3 Mechanical properties of vascular grafts

Mechanical properties of vascular grafts should match those of natural blood vessels but currently used commercial grafts made from PET or PTFE have much stronger mechanical properties. Our tubular scaffolds made from PCL possess average engineering tension of 3,3 ± 1,1 MPa compared to PLC tubular scaffold with 37,2 ± 9,2 MPa that is slightly higher than that of native blood vessels. Abdominal aorta in the same longitudinal direction has the tensile strength of 1,47 MPa and commercial graft Teflon TF-208 85,2 MPa (*How, 1992).* Biodegradable vascular grafts have to ensure the mechanical strength in time of suturing that is followed by tissue remodelation accompanied by changing of mechanical behavior. Higher values of mechanical strength that has been achieved in tubular samples made from PCL and PLC are beneficial since degradation of the polymer will weaken the scaffold following the implantation. Electrospun PCL exhibit low engineering tension that could be potentially improved by using polycaprolactone with higher molecular weight. Measured elasticity of PCL tubular samples was much lower with the average elongation of 37,5 ± 8,8 % compared to PLC reaching the average values of 377,4 ± 157,4 %.

Measurement of mechanical properties could be done in axial direction as well. Such a study was carried out previously in our department. Electrospun vascular grafts made from PCL with different degree of fibre orientation were measured at both directions to obtain the values of tensile strength and elongation at break. Isotropic fibrous structures possess tensile strength between 0,3 and 0,4 MPa and elongation at break up to 100% in both directions. When the fibers were oriented in radial

direction, tensile strength in the same direction decreased to 0,1 MPa with increasing tensile strength in axial direction to 1 MPa and elongation at break to 200% (*Yalcin, 2014).*

Besides engineering strength and elongation at break, other parameters related to the mechanical behavior of the grafts have to be tested. One of the most important parameter is burst pressure that has to be determined in order to verify that the grafts will not leak after suturing. Another important aspect is the suture retention. The above mentioned tests are under development in our laboratories. However, preliminary *in vivo* tests revealed that vascular grafts made from PCL worked well as replacement of rat abdominal aorta. No troubles in suturing positions or blood leakage through the wall of vascular graft to the abdomen were observed (see figure 65).

6.4 Biocompatibility of electrospun layers tested in vitro

Electrospun PCL and PLC with similar fibrous morphologies having fiber diameter of about 1 μm were tested with fibroblast cell line. It has been assumed that PLC with lower contact angle than PCL would support cellular adhesion and proliferation due to the adsorption of adhesion molecules in right conformations. The results showed significantly higher proliferation rate on PLC after 7 and 14 days of incubation with 3T3 mouse fibroblasts. The outcome corresponds with surface properties of the scaffolds, mostly with appropriate surface wettability of PLC discussed above.

Electrospun layers were tested in a similar manner using endothelial cell line. Since PCL was able to create nanofibers that had been supposed to fasten endothelialization, two different fibrous morphologies were tested assign as PCL nm (fiber diameter 230 ± 190 nm) and PCL μm (fiber diameter 960 ± 760 nm). Copolymer PLC created fibrous structure with average fiber diameter of 1030 ± 710 nm. Obtained results were similar to previous experiment - copolymer PLC support endothelial cell proliferation more than PCL. When different fibrous morphologies of PCL were compared, contradictory to the assumption, microfibers supported endothelial cell proliferation more than nanofibers. One of the limitations of the study is the static incubation of the scaffolds. It is possible that flowing conditions would result in different outcomes. This assumption has to be clarified after cultivation of tubular scaffolds in bioreactor that enables medium flow similar as in blood vessels.

Based on the *in vitro* test results the design of double layered graft should be re-make. The thesis was focused on characterization of electrospun layers made from either PCL or copolymer PLC. Both polymers possess certain advantages and disadvantages. Appropriate combination of those 2 polymers could improve the function of final ideal prosthesis and further tests are expected to be carried out.

6.5 Thrombogenicity of vascular grafts

Thrombosis is a major cause of poor patency in synthetic vascular grafts for small diameter blood vessel replacement. Endothelial cells provide a constant non-thrombogenic environment. Platelets having negative charge adhere to positively charged hydrophobic surfaces *(Sarkar, 2006)*. Due to the difficulties of spontaneous endothelialization in humans, an investigation of thrombogenic potential of new materials has to be carried out.

The evaluation of thrombogenicity of tested layers (microfibrous and nanofibrous PCL and microfibrous PLC) with thrombocyte rich solution showed no statistical significant difference between the samples in case of thrombocytes viability measured by MTT test (see figure 42). Thrombocytes adhered and became activated as seen from SEM images. Platelets changed their shape from circular to the structure with multiple pseudopodia. Microscopic techniques revealed the difference in platelet spreading through the layers. Since nanofibrous layers were covered abundantly in the surface, microfibrous layers allow platelets to penetrate into the inner structures and create aggregates. However, quantification of the platelets by microscopic techniques was not possible to carry out due to the spread structure of thrombocytes where single platelets could have not been distinguished. Qualitative description of thrombocyte shape is a regular technique for evaluation of thrombogenic potential. When platelets are in resting state, their shape is circular. Once became activated, the structure undergo changes and multiple pseudopodia are created. When the activation continues, the platelets start to aggregate and spread through the surface.

Different surface morphologies were compared in order to examine its contribution to thrombogenicity. Interestingly, it was found that electrospun fibrous layers activated platelets more than corresponding foils. Surface roughness play very important role in thrombogenicity. While electrospun layers were fully covered with spread thrombocytes, platelets in foils occurred isolated in different stage of their

activation. In the figure 48 there are resting circular platelets as well as spread thrombocytes with pseudopodia.

Experiments in static and dynamic conditions showed different platelet morphologies after incubation with vascular grafts pointing the necessity of testing in natural environment. When dynamic conditions were employed, platelets completely lost their circular shape and became completely spread that indicates their higher degree of activation. This activation was higher in nanofibrous PCL structure compared to PLC microfibrous structure where sporadic not fully spread platelets could be found (see figure 51).

Milleret et al. tested the influence of electrospun fiber diameter, roughness and surface wettability on blood activation. They found out that nanofibers exhibit low coagulation with almost no adhered platelets. The microfibrous structure caused thrombin formation and coagulation cascade activation when incubated with whole blood *(Milleret, 2012).* Our results showed higher degree of thrombocyte activation in nanofibers. However, the difference did not claim significance and further hemocompatibility tests have to be carried out. Platelet activation is just a part of blood-material interaction assessment that is planned to study in further experiments.

When thrombocytes are incubated with materials, they can adhere to the surface of material, undergo the process of activation and create aggregates. These reactions could be beneficial but also harmful. Vascular grafts that will allow the blood leakage could not work after suturing into blood circulation. Platelet activation leading to the creation of microthrombi within the graft wall could have a positive effect on blood permeability. On the other hand, thrombogenic potential of materials can cause thrombus formation in the lumen of the graft making the bypass occluded. The equilibrium of those two contradictory processes is difficult to evaluate without *in vivo* or *ex vivo* testing.

6.6 Vascular grafts releasing nitric oxide

One of the main limitations of state-of-the-art NO-releasing biomedical devices is short-term delivery of NO. In the experiments described above in chapter 5, incorporation of SNAP-cyclam, newly synthesized compound, into a PCL nanofibrous vascular graft led to long-term NO release. The initial burst of NO after exposure to an aqueous environment was between 200 and 450 pmol min^{-1} cm^{-2} (figure 61),

which was of similar to the physiological levels of NO produced by endothelial cells *(Vaughn, 1998)*.The measurement of NO release was strongly influenced by the presence of Cu^{2+} and ascorbic acid. Copper is known to catalytically decompose RSNOs to release NO, provided that the appropriate reducing equivalents are present to convert Cu^{+2} to Cu^{+1}. PBS and complete medium were both used to soak the NO-releasing PCL to demonstrate that biological agents present in the medium do not coat the polymer and prevent NO release. Even after 42 days of immersion in PBS, NO-releasing groups were still present within the fibers and were capable of NO generation. These *in vitro* results suggest that physiological levels of NO were still being developed at the NO-releasing PCL graft surface after 10 days *in vivo*. In the *in vivo* environment, many endogenous agents (including Cu^{2+} and ascorbate) are present that are able to release NO from RSNOs present in the polymer *(Singh, 1996)*.

Nanofibrous structures mimic the extracellular matrix and therefore promote cellular adhesion *(Bhardwaj, 2010)*. However, cellular infiltration of complex 3D nanofibrous structures can be limited by the small pore size of nanofibrous scaffolds *(Nam, 2007)*. The vascular grafts prepared by electrospinning of PCL composed primarily of 150 nm-diameter fibers which allowed uniform cellular infiltration throughout control PCL grafts after 10 days of implantation (see figure 68). In striking contrast, we found that cellular infiltration was strongly inhibited by NO release. Nanofibrous PCL vascular grafts were uniformly infiltrated with inflammatory cells, and their presence was significantly reduced in the NO-releasing graft. Most of the cells present had colonized the NO graft from the adventitial side, with relatively few cells present on the luminal side, and a near absence of cells in the mid-section of the graft. The results show a clear protection of the middle and luminal part of the implanted graft from inflammatory cell infiltration, which comprise the approximate region where neointimal hyperplasia occurs. The results also show that inflammatory cells migrate into the graft primarily from the surrounding microcirculation relative to the circulating blood. Thus, the NO release was very effective in creating a barrier that inhibited the transmigration of adventitial inflammatory cells into the middle and inner regions of the graft (Figure 67). Because SMCs are stimulated by inflammatory cells to migrate to the intima of vascular grafts where they promote neointimal hyperplasia and eventual graft failure, we speculate that the reduced presence of inflammatory cells in the inner and middle regions of NO-releasing grafts may reduce later intimal hyperplasia of SMCs.

Whereas the transmigration of harmful inflammatory cells was strongly inhibited, the presence of a thin band of cells along the blood-contacting surface of the vascular graft suggests that re-endothelialization may not be impaired by the NO release. Indeed, there is evidence that NO release may be beneficial for endothelial cell migration and proliferation *(Taite, 2008; Kushwaha, 2010)*. After the implantation of a conventional vascular graft, endothelial cells typically begin to migrate from the adjacent host artery. After 6 weeks of implantation into the rat abdominal aorta, endothelial cells cover 80% of a conventional graft's lumen, and complete endothelialization is achieved after 6 months *(Valence, 2012)*. Because of the short duration of the present study (10 days), we were not able to assess the contribution of continuous exogenous NO release to restore endothelial cell coverage. A long-term study is required to determine to what extent endothelial cell coverage may be enhanced by NO release.

6.7 Future perspectives

The thesis offers the technological tools for production of vascular grafts, their fabrication from biodegradable polyesters PCL and PLC and the characterization of such scaffolds. To assess the function of tissue engineering scaffolds, further studies have to be carried out. Further *in vitro* tests with vascular smooth muscle cells that are another important part of functional blood vessel are ongoing. Assessment of thrombogenicity will be repeated with new model of bioreactor. Meanwhile static incubation of thrombocytes with fibrous layers modified by NO releasing compounds will be tested.

Materials used for vascular grafts will be also examined for complex hemocompatibility testing including hemolysis assay and different coagulation pathways assessment to understand the blood material interactions.

Since both used polymers are biodegradable, the degradation rate has to be studied as well. Previously, there were carried out tests with degradation of PCL that had taken several months to degrade. On the other hand, copolymer PLC is a new material that has to be characterized over a period of time for the progress of its degradation and its mechanical and structural changes after implantation *in vivo*. It is assumed that the degradation will be faster in case of copolymer PLC because of its

amorphous state slightly more hydrophilic than PCL. Degradation studies have to follow the molecular weight loss and mechanical behavior shift.

Long term performance of vascular grafts implanted in animal models such as rats, rabbits and pigs will be evaluated. These outcomes will bring very important insight into the function of presented scaffolds for vascular tissue engineering since the results from complex *in vivo* testing are the most valuable for further directions.

7 General conclusions

The aim of the thesis was the contribution to the development of ideal vascular graft that will fulfill its requirements listed in the theoretical part. The hypothesis of mimicking extracellular matrix was employed and proposed structure composed of two layers mimicking native vessels (tunica intima and tunica media) had been designed. Biodegradable polymers were chosen for production of vascular grafts because those materials enable tissue remodeling after implantation. The concept of *in situ* tissue engineering was accepted leading to readily available grafts in various sizes and thicknesses of final products. Polycaprolactone was electrospun into planar and tubular samples with different morphologies. Nanofibers as well as microfibers were created by changing electrospinning solution properties and electrospinning conditions. PCL enabled the creation of proposed double layered vascular graft where inner layer was composed of nanofibers and outer layer was created by oriented microfibers as in native vessels. The first hypothesis based on the mimicking of native extracellular matrix by electrospinning was achieved using electrospinning of polycaprolactone.

Novel material from the same group of biodegradable polyesters, copolymer polylactide and polycaprolactone, was electrospun into planar and tubular form. However, the morphology remained similar even if conditions or composition of electrospinning solution was changed. Therefore a single layered graft was prepared from this polymer.

The second hypothesis was based on mechanical performance of produced tubular scaffolds. Mechanical properties of electrospun vascular grafts made from PCL and copolymer PLC were compared by measurement of stress-strain curves. Copolymer PLC possessed higher strength and elasticity compared to electrospun PCL making it ideal material for vascular tissue engineering. The values of mechanical strength were higher compared to native blood vessels. However, it is beneficial since degradation of the polymer will weaken the scaffold following the implantation. In terms of appropriate mechanical behavior, copolymer PLC is preferred over polycaprolactone in time of suturing.

Materials properties were evaluated in order to characterize these candidates potentially employed in the field of vascular tissue engineering. Surface wettability

showed that copolymer PLC is more hydrophilic than PCL that was hypothesized from their chemical structures. Slightly more hydrophilic surface of PLC facilitated fibroblast and endothelial cells adhesion and proliferation *in vitro.* Higher proliferation rate of fibroblasts and endothelial cells was observed with copolymer PLC that possess lower contact angle compared to PCL.

Nanofibers were assumed to promote endothelialization of vascular lumen as proposed for the inner layer of ideal vascular graft. Nevertheless, this hypothesis has been rejected after incubation of nano- and microfibrous PCL in static conditions. Endothelial cells showed higher viability on microfibrous PCL layers than on nanofibrous PCL layers. Nanofibers also activated thrombocytes in static and dynamic conditions due to their high surface to volume ratio. Based on these complex results, the proposed structure has to be re-designed according to the outcomes. Material properties are probably more important than morphology of the fibers. Copolymer PLC made from microfibers fitted more to the requirements for vascular grafts however the native ECM has not been fully mimicked by electrospinning. Further steps in evaluation of *in vivo* tests have to be carried out to verify this statement.

Another important part of the thesis was the functionalization of vascular graft made from PCL by nitric oxide releasing compound. Long term release has not been achieved in the literature before. Newly synthesized compound, SNAP-cyclam was added to polymeric fibers ensuring stable long term NO release in physiological levels up to 42 days *in vitro.* Nitric oxide beneficial properties were confirmed *in vitro* by culturing the scaffolds with endothelial cells that were supported in the presence of NO donors compared to controls during the first week of culturing. More importantly, the effect of NO was observed *in vivo* after implantation in rats as a replacement of abdominal aorta. After 10 days of implantation, nitric oxide suppressed the inflammatory reaction within the graft compared to control PCL grafts. The NO release strongly inhibits the harmful infiltration of inflammatory cells into the middle and inner regions of the vascular grafts. The protection against inflammation in this region of the graft is anticipated to confer increased resistance against neointimal hyperplasia from smooth muscle cells. Additional long-term studies should be conducted to confirm a reduced intimal hyperplasia relative to control grafts and measure the rate of re-endothelialization.

The development of tissue engineering scaffold requires wide range of knowledge and skills in material science field, biology and medicine. The thesis is

focused on characterization of electrospun vascular grafts made from polycaprolactone or copolymer polylactide-polycaprolactone. The material bulk and surface properties were investigated followed by *in vitro* tests and preliminary *in vivo* tests. Further investigation before translation into clinic is needed. However, the first steps towards the development of suitable vascular graft were conducted.

8 References

Abbate M, Lomeo A, Gentile M, Bianca I, Bartoloni A, Pilato M. Our experience utilizing the bovine internal mammary artery in the myocardial revascularization, J Cardiovasc Surg 1988;29:76.

Ahanchi SS, Tsihlis ND, Kibbe MR. The role of nitric oxide in the pathophysiology of intimal hyperplasia, J Vasc Surg 2007;45:64A-73A.

Angelini GD, Newby AC. The future of saphenous vein as a coronary artery bypass conduit, Eur Heart J 1989;10(3):273-80.

Arrigoni C, Camozzi D, Remuzzi A. Vascular Tissue Engineering, Cell Transplantation 2006;15:119-125.

Bacakova L, Filova E, Parizek M, Ruml T, Svorcik V. Modulation of cell adhesion, proliferation and differentiation on materials designed for body implants, Biotechnology Advance 2011;29:739-767.

Bauer S, Schmuki P, von der Mark K, Park J. Engineering Biocompatible Implant Surfaces Part I: Materials and Surfaces, Progress in Materials Sciences 2013;58:261-326.

Berger K, Sauvage LR, Rao AM, Wood SJ. Healing of arterial prostheses in man: its incompleteness, Ann Surg 1972;175(1):118—27.

Bergstrom K, Osterberg E, Hoffman AS, Schuman P TP, Kozlowski A, Harris JM. Effects of branching and molecular weight of surface-bound poly(ethylene oxide) on protein rejection, J Biomater Sci Polym Ed 1994;6:123-132.

Bertleff M, Meek MF, Nicolai JPA. A prospective clinical evaluation of biodegradable neurolac nerve guides for sensory nerve repair in the hand, J Hand Surg Am Vol 2005;30A:513-8.

Beyuidenhout D, Zilla P. Vascular grafts. In *Encyclopedia of Biomaterials and Biomedical Engineering*: Wnek G, Bowlin GL. ISBN 0-8247-4798-4. p.1715-25.

Bhardwaj N, Kundu SC. Electrospinning: A fascinating fiber fabrication technique, Biotechnol Adv 2010;28:325-347.

Boland ED, Espy PG, Bowlin GL. Tissue Engineering Scaffolds. In *Encyclopedia of Biomaterials and Biomedical Engineering*; Wnek G, Bowlin GL. ISBN 0-8247-4798-4. p.1630-1638.

Brisbois EJ, Handa H, Major TC, Bartlett RH, Meyerhoff ME. Long-term nitric oxide release and elevated temperature stability with S-nitroso-N-acetylpenicillamine (SNAP)-doped Elast-eon E2As, Biomaterials 2013;34:6957-66.

Brooke BS, Satyajit KK, Li DY. Extracellular matrix in vascular morphogenesis and disease: structure versus signal, Trends in Cell Biology 2003;13:51-56.

Brothers T, Stanley J, Burkel W, Graham L. Small-caliber polyurethane and polytetrafluoroethylene grafts: a comparative study in a canine aortoiliac model, J Biomed Mat Res 1990;24:761-771.

Cameron A, Davis KB, Green G, Schaff HV. Coronary bypass surgery with internal-thoracic-artery grafts - effects on survival over a 15-year period, N Engl J Med 1996;334(4):216—9.

Chen S, An J, Weng L, Li Y, Xu H, Wang Y, Ding D, Kong D, Wang S. Construction and biofunctional evaluation of electrospun vascular graft loaded with selenocystamine for in situ catalytic generation of nitric oxide, Materials Science and Engineering 2014;C 45:491-6.

Chlupac J, Filova E, Bacakova L. Blood Vessel Replacement: 50 years of Development and Tissue Engineering Paradigms in Vascular Surgery, Physiol Res 2009;58:119-139.

Dahlin RL, Kasper FK, Mikos AG. Polymeric nanofibers in tissue engineering, Tissue Eng Part B Rev 2011;17(5):349-64.

Davis GE, Senger DR, Endothelial Extracellular Matrix Biosynthesis, Remodeling, and Functions During Vascular Morphogenesis and Neovessel Stabilization, Circulation Research 2005; 97:1093-1107.

Diban H, Haimi S, Bolhuis-Versteeg L, Teixeira S, Miettinen S, Poot A, Grijpma D, Stamatialis D. Hollow fibers of Poly (lactide-co-glycolide) and Poly(ε-caprolactone) blends for vascular tissue engineering applications, Acta Biomater 2013;9:6450-8.

Dicks AP, Williams DLH. Generation of nitric oxide from S-nitrosothiols using protein-bound Cu 2+ sources, Chemistry & Biology 1996;3:655-659.

Dong Y, Yong T, Liao S, Chan CK, Ramakrishna S. Long-term viability of coronary artery smooth muscel cells on poly(l-lactide-co-caprolactone) nanofibrous scaffold indicates its potential for blood vessel tissue engineering, J R Soc Interface 2008;5:1109-1118.

Du F, Wang H, Zhao W, Li D, Kong D, Yang J, Zhang Y. Gradient nanofibrous chitosan/poly ε-caprolactone scaffolds as extracellular microenvironments for vascular tissue engineering, Biomat 2012;33:762-70.

Ducasse E, Cosset JM, Eschwege F, Chevalier J, De Ravignan D, Puppinck P, Lartigau E. Hyperplasia of the arterial intima due to smooth muscle cell proliferation. Current data, experimental treatments and perspectives, J Mal Vasc 2003;28:130-44.

Engbers GH, Feijen J. Current techniques to improve the blood compatibility of biomaterial surfaces, Int J Artif Organs 1991;14(4):199-215.

Erben J, Pilarova K, Sanetrnik F, Chvojka J, Jencova V, Blazkova L, Havlicek J, Novak O, Mikes P, Prosecka E, Lukas D, Kuzelova Kostakova E. The combination of meltblown and electrospinning for bone tissue engineering, Materials Letters 2015;143:172-176.

Esquivel CO, Blaisdell FW. Why small caliber vascular grafts fail: a review of clinical and experimental experience and the significance of the interaction of blood at the interface, J Surg Res 1986;41(1):1-15.

Fleser PS, Nuthakki VK, Malinzak LE, Callahan RE, Seymour ML, Reynolds MM, Merz SI, Meyerhoff ME, Bendick PJ, Zelenock GB, Shanley CJ. Nitric oxide-releasing biopolymers inhibit thrombus formation in a sheep model of arteriovenous bridge grafts, J Vasc Surg 2004;40:803-11.

Freshney RI. Culture of Animal Cells: A Manual of Basic Technique and Specialized Applications, John Wiley & Sons, Inc. 2010, ISBN 978-0-470-52812-9.

Frost MC, Reynolds MM, Meyerhoff ME. Polymers incorporating nitric oxide releasing/generating substances for improved biocompatibility of blood-contacting medical devices, Biomaterials 2005;26:1685-93.

Garg UC, Hassid A. Nitric oxide-generating vasodilators and 8-bromo-cyclic guanosine monophosphate inhibit mitogenesis and proliferation of cultured rat vascular smooth muscle cells, J Clin Invest 1989;83:1774-7.

Gierke GE, Nielsen M, Frost MC. S-Nitroso-N-acetyl-D-penicillamine covalently linked to polydimethylsiloxane (SNAPPDMS) for use as a controlled photoinitiated nitric oxide release polymer, Sci Technol Adv Mater 2011;12:1-5.

Giudiceandrea A, Seifalian AM, Krijgsman B, Hamilton G. Effect of prolonged pulsatile shear stress in vitro on endothelial cell seeded PTFE and compliant polyurethane vascular grafts, Eur J Vasc Endovasc Surg 1998;15(2):147—54.

Greenwald SE, Berry CL. Improving vascular grafts: the importance of mechanical and haemodynamic properties, J Pathol 2000;190(3):292—9.

Guidon R, Chakfe N, Maurel S, How T, Batt M, Marois M. Expanded polytetrafluorethylene arterial prostheses in humans: A histopathological study of 298 surgically excised grafts, Biomaterials 1993;14:678-693.

Gunatillake PA, Adhikari R. Biodegradable Synthetic Polymers for Tissue Engineering, European Cells and Materials 2003;5:1-16.

Han F, Jia X, Dai D, Yang X, Zhao J, Zhao Y, Fan Y, Yuan X. Performance of a multilayered small-diameter vascular scaffold dual-loaded with VEGF and PDGF. Biomaterials 2013;34:7302-13.

Hasegawa T, Okada K, Takano Y, Hiraishi Y, Yoshida Y, Okita Y. Hybrid small caliber vascular prosthesis for coronary artery bypass grafting: a preliminary study of plasmin-treated fibrin-coated vascular prosthesis. ASAIO J 2005;51(6):725-9.

He W, Ma Z, Teo WE, Dong YX, Robless PA, Lim TC, Ramakrishna S. Tubular nanofiber scaffolds for tissue engineered small-diameter vascular grafts, J Biomed Mater Res A 2008;90:205-16.

Hetrick EM, Prichard HL, Klitzman B, Schoenfisch MH. Reduced foreign body response at nitric oxide-releasing subcutaneous implants, Biomaterials 2007;28:4571-80.

Hoenig MR, Campbell GR, Rolfe BE, Campbell JH. Tissue-engineered blood vessels: alternative to autologous grafts? Arterioscler Thromb Vasc Biol 2005;25(6):1128-34.

How TV. Mechanical properties of arteries and arterial grafts. In: Hastings GW, Cardiovascular Biomaterials. New York: Springer-Verlag;1992,1-28.

Hu JJ, Chao WC, Lee PY, Huang CH. Construction and characterization of an electrospun tubular scaffold for small-diameter tissue-engineered vascular grafts: A scaffold membrane approach, Journal of the Mechanical behavior of Biomedical Materials 2012;13:140-155.

Huang Ch, Geng X, Qinfei K, Xiumei M, Al-Deyab S, El-Newehy M. Preparation of composite tubular grafts for vascular repair via electrospinning, Progress in Natural Science: Materials International 2012;22:108-114.

Jacob RA, Sotoudeh G. Vitamin C funtion and status in chronic disease, Nutr Clin Care 2002;5(2):66-74.

Jardine S, Wilson JIB. Plasma Surface Modification of ePTFE Vascular Graft, Plasma Processes and Polymers 2005;2:328-333.

Jenkins MJ, Harrison KL. The effect of molecular weight on the crystallization kinetics of polycaprolactone. Polymers for Advanced Technologies 2006;17:474-78.

Jourd'heuil D, Hallen K, Feelisch M, Grisham MB. Dynamic state of S-nitrosothiols in human plasma and whole blood, Free Radical Biol Med 2000;28(3):409−417.

Kakisis JD, Liapis CD, Breuer C, Sumpio BE. Artificial blood vessel: the Holy Grail of peripheral vascular surgery, J Vasc Surg 2005;41:349-354.

Kallmes DF, McGraw JK, Evans AJ, Mathis JM. Hergenrother RW, Jensen ME, Cloft HJ, Lopes MB, Dion JE. Thrombogenicity of hydrophilic and nonhydrophlic microcatheters and guiding wires, Am J Neuroradiol 1997;18:1243-1251.

Kamath S, Blann AD, Lip GYH. Platelet activation: assessment and quantification, European Heart Journal 2001;22:1561-1571.

Kapadia MR, Popowich DA, Kibbe MR. Modified Prosthetic Vascular Conduits, Circulation 2008;117:1873-1882.

Karrer L, Duwe J, Zisch AH, Khabiri E, Cikirikcioglu M, Napoli A, Goessi A, Schaffner T, Hess OM, Carrel T, Kalangos A, Hubbell JA, Walpoth BH. PPS-PEG surface coating to reduce thrombogenicity of small diameter ePTFE vascular grafts, Int J Artif Organs 2005;28:993-1002.

Kim HN, Jiao A, Hwang NS, Kim MS, Kang DH, Kim DH, Suh KY. Nanotopography-guided tissue engineering and regenerative medicine, Advanced Drug Delivery Reviews 2013;65:536-58.

Klopp LS, Simon BJ, Bush JM, Enns RM, Turner AS. Comparison of a caprolactone/lactide film (Mesofol) to two polylactide film products as a barrier to postoperative peridural adhesion in an ovine dorsal laminectomy model, Spine 2008;33:1518-26.

Koh A, Carpenter AW, Slomberg DL, Schoenfisch MH. Nitric oxide-releasing silica nanoparticle-doped polyurethane electrospun fibers, ACS Appl Mater Interface 2013;5:7956-64.

Kolacna L, Bakesova J, Varga F, Kostakova E., Planka L. Necas A, Lukas D, Amler E, Pelouch V. Biochemical and Biophysical Aspects of Collagen Nanostructure in the Extracellular Matrix, Physiol Res 2007;56(1):S51-S60.

Kushwaha M, Anderson JM, Bosworth CA, Andukuri A, Minor WP, Lancaster JR, Anderson PG, Brott BC, Jun HW. A nitric oxide releasing, self assembler amphiphile matrix that mimics native endothelium for coating implantable cardiovascular devices, Biomaterials 2010;31:1502-8.

Langer R, Vacanti JP. Tissue engineering, Science 1993;260:920-6.

Lefer AM. Nitric oxide: nature's naturally occurring leukocyte inhibitor, Circulation 1997;95:553-4.

Lemson MS, Tordoir JHM, Daemen MJAP, Kitslaar PJEHM. Intimal hyperplasia in vascular grafts, Eur J Vasc Endovasc Surg 2000;19:336-50.

L'Hereux N, Paquet S, Labbe R, Germain L, Auger FA. A completely biological tissue-engineered human blood vessel, FASEB J 1998;12:47-56.

Li S, Sengupta D, Chien S. Vascular tissue engineering: from *in vitro* to *in situ*, Wiley Interdiscip Rev Syst Biol Med 2014;6(1):61-76.

McClure MJ, Sell SA, Simpson DG, Walpoth BH, Bowlin GL. A three-layered electrospun matrix to mimic native arterial architecture using polycaprolactone, elastin, and collagen: A preliminary study, Acta Biomaterialia 2010;6:2422-2433.

Middleton JC, Tipton AJ. Synthetic Biodegradable Polymers as orthopedic device, Biomaterials 2000;21:2335-46.

Milleret V, Hefti T, Hall H, Vogel V, Eberli D. Influence of the fiber diameter and surface roughness of electrospun vascular grafts on blood activation, Acta Biomaterialia 2012;8(12): 4349-4356.

Mitchell IM, Essop AR, Scott PJ, Martin PG, Gupta NK, Saunders NR, Nair RU, Williams GJ. Bovine internal mammary artery as a conduit for coronary revascularization: long-term results, Ann Thorac Surg 1993;55(1):120-2.

Mo XM, Xu CY, Kotaki M, Ramakrishna S. Electrospun P(LLA-CL) nanofiber: a biomimetic extracellular matrix for smooth muscle cell and endothelial cell proliferation, Biomat 2004;25:1883-1890.

Mooradian DL, Hutsell TC, Keefer LK. Nitric-oxide (NO) donor molecules: effect of NO release rate on vascular smooth muscle cell proliferation in vitro, J Cardiovasc Pharmacol 1995;25:674-8.

Mrowczynski W, Mugnai D, Valence S, Tille J, Khabiri E, Cikirikcioglu M, Moller M,Nalpoth BH. Porcine carotid artery replacement with biodegradable electrospun poly-ε-caprolactone vascular prosthesis, J of Vasc Surgery 2014;59: 210-219.

Nair LS, Laurencin CT. Biodegradable polymers as Biomaterials, Prog Poly Sci 2007;32:762-798.

Nam J, Huang Y, Agarwal S, Lannutti J. Improved cellular infiltration in electrospun fiber via engineering porosity, Tissue Eng 2007;13:2249-57.

Nerem RM, Seliktar D. Vascular tissue engineering, Biomed Eng 2001;3:225–43.

Nichols SP, Koh A, Brown NL, Rose MB, Sun B, Slomberg DL, Riccio DA, Klitzman B, Schoenfisch MH. The effect of nitric oxide surface flux on the foreign body response to subcutaneous implants, Biomaterials 2012;33:6305-12.

Niklason LE, Gao J, Abbott WM, Hirschi KK, Houser S, Marini R, Langer R. Functional arteries grown in vitro, Science 1999;284:489-493.

Nilsson A, Wiig M, Alnehill H, Berggren M, Bjornum S, Geijev M, Kopylov P, Sollerman C. The Artelon CMC Spacer Compared with Tendon Interposition Arthroplasty, Acta Orthop 2010;81(2):237-244.

Nottelet B, Pektok E, Mandracchia D, Tille JC, Walpoth B, Gurny R, Moller M. Factorial design optimization and in vivo feasibility of poly(ε-caprolactone)-micro- and nanofiber-based small diameter vascular grafts, J Biomed Mater Res A 2009;89:865-75.

Patel A, Fine B, Sandig M, Mequanint K. Elastin Biosynthesis: The missing link in tissue-engineered blood vessels, Cardiovascular Research 2006;71:40-49.

Pektok E, Nottelet B, Tille JC, Gurny R, Kalangos A, Moeller M, Walpoth BH. Vascular grafts in the rat systemic arterial circulation degradation and healing characteristics of small-diameter poly(e-caprolactone), Circulation 2008;118:2563-2570.

Pham QP, Sharma U, Mikos AG. Electrospinning of polymeric nanofibers for tissue engineering applications: a review, Tissue Eng 2006;12(5):1197-211.

Popowich DA, Varu V, Kibbe MR. Nitric Oxide: What a Vascular Surgeon Needs to Know, Vascular 2007;15:324-335.

Radomski MW, Palmer RMJ, Moncada S. The role of nitric oxide and CGMP in platelet adhesion to vascular endothelium, Biochem Biophys Res Commun 1987;148:1482-9.

Rampichova M, Chvojka J, Buzgo M, Prosecka E, Mikes P, Vyslouzilova L, Tvrdik D, Kochova P, Gregor T, Lukas D, Amler E. An elastic three dimensional poly (ε-caprolactone) nanofibre scaffold enhanced the migration, proliferation, and osteogenic differentiation of mesenchymal stem cells, Cell Proliferation 2013;46:23-37.

Rasband WS. ImageJ, U. S. National Institutes of Health, Bethesda, Maryland, USA, http://imagej.nih.gov/ij/, 1997-2014.

Rensen SSM, Doevendans PAFM, van Eys GJJM. Regulation and characteristics of vascular smooth muscle cell phenotypic diversity, Neth Heart J 2007;15:100-108.

Riccio DA, Coneski PN, Nichols SP, Broadnax AP, Schoenfisch MH. Photoinitiated nitric oxide-releasing tertiary S-nitrosothiol-modified xerogels, ACS Appl Mater Interface 2012;4:796-804.

Rukgauer M, Klei J, Krause-Jarres JD. Reference values for the trace elements copper, manganese, selenium, and zinc in the serum/plasma of children, adolescents, and adults, Journal of Trace Elements in Medicine and Biology 1997;11(2):92-98.

Salacinski HJ, Goldner S, Giudiceandrea A, Hamilton G, Seifalian AM, Edwards A, Carson RJ. The mechanical behavior of vascular grafts: a review, J Biomater Appl 2001;15(3):241-78.

Sarkar S, Sales KM, Hamilton G, Seifalian AM. Addressing thrombogenicity in Vascular Graft Construction, Journal of Biomedical Materials Research Part B: Applied Biomaterials 2006,100-108.

Sauvage L, Berger K, Wook S, Nakagawa Y, Mansfield P. An external velour surface for porous arterial prothese, Surgery 1971;70(6):940-953.

Seifalian AM, Salacinski HJ, Tiwari A, Edwards A, Bowald S, Hamilton G. In vivo biostability of a poly(carbonate-urea)urethane graft, Biomaterials 2003;24(14):2549-57.

Sell SA, McClure MJ, Garg K, Wolfe PS, Bowlin GL. Electrospinning of collagen/biopolymers for regenerative medicine and cardiovascular tissue engineering, Advanced Drug Delivery Reviews 2009;61:1007–1019.

Shi Q, Wu MH-D, Sauvage LR. Clinical and experimental demonstration of complete healing of porous Dacron patch grafts used for closure of the arteriotomy after carotid endarterectomy, Ann Vasc Surg 1999;13:313-317.

Shin'oka T, Imai Y, Ikada Y. Transplantation of a tissue-engineered pulmonary artery, N Engl J Med 2001;44:532-533.

Silver GM, Katske GE, Stutzman FL, Wood NE. Umbilical vein for aortocoronary bypass, Angiology 1982;33(7):450-3.

Singh RJ, Hogg N, Joseph J, Kalyanaraman B. Mechanism of Nitric Oxide Release from S-Nitrosothiols, The Journal of Biological Chemistry 1996;271:18596-603.

Soldani G, Losi P, Bernabei M, Burchielli S, Chiappino D, Kull S, Briganti E, Spiller D. Long term performance of small-diameter vascular grafts made of a poly(ether)urethane-polydimethylsiloxane semi-interpenetrating polymeric network, Biomaterials 2010;31(9):2592-605.

Srouji S, Kizhner T, Suss-Tobi E, Livne E, Zussman E. 3D Nanofibrous electrospun multilayered construct is an alternative ECM mimicking scaffold, J Mater Sci: Mater Med 2008;19:1249-55.

Suma H, Wanibuchi Y, Terada Y, Fukuda S, Saito T, Isshiki T, Yamaguchi T. Bovine internal thoracic artery graft. Successful use at urgent coronary bypass Sumery, J Cardiovasc Surg 1991;32(2):268-70.

Sumpio BE, Riley JT, Dardik A. Cells in focus: endothelial cell, Int J Biochem Cell Biol 2002;34:1508-12.

Sun H, Mei L, Song C, Cui X, Wang P. The in vivo degradation, absorption and excretion of PCL-based implants, Biomaterials 2006;27:1735-40.

Tai NR, Salacinski HJ, Edwards A, Hamilton G, Seifalian AM. Compliance properties of conduits used in vascular reconstruction, Br J Surg 2000;87(11):1516—24.

Taite LJ, Yang P, Jun HW, West JL. Nitric oxide-releasing polyurethane-PEG copolymer containing the YIGSR peptide promotes endothelialization with decreased platelet adhesion, J Biomed Mater Res B Appl Biomater 2008;84:108-116.

Thomas AC, Campbell GR, Campbell JH. Advances in vascular tissue engineering, Cardiovascular Pathology 2003;12:271-276.

Tillman BW, Yazdani SK, Lee SJ, Geavy RL, Atala A, Yoo JJ. The *in vivo* stability of electrospun polycaprolactone-collagen scaffolds in vascular reconstruction, Biomat 2009;30:583-588.

Tomizawa Y, Moon MR, DeAnda A, Castro LJ, Kosek J, Miller DC. Coronary bypass grafting with biological grafts in a canine model, Circulation 1994;90(5 Pt 2):II160-6.

Tzeng E, Kim YM, Pitt BR, Litonova A, Kovesdi I, Billiar TR. Adenoviral transfer of the inducible nitric oxide synthase gene blocks endothelial cell apoptosis, Surgery 1997;122:255-63.

Valence S, Tille JC, Chaabane C, Gurny R, Bochaton-Piallat BH, Moller M. Plasma treatment for improving cell biocompatibility of a biodegradable polymer scaffold for vascular graft applications, Eur J Pharm Biopharm 2013;85:78-86.

Valence S, Tille JC, Mugnai D, Mrowczynski W, Gurny R, Moller M, Walpoth BH. Long term performance of polycaprolactone vascular grafts in a rat abdominal aorta replacement model, Biomaterials 2012;33:38-47.

Vaughn MW, Kuo L, Liao JC. Estimation of nitric oxide production and reaction rates in tissue by use of a mathematical model, Am J Physiol Heart C 1998;274:H2163-76.

Vaz CM, Tuij S, Bouten CVC, Baaijens FPT. Design of scaffolds for blood vessel tissue engineering using a multi-layering electrospinning technique, Acta Biomaterialia 2005;1: 575–582.

Von Oppel U, Zilla P. Tissue adhesives in cardiovascular surgery, J Long-Term Eff Med Implants 1998;8(2):87-101.

Vrandecic MOP. New graft for the surgical-treatment of small vessel diseases, J Cardiovasc Surg (Torino) 1987;28(6):711-4.

Wang TG, Cai TB, Taniguchi N. Nitric Oxide Donors: For Pharmaceutical and Biological Applications, WILEY-VCH, 2005, ISBN: 3-527-31015-0.

Wang X, Lin P, Yao Q, Chen C. Development of small-diameter vascular grafts, World J Surg 2007;31(4):682-9.

Wang Z, Cui Y, Wang J, Yang X, Wu Y, Wang K, Gao X, Li D, Li Y, Zheng XL, Zhu Y, Kong D, Zhao Q. The effect of thick fibers and large pores of electrospun poly(ε-caprolactone) vascular grafts on macrophage polarization and arterial regeneration, Biomaterials 2014;35(22):5700-10.

Watanabe M, Shin'oka T, Tohyama S, Hibino N, Konuma T, Matsumura G, Kosaka Y, Ishida T, Imai Y, Yamakawa M, Ikada Y, Morita S. Tissue-Engineered Vascular Autograft: Inferior Vena Cava Replacement in a Dog Model, Tissue Engineering 2001;7:429-439.

Weinberg C, Bell E. A blood vessel model constructed from collagen and cultured vascular cells, Science 1986;231:397–400.

Williams JK, Heistad, DD. Structure and function of vasa vasorum, Trends in Cardiovascular Medicine 1996;6:53-57.

Woodruff MA, Hutmacher DW. The Return of a Forgotten Polymer - Polycaprolactone in the 21st Century. Prog Polym Sci 2010;35:1217-1256.

Wu H, Fan J, Chu CC, Wu J. Electrospinning of small diameter 3-D nanofibrous tubular scaffolds with controllable nanofiber orientations for vascular grafts, J. Mater Sci: Mater Med 2010;21:3207–3215.

Xue L, Greisler HP. Biomaterials in the development and future of vascular grafts, J Vasc Surg 2003;37(2):472-80.

Yalcin I, Horakova J, Mikes P, Gok Sadikoglu T, Domin R, Lukas D. Design of Polycaprolactone Vascular Grafts, Journal of Industrial Textiles 2014, 1-21.

Yarin AL, Pourdeyhimi B, Ramakrishna S. Fundamentals and Applications of Micro- and Nanofibers, Cambridge University Press, 2014, ISBN 978-1-107-06029-6.

Zhang X, Thomas V, Xu Y, Bellis SL, Vohra YK. An *in vitro* regenerated functional human endothelium on a nanofibrous electrospun scaffold, Biomaterials 2010;31:4376-4381.

Zhang X. Fundamentals of Fiber Science, DEStech Publications, 2014, ISBN 978-1-160595-119-5.

Zheng W, Wang Z, Song L, Zhao Q, Zhang J, Li D, Wang S, Han J, Zheng XL, Yang Z, Kong D. Endothelialization and patency of RGD-functionalized vascular grafts in a rabbit carotid artery model, Biomaterials 2012;33:2880-91.

Ziche M, Morbidelli L, Masini E, Amerini S, Granger HJ, Maggi CA, Geppetti P, Ledda F. Nitric oxide mediates angiogenesis in vivo and endothelial cell growth and migration in vitro promoted by substance P, J Clin Invest 1994;94:2036-44.

Zilla P, Bezuidenhout D., Human P. Prosthetic vascular grafts: Wrong models, wrong questions and no healing, Biomat 2007;28:5009-5027.